arXiv:1006.5394v2 [astro-ph.CO] 12 Jul 2010

Galaxy Formation Theory

Andrew J. Benson

California Institute of Technology, MC350-17, 1200 E. California Blvd., Pasadena, CA 91125, U.S.A. (E-Mail: abenson@caltech.edu*)*

Abstract

We review the current theory of how galaxies form within the cosmological framework provided by the cold dark matter paradigm for structure formation. Beginning with the pre-galactic evolution of baryonic material we describe the analytical and numerical understanding of how baryons condense into galaxies, what determines the structure of those galaxies and how internal and external processes (including star formation, merging, active galactic nuclei, etc.) determine their gross properties and evolution. Throughout, we highlight successes and failures of current galaxy formation theory. We include a review of computational implementations of galaxy formation theory and assess their ability to provide reliable modeling of this complex phenomenon. We finish with a discussion of several "hot topics" in contemporary galaxy formation theory and assess future directions for this field.

Keywords: galaxies, cosmology, galactic structure, galaxy evolution, galaxy formation

Contents

1 Introduction **2**

2 Background Material **3**
2.1 Background Cosmology . . . 3
2.2 Structure Formation . . . 3
2.3 Halo Formation . . . 4
2.3.1 Halo Mass Distribution . . . 4
2.3.2 Halo Formation Distribution . . . 5
2.4 Halo Structure . . . 5

3 Pre-Galactic Evolution of Baryons **6**
3.1 Cold or Hot Accretion (Shocks) . . . 7
3.2 Cooling . . . 9
3.2.1 Atomic . . . 9
3.2.2 Compton Cooling . . . 10
3.2.3 Molecular Hydrogen Cooling . . . 12
3.3 Heating . . . 13
3.3.1 Photoheating . . . 13
3.3.2 Heating from Feedback . . . 14
3.3.3 Preheating . . . 15
3.3.4 Thermal Conduction . . . 16
3.4 Fate of Cooling Gas . . . 16

4 Galaxy Interactions **17**
4.1 Galaxy Orbits . . . 17
4.2 Gravitational Interactions . . . 17
4.2.1 Mergers . . . 17
4.2.2 Tidal Destruction . . . 19

4.2.3 Harassment . . . 20
4.3 Hydrodynamical Interactions . . . 21
4.3.1 Ram pressure . . . 21

5 Galactic Structure **22**
5.1 Disk Formation . . . 22
5.1.1 Sizes . . . 23
5.1.2 Stability . . . 25
5.1.3 Bars/Spiral Arms . . . 26
5.2 Spheroid Formation . . . 27
5.2.1 Major Mergers . . . 28
5.2.2 Secular Evolution . . . 29
5.2.3 Sizes . . . 30

6 Star Formation, AGN and Feedback **31**
6.1 Star Formation . . . 31
6.2 Black Hole Formation . . . 32
6.3 Feedback . . . 36
6.3.1 Supernovae/Stellar Winds . . . 36
6.3.2 AGN . . . 38
6.4 Chemical Enrichment . . . 39
6.5 Stellar Populations . . . 41
6.5.1 Steller Population Synthesis . . . 41
6.5.2 Dust Absorption and Re-emission . . . 42
6.6 Absorption by the Intergalactic Medium . . . 44

7 Computational Techniques **44**
7.1 N-body/Hydro . . . 45
7.2 Semi-Analytic . . . 47
7.3 Halo Occupation Distributions . . . 48

8 Topics of Current Interest **48**
8.1 The First Galaxies . . . 48
8.2 The Formation and Sizes of Galaxy Disks . . . 50
8.3 The Overcooling Problem . . . 52
8.4 Local Group Dwarf Satellites . . . 53
8.5 The Origins of the Hubble Sequence . . . 54

9 Future Directions **55**

10 Summary **55**

1. Introduction

While the concept of galaxies as "island universes" can be traced back to Wright (1750) and Kant (1755) the study of the formation of galaxies did not begin until after their extra-Galactic status was confirmed by Hubble (1929). In fact, much of the early work on galaxy evolution and formation was driven by the necessity of understanding galaxies in order to answer questions of cosmology (such as whether or not the Universe began with a Big Bang). While an understanding of galaxies remains necessary for such reasons even today, the field has since become an important one in its own right.

Modern galaxy formation theory therefore grew out of early studies of cosmology and structure formation and is set within the cold dark matter cosmological model and so proceeds via a fundamentally hierarchical paradigm.

Observational evidence and theoretical expectations indicate that galaxy formation is an ongoing process which has been occurring over the vast majority of the Universe's history. The goal of galaxy formation theory then is to describe how simple physics gives rise to the complicated set of phenomena which galaxies encompass.

Galaxy formation is very much an observationally driven field in the sense that we are still decidedly in the stage of making new experimental discoveries rather than performing precision tests of well-specified theoretical models. While this situation shows signs of a gradual shift to the "precision tests" phase it seems unlikely that the transition will be completed any time soon. In addition, astronomy is perhaps uniquely hindered by experimental biases, since we are not able to design the experiment, merely to observe what the Universe has decided to put on show. The complicated nature of the resulting selection effects result in a secondary, but very important, role for theoretical models, namely in quantifying these biases and interpreting the data. While this secondary role is well established it needs to become more so, in particular it should become an integral part of any observational campaign and will require direct and simple access to modeling capabilities for all.

2. Background Material

Modern galaxy formation theory is set within the larger scale cold dark matter cosmological model (Blumenthal et al. 1984). The success of that model in explaining the cosmic microwave background (CMB) (Komatsu et al., 2009) and large scale structure (Seljak et al., 2005; Percival et al., 2007a; Ferramacho et al., 2008; Sanchez et al., 2009) of the Universe makes it the *de facto* standard. However, it is important to recognize that the scales on which the simplest cold dark matter (CDM) model has been most precisely tested are much larger than those that matter for galaxy formation[1]. As such, we cannot fully rule out that dark matter is warm or self-interacting, although good constraints exist on both of these properties (Markevitch et al., 2004; Boehm and Schaeffer, 2005; Ahn and Shapiro, 2005; Miranda and Macciò, 2007; Randall et al., 2008; Yüksel et al., 2008; Boyarsky et al., 2008).

More extensive reviews of the cold dark matter cosmological model can be found in, for example, Narlikar and Padmanabhan (2001), Frenk (2002) and Bertone et al. (2005).

2.1. Background Cosmology

A combination of experimental measures, including studies of the CMB (Dunkley et al. 2009), large scale structure (Tegmark et al. 2004; Cole et al. 2005; Tegmark et al. 2006; Percival et al. 2007a,b), the Type Ia supernovae magnitude–redshift relation (Kowalski et al. 2008) and galaxy clusters (Mantz et al., 2009; Vikhlinin et al., 2009; Rozo et al., 2010), have now placed strong constraints on the parameters of the cold dark matter cosmogony. The picture that emerges (Komatsu et al., 2010) is one in which the energy density of the Universe is shared between dark energy ($\Omega_\Lambda = 0.728^{+0.015}_{-0.016}$), dark matter ($\Omega_c = 0.227 \pm 0.014$) and baryonic matter ($\Omega_b = 0.0456 \pm 0.0016$), with a Hubble parameter of $70.4^{+1.3}_{-1.4}$ km/s/Mpc. Perturbations on the uniform model seem to be well described by a scale-free primordial power spectrum with power-law index $n_s = 0.963 \pm 0.012$ and amplitude $\sigma_8 = 0.809 \pm 0.024$.

Given such a cosmological model, the Universe is 13.75 ± 0.11 Gyr old. Galaxies probably began forming at $z \sim 20 - 50$ when the first sufficiently deep dark matter potential wells formed to allow gas to cool and condense to form galaxies (Tegmark et al. 1997; Gao et al. 2007).

2.2. Structure Formation

The formation of structure in the Universe is seeded by minute perturbations in matter density expanded to cosmological scales by inflation. The dark matter component, having no pressure, must undergo gravitational collapse and, as such, these perturbations will grow. The linear theory of cosmological perturbations is well understood and provides an accurate description of the early evolution of these perturbations. Once the perturbations become nonlinear, their evolution is significantly more complicated, but simple arguments (e.g. spherical top-hat collapse and developments thereof; Gunn 1977; Shaw and Mota 2008) provide insight into the basic behavior. Empirical methods to

[1] Although measurements of the Lyman-α forest (Slosar et al., 2007; Viel et al., 2008) and weak-lensing (Mandelbaum et al., 2006) give interesting constraints on the distribution of dark matter on small scales they typically require modeling of either the nonlinear evolution of dark matter or the behavior of baryons (or both) which complicate any interpretation. They are therefore not as "clean" as CMB and large scale structure constraints.

determine the statistical distribution of matter in the nonlinear regime exist (Hamilton et al. 1991; Peacock and Dodds 1996; Smith et al. 2003; Heitmann et al. 2009). These, together with N-body simulations (e.g. Klypin and Shandarin 1983; Springel et al. 2005b; Heitmann et al. 2008) show that a network of halos strung along walls and filaments forms, creating a cosmic web. This web is consistent with measurements of galaxy and quasar clustering on a wide range of scales.

2.3. Halo Formation

The final result of the nonlinear evolution of a dark matter density perturbation is the formation of a dark matter halo: an approximately stable, near-equilibrium state supported against its own self-gravity by the random motions of its constituent particles. In a hierarchical universe the first halos to form will do so from fluctuations on the smallest scales. Later generations of halos can be thought of as forming from the merging of these earlier generations of halos. For the purposes of galaxy formation, two fundamental properties of the dark matter halos are of primary concern: (i) the distribution of their masses at any given redshift and (ii) the distribution of their formation histories (i.e. the statistical properties of the halos from which they formed).

2.3.1. Halo Mass Distribution

The insight of Press and Schechter (1974) was that halos could be associated with peaks in the Gaussian random density field of dark matter in the early universe. Using the relatively simple statistics of Gaussian random fields they were able to derive the following form for the distribution of dark matter halo masses such that the number of halos per unit volume in the mass range M to $M + \delta M$ is $\delta M(\mathrm{d}n/\mathrm{d}M)$ where[2]:

$$\begin{aligned}\frac{\mathrm{d}n}{\mathrm{d}M}(M,t) &= \left(\frac{2}{\pi}\right)^{1/2}\frac{\rho_0}{M^2}\frac{\delta_\mathrm{c}(t)}{\sigma(M)}\left|\frac{\mathrm{d}\ln\sigma}{\mathrm{d}\ln M}\right| \\ &\quad\times\exp\left[-\frac{\delta_\mathrm{c}^2(t)}{2\sigma^2(M)}\right],\end{aligned} \tag{1}$$

where ρ_0 is the mean density of the Universe, $\sigma(M)$ is the fractional root variance in the density field smoothed using a top-hat filter that contains, on average, a mass M, and $\delta_\mathrm{c}(t)$ is the critical overdensity for spherical top-hat collapse at time t (Eke et al. 1996).

While the Press and Schechter (1974) expression is remarkably accurate given its simplicity, it does not provide a sufficiently accurate description of modern N-body measures of the halo mass function. Several attempts have been made to "fix" the Press and Schechter (1974) theory by appealing to different filters and barriers (e.g. Sheth et al. 2001) although to date none are able to accurately predict the measured form without adjusting tunable parameters. The most accurate fitting formulae currently available are those of Tinker et al. (2008; see also Reed et al. 2007; Robertson et al. 2009). Specifically, the mass function is given by

$$\frac{\mathrm{d}n}{\mathrm{d}M} = f(\sigma)\frac{\bar{\rho}}{M}\frac{\mathrm{d}\ln\sigma^{-1}}{\mathrm{d}M}, \tag{2}$$

where

$$f(\sigma) = A\left[\left(\frac{\sigma}{b}\right)^{-a} + 1\right]\exp\left(-\frac{c}{\sigma^2}\right), \tag{3}$$

and where A, a, b and c are parameters determined by fitting to the results of N-body simulations. The mass variance $\sigma^2(M)$ is determined from the power spectrum of density fluctuations

$$\sigma^2(M) = \frac{1}{2\pi^2}\int_0^\infty P(k)T^2(k)\hat{W}_M^2(k)k^2\mathrm{d}k \tag{4}$$

[2]The original derivation by Press and Schechter (1974) differed by a factor of 2, resulting in only half of the mass of the Universe being locked up in halos. Later derivations placed the method on a firmer mathematical basis and resolved this problem, a symptom of the "cloud-in-cloud" problem (Bond et al. 1991; Bower 1991; Lacey and Cole 1993).

where $P_(k)$ is the primordial power spectrum (usually taken to be a scale-free power spectrum with index n_s), $T(k)$ is the cold dark matter transfer function (Eisenstein and Hu 1999) and $\hat{W}_M(k)$ is the Fourier transform of the real-space top-hat window function. Tinker et al. (2008) give values for these parameters as a function of the overdensity, Δ, used to define what we consider to be a halo. Additionally, they find that the best fit values are functions of redshift. Earlier studies had hoped to find a "universal" form for the mass function (such that the functional form was always the same when expressed in terms of $\nu = \sigma/\delta_c$). While this is approximately true, the work of Tinker et al. (2008) demonstrates that universality does not hold when high precision results are considered.

2.3.2. Halo Formation Distribution

A statistical description of the formation of halos, specifically the sequence of merging events and the masses of halos involved in those events, can be extracted using similar arguments as the original Press and Schechter (1974) approach (Lacey and Cole 1993). These show that the distribution of halo progenitor masses, M_1m at redshift z_1 for a halo of mass M_2 at later redshift z_2 is given by

$$\begin{aligned}\frac{\mathrm{d}N}{\mathrm{d}M_1} &= \left(\frac{2}{\pi}\right)^{1/2} \frac{\mathrm{d}\ln\sigma}{\mathrm{d}\ln M}_1 M_2 \frac{\sigma_1^2}{M_1^2} \frac{\delta_{c1}-\delta_{c2}}{(\sigma_1^2-\sigma_2^2)^{3/2}} \\ &\quad \times \exp\left[-\frac{(\delta_{c1}-\delta_{c2})^2}{(\sigma_1^2-\sigma_2^2)}\right], \end{aligned} \tag{5}$$

where $\sigma_1 = \sigma(M_1)$, $\sigma_2 = \sigma(M_2)$, $\delta_{c1} = \delta_c(z_1)$, $\delta_{c2} = \delta_c(z_2)$. With a zero time-lag (i.e. as $z_1 \rightarrow z_2$ and therefore $\delta_{c1} \rightarrow \delta_{c2}$) this can be interpreted as a merging rate (although see Neistein and Dekel (2008) for a counter argument). Repeated application of this merging rate can be used to build a merger tree. Finding a suitable algorithm is non-trivial and many attempts have been made (Kauffmann and White 1993; Somerville and Primack 1999; Cole et al. 2000; Parkinson et al. 2008). A recent examination of alternative algorithms is given by Zhang et al. (2008). Current implementations of merger tree algorithms are highly accurate and can reproduce the progenitor halo mass distribution over large spans of redshift (Parkinson et al. 2008).

A fundamental limitation of any Press and Schechter (1974) based approach is that the merger rates are not symmetric, in the sense that switching the masses M_1 and M_2 results in two different predictions for the rate of mergers between halos of mass M_1 and M_2. Benson et al. (2005) and Benson (2008) showed that a symmetrized form of the Parkinson et al. (2008) merger rate function could be made to approximately solve Smoluchowski's coagulation equation (Smoluchowksi 1916) and thereby provide a solution free from ambiguities. Other empirical determinations of merger rates have been made (Cole et al. 2008; Fakhouri and Ma 2008a,b).

In addition to these purely analytic approaches, numerical studies utilizing N-body simulations have lead to the development of an empirical understanding of halo formation histories (Wechsler et al., 2002; van den Bosch, 2002) and halo–halo merger rates (Fakhouri and Ma, 2008a, 2009; Stewart et al., 2009; Fakhouri et al., 2010; Hopkins et al., 2010). Merger trees can also be extracted directly from N-body simulations (e.g. Helly et al. 2003a; Springel et al. 2005b) which sidesteps these problems but incorporates any limitations of the simulation (spatial, mass and time resolution), and additionally provides information on the spatial distribution of halos. Such N-body merger trees also serve to highlight some, perhaps fundamental, limitations of the Press and Schechter (1974) type approach. For example, halos in N-body simulations undergo periods of mass loss, which is not expected in pure coagulation scenarios. The existence of systems of substructures within halos (see Section refsec:galaxyOrbits) can even lead to three-body encounters which cause subhalos to be ejected (Sales et al. 2007).

2.4. Halo Structure

Dark matter halos are characterized by their large overdensity with respect to the background density. Spherical top-hat collapse models (e.g. Eke et al. 1996) show that the overdensity, Δ, of a just collapsed halo is approximately 200, with some dependence on cosmological parameters. This overdensity corresponds, approximately, to the virialized region of a halo, and allows us to define a virial radius as

$$r_v = \left(\frac{3M}{4\pi\rho_0\Delta}\right)^{1/3}. \tag{6}$$

Studies utilizing N-body simulations show that halos approximately obey the virial theorem within this radius and that r_v is a characteristic radius for the transition from ordered inflow of matter (on larger scales) to virialized random motions (on smaller scales) (Cole and Lacey 1996). Dark matter halos have triaxial shapes and the distribution of axial ratios has been well characterized from N-body simulations (Frenk et al. 1988; Jing and Suto 2002; Bett et al. 2007).

Recent N-body studies (Navarro et al. 2004; Merritt et al. 2005; Prada et al. 2006) indicate that density profiles of dark matter halos have an approximately universal form in CDM cosmologies that is better described by the Einasto profile (Einasto 1965) than the Navarro-Frenk-White (NFW) profile (Navarro et al. 1996, 1997). The Einasto density profile is given by

$$\rho(r) = \rho_{-2} \exp\left(-\frac{2}{\alpha}\left[\left(\frac{r}{r_{-2}}\right)^{\alpha} - 1\right]\right), \tag{7}$$

where r_{-2} is a characteristic radius at which the logarithmic slope of the density profile equals -2 and α is a parameter which controls how rapidly the logarithmic slope varies with radius. The parameter α seems to correlate well with the height of the peak from which a halo formed, $\nu = \delta_c(z)/\sigma(M)$ as has been shown by Gao et al. (2008) who provide a fitting formula,

$$\alpha = \begin{cases} 0.155 + 0.0095\nu^2 & \text{if } \nu < 3.907 \\ 0.3 & \text{if } \nu \geq 3.907, \end{cases} \tag{8}$$

which is a good match to halos in the Millennium Simulation[3] (Springel et al. 2005b). The value of r_{-2} for each halo is determined from the known virial radius, r_v, and the concentration, $c_{-2} \equiv r_v/r_{-2}$. The NFW profile has a significantly simpler form and is good to within 10–20% making it still useful. It is given by

$$\rho(r) = 4\frac{\rho_s}{(r/r_s)[1 + r/r_s]^2}, \tag{9}$$

where r_s is a characteristic scale radius and ρ_s is the density at $r = r_s$. For NFW halos, the concentration is defined as $c_{NFW} = r_v/r_s$.

Concentrations are found to depend weakly on halo mass and on redshift and can be predicted from the formation history of a halo (Wechsler et al. 2002). Simple algorithms to approximately determine concentrations have been proposed by Navarro et al. (1997), Eke et al. (2001) and Bullock et al. (2001b). More accurate power-law fits have also been determined from N-body simulations (Gao et al. 2008; Zhao et al. 2009).

Integrals over the density and mass distribution are needed to compute the enclosed mass, velocity dispersion, gravitational energy and so on for the halo density profile. For NFW halos the integrals are mostly straightforward, although some require numerical calculation. For the Einasto profile some of these may be expressed analytically in terms of incomplete gamma functions (Cardone et al. 2005). Specifically, expressions for the mass and gravitational potential are provided by Cardone et al. (2005), other integrals (e.g. gravitational energy) must be computed numerically.

3. Pre-Galactic Evolution of Baryons

Baryons are initially distributed near uniformly—they are expected to trace the dark matter distribution on scales above the Jeans length (Arons and Silk 1968; Gnedin and Hui 1998). To form galaxies they must first be concentrated by the forces of gravity which are dominated by the distribution of dark matter. In particular, we expect that baryons will concentrate towards the deep potential wells of dark matter halos. These should therefore be the sites of galaxy formation.

[3]We have truncated this fit so that α never exceeds 0.3. Gao et al. (2008) were not able to probe the behavior of α in the very high ν regime. Extrapolating their formula to $\nu > 4$ is not justified and we instead choose to truncate it at a maximum of $\alpha = 0.3$.

3.1. Cold or Hot Accretion (Shocks)

Baryonic material will be dragged along by the gravitationally dominant dark matter such that dark matter halos are expected to accrete baryonic material. How much baryonic material they accrete depends upon the depth of their potential well and the pressure of the baryons.

According to Okamoto et al. (2008a), the mass of baryons which accrete from the intergalactic medium into a galaxy halo during some interval δt after the Universe has been reionized (i.e. the hydrogen content of the Universe has been almost fully ionized as a result of emission from stars and active galactic nuclei (AGN)) is given by

$$M_{\rm b} = M'_{\rm b} + M_{\rm acc}, \tag{10}$$

where $M_{\rm acc}$ is given below,

$$M'_{\rm b} = \sum_{\rm prog} \exp\left(-\frac{\delta t}{t_{\rm evp}}\right) M_{\rm b}, \tag{11}$$

and where the sum is taken over all progenitors of the current halo, and $t_{\rm evp}$ is the timescale for gas to evaporate from the progenitor halo and is given by

$$t_{\rm evp} = \begin{cases} r_{\rm v}/c_{\rm s}(\Delta_{\rm evp}) & \text{if } T_{\rm v} < T_{\rm evp}, \\ \infty & \text{if } T_{\rm v} > T_{\rm evp}, \end{cases} \tag{12}$$

where $T_{\rm evp}$ is the temperature below which gas will be heated and evaporated from the halo, $c_{\rm s}$ is the sound speed in the halo gas. Okamoto et al. (2008a) compute $T_{\rm evp}$ by finding the equilibrium temperature of gas at an overdensity of $\Delta_{\rm evp} = 10^6$. The accreted mass, $M_{\rm acc}$, is given by

$$M_{\rm acc} = \begin{cases} \frac{\Omega_{\rm b}}{\Omega_0} M_{\rm H} - M'_{\rm b} & \text{if } T_{\rm vir} > T_{\rm acc}, \\ 0 & \text{if } T_{\rm vir} < T_{\rm acc}. \end{cases} \tag{13}$$

Here, $T_{\rm acc}$ is the larger of $T_{\rm eq}$ and the temperature of intergalactic medium gas adiabatically compressed to the density of accreting gas where $T_{\rm eq}$ is the equilibrium temperature at which radiative cooling balances photoheating for gas at the density expected at the virial radius, for which Okamoto et al. (2008a) use one third of the halo overdensity.

An accretion shock is a generic expectation whenever the gas accretes supersonically as it will do if the halo virial temperature exceeds the temperature of the accreting gas (Binney 1977a). Models of accretion shocks have been presented by several authors (Bertschinger 1985; Tozzi and Norman 2001; Voit et al. 2003; Book and Benson 2010) with the general conclusion that the shock occurs at a radius comparable to (or perhaps slightly larger than) the virial radius when cooling times are long compared to dynamical times. In the other limit of short cooling times, it has long been understood that the shock must instead form at much smaller radii, close to the forming galaxy (Rees and Ostriker, 1977; White and Frenk, 1991). For example, according to Rees and Ostriker (1977): "Unless pre-galactic clouds collapse in an exceedingly homogeneous fashion, their kinetic energy of infall will be thermalized by shocks before collapse has proceeded by more than a factor ~ 2. What happens next depends on the relative value of the cooling and collapse timescales. Masses in the range 10^{10}–$10^{12} M_\odot$ cool so efficiently that they always collapse at the free-fall rate, and probably quickly fragment into stars. Larger masses may, however, experience a quasistatic contraction phase…". Thus, Rees and Ostriker (1977) clearly understood the difference between the rapid inflow and hydrostatic cooling regimes, and correctly identified the transition mass, suggesting that this be identified this with the characteristic stellar mass of galaxies. Accretion in these two regimes may be expected to result in very different spatial and spectral distributions of cooling radiation, leading to the possibility of observationally distinguishing the two types of accretion (Fardal et al., 2001).

The distinction between these two regimes has always been an integral part of analytic models of galaxy formation, beginning with Rees and Ostriker (1977). For example, White and Frenk (1991) introduced a transition between rapid and slow cooling regimes at the point where cooling and virial radii become equal, or, equivalently, the point at which cooling and dynamical times at the halo virial radius become equal. In the rapid cooling regime, the accretion rate of gas into the central galaxy was then determined by the cosmological infall rate, while in the slow cooling regime the accretion rate was determined by the cooling time in the gas. Their Figure 2 illustrates that the rapid cooling regime will occur in low mass halos and at high redshifts. All subsequent semi-analytic models of galaxy formation (e.g. Kauffmann et al. 1993; Cole et al. 1994) have adopted this prescription, or some variant of it, and it

has also been validated by 1D hydrodynamical simulations (e.g Forcada-Miro and White 1997). The validity of this prescription has been confirmed by studies which compared its predictions for the condensed masses of galaxies with those from smoothed particle hydrodynamics simulations across the boundary of the rapid to slow cooling transition (Benson et al., 2001b; Yoshida et al., 2002; Helly et al., 2003b), although it should be noted that the accuracy of these comparisons is less than that at which semi-analytic models are now being used.

Recent work has once again focused on the formation of accretion shocks. Recent 3D hydrodynamical simulations (Fardal et al. 2001; see also Kereš et al. 2005; Ocvirk et al. 2008; Kereš et al. 2009), have suggested that a significant fraction of gas in low mass galaxies has never been shock heated (at least within regions adequately resolved by the simulations; for example numerical simulations may not adequately resolve shocks in the radiative regime due to artificial viscosity, numerical diffusion and other numerical artifacts; Agertz et al. 2007). Motivated by these results Birnboim and Dekel (2003) developed an analytic treatment of accretion shock stability[4]. The accretion shock relies on the presence of a stable atmosphere of post-shock gas to support itself. If cooling times in the post-shock gas are sufficiently short, this atmosphere cools and collapses and can no longer support the shock. The shock therefore shrinks to smaller radii, where it can be stable. Birnboim and Dekel (2003) find that

$$\rho r \Lambda(T_1)/u^3 \mu^2 m_{\rm H}^2 < 0.0126, \tag{14}$$

where ρ is gas density, $\Lambda(T)$ is the cooling function for gas at temperature T, $T_1 = (3/16)\mu u_0^2/k_{\rm B}N_a$ is the post-shock temperature and u is the infall velocity, all evaluated for the pre-shock gas at radius r, is required for the shock to be stable[5]. For cosmological halos this implies that shocks can only form close to the virial radius in halos with mass greater than $10^{11}M_\odot$ for primordial gas (or around $10^{12}M_\odot$ for gas of Solar metallicity). These values are found to depend only weakly on redshift and are in good agreement with the results of hydrodynamical simulations. It is crucial to note that these new criteria are equivalent to that of White and Frenk (1991) up to factors of order unity.

As a result, in low mass halos gas tends to accrete into halos "cold[6]"—never being shock heated to the virial temperature and proceeding to flow along filaments towards the center of the halo where it will eventually shock[7]. Halos which do support shocks close to the virial radius are expected to contain a quasi-hydrostatic atmosphere of hot gas. The structure of this atmosphere is determined by the entropy that the gas gains at the accretion shock and that may be later modified by radiative cooling and feedback (Voit et al. 2003; McCarthy et al. 2007). In practice, the transition from rapid to slow cooling regimes is not sharp—halos able to support a shock at their virial radius still contain some unshocked gas; because the halos retain a memory of past accretion and because cold filaments may penetrate through the hot halo. At high redshifts in particular, the "cold" accretion mode may be active even in halos whose accretion of gas is primarily via an accretion shock close to the virial radius.

The consequences of rapid vs. slow cooling regimes for the properties of the galaxy forming warrant further study. As Croton et al. (2006) have stressed, the absence of a more detailed treatment of the rapid cooling regime may not be important since, by definition the gas accretion rate in small halos is limited by the growth of the halo rather than by the system's cooling time. In contrast, Brooks et al. (2009) demonstrate in hydrodynamical simulations that in the rapid cooling regime accreted gas can reach the galaxy more rapidly, by virtue of the fact that it does not have to cool but instead merely has to free-fall to the center of the halo (starting with a velocity comparable to the virial velocity). This results in earlier star formation than if all gas were assumed to be initially shock heated to the virial temperature close to the virial radius of the halo. It is also clear that the situation needs to be carefully reassessed in the presence of effective feedback schemes that prevent excessive star formation, particularly in the high redshift universe.

While hot atmospheres of gas are clearly present in massive systems such as groups and clusters of galaxies (where the hot gas is easily detected by virtue of its X-ray emission), observational evidence for hot atmospheres of gas arising from cosmological infall surrounding lower mass systems, such as massive but isolated galaxies is sparse. Interesting upper limits have been placed on the X-ray emission from massive, nearby spiral galaxies (Benson et al. 2000b; Rasmussen et al. 2009), and the hot component of the Milky Way's halo is constrained by the ram pressure

[4]Unpublished work by Forcada-Miro and White (1997), also utilizing a 1D hydrodynamics code, reached similar conclusions.

[5]The left-hand side of this expression is equivalent, to order of magnitude, to $t_{\rm sc}/t_{\rm cool}$ where $t_{\rm sc}$ is the sound-crossing time in the halo and $t_{\rm cool}$ is the cooling time in the post-shock gas. This provides some physical insight into this condition: if the post-shock gas can cool too quickly sound waves cannot communicate across the halo and thereby form a hydrostatic atmosphere which can support a shock front).

[6]Or, more likely, warm (Bland-Hawthorn, 2009).

[7]While this picture seems reasonable on theoretical grounds, it as yet has little direct observational support (Steidel et al., 2010).

that it exerts on the Magellanic Stream (Moore and Davis 1994; Mastropietro et al. 2005b). Additionally, ultraviolet line detections of the so-called warm-hot intergalactic medium (intergalactic gas at temperatures of 10^5–10^6K) show that some of this material must lie close to the Milky Way (Wang et al. 2005; Williams et al. 2006). What is known is that the Milky Way's halo contains a significant mass of cold, neutral gas in the form of high velocity clouds (Putman et al. 2003). This may indicate, as expected on theoretical grounds (Crain et al., 2009), that the Milky Way is in the transition mass range between purely cold and purely hot accretion.

3.2. Cooling

Gas which does experience a strong virial shock will have its kinetic infall energy thermalized and therefore be heated to of order the virial temperature

$$T_{\rm v} = \frac{2}{3}\frac{{\rm G}M_{\rm v}}{r_{\rm v}}\frac{\mu m_{\rm H}}{k_{\rm B}}. \tag{15}$$

This gas will proceed to form a hydrostatically supported atmosphere obeying the usual hydrostatic equilibrium equation:

$$\frac{{\rm d}P}{{\rm d}r} = -\frac{{\rm G}M(r)}{r^2}\rho(r), \tag{16}$$

where P is the gas pressure, $\rho(r)$ the gas density and $M(r)$ the total (i.e. dark matter plus baryonic) mass within radius r. This distribution may be modified, particularly on small scales, by other contributors to supporting the halo against gravity, such as turbulence (Frenk et al. 1999), cosmic ray pressure (Guo and Oh 2008) and magnetic pressure (Gonçalves and Friaça 1999). In any case, the resulting hot atmosphere will fill the dark matter halo with a density still several orders of magnitude lower than typical galactic densities. In the absence of any dissipitative process, the gas would remain in this state indefinitely. Fortunately, however, gas is able to cool radiatively and so will eventually lose energy and, consequently, pressure support, at which point it must fall towards the center of the gravitational potential of the dark matter halo thereby increasing its density. Gas which does not experience a shock close to the virial radius can fall almost ballistically towards the halo center. It must still lose its infall energy at some point, however, shocking closer to the halo center near the forming galaxy. As such, it too will eventually be heated and must cool down (although it will presumably do so much more rapidly due to its higher density).

In the remainder of this subsection we will review the various mechanisms by which such gas cools.

3.2.1. Atomic

For metal rich gas, or gas hot enough to begin to collisionally ionize hydrogen (i.e. $T \gtrsim 10^4$K), the primary cooling mechanisms at low redshifts are a combination of various atomic processes including recombination radiation, collisional excitation and subsequent decay and Bremmsstahlung. In the absence of any external radiation field (see Section refsec:PhotoHeat), these are all two-body processes and so the cooling rate is expected to scale as the square of the density for gas of fixed chemical composition and temperature. It is usual, therefore, to write the cooling rate per unit volume of gas as

$$\mathcal{L} = n_{\rm H}^2 \Lambda(T, \boldsymbol{Z}), \tag{17}$$

where $n_{\rm H}$ is the number density of hydrogen (both neutral and ionized) and $\Lambda(T, \boldsymbol{Z})$ is the "cooling function" and depends on temperature and chemical composition. Typically, the chemical composition is described by a single number, the metallicity Z (defined as the mass fraction of elements heavier than helium), and an assumed set of abundance ratios (e.g. primordial or Solar). The cooling function can then be found by first solving for the ionization state of the gas assuming collisional ionization equilibrium and then summing the cooling rates from the various above mentioned cooling mechanisms. Such calculations can be carried out by using, for example, Cloudy (Ferland et al. 1998). Examples of cooling functions computed in this way are shown in Fig. 1.

In detail, the cooling function depends not just on the overall metallicity, but on the detailed chemical composition of the gas. If the abundances of individual elements are known, the corresponding cooling function is easily calculated. In theoretical calculations of galaxy formation it is often computationally impractical to follow the abundance of numerous chemical species in a large number of galaxies and dark matter halos. Fortunately, Martínez-Serrano et al. (2008) have demonstrated that an optimal linear combination of abundances, which minimizes the variance between cooling/heating rates computed using that linear combination as a parameter and a full calculation using all abundances, provides very accurate estimates of cooling rates. The best linear combination turns out to be a function

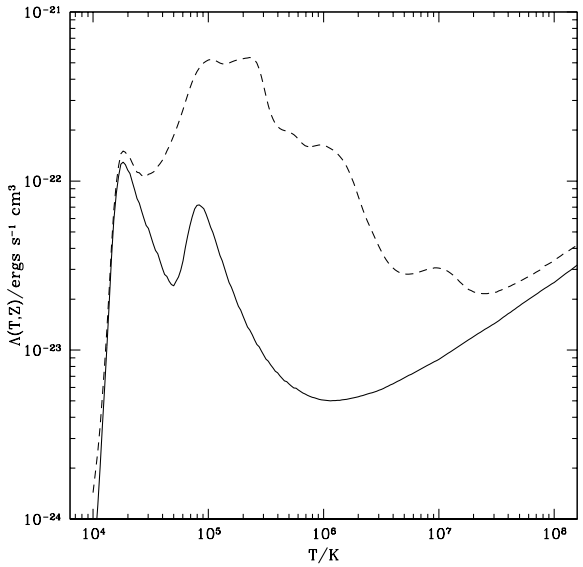

Figure 1: Cooling functions for gas in collisional ionization equilibrium are shown as a function of temperature. The solid line corresponds to gas of primordial composition, while the dashed line corresponds to gas of Solar composition.

of temperature. This reduces the problem to tracking the optimal combination of elements for a small number of temperatures. This number can then be used in place of metallicity when computing cooling functions.

Most calculations of cooling rates in cosmological halos assume that the gas is in collisional or photoionization equilibrium. Even if the gas begins in such a state, as it cools it can drift away from equilibrium as, particularly at low temperatures, the ion–electron recombination timescales can significantly exceed the cooling timescales—as such, the ionization state always lags behind the equilibrium state due to the rapidly changing gas temperature. Figure 2 shows calculations of effective cooling functions for gas initially in collisional ionization equilibrium (and with no external radiation field) with a fully time-dependent calculation of cooling and ionization state (Gnat and Sternberg 2007). Significant differences can be seen, resulting in cooling timescales being a factor of 2–3 longer when non-equilibrium effects are taken into account.

3.2.2. Compton Cooling

At high redshifts, the density of cosmic microwave background photons becomes sufficiently high that the frequent Compton scattering of these photons from electrons in the ionized plasma inside dark matter halos results in significant cooling of that plasma (assuming that its temperature exceeds that of the cosmic microwave background). The Compton cooling timescale is given by (Peebles 1968)

$$\tau_{\rm Compton} = \frac{3 m_{\rm e} c (1 + 1/x_{\rm e})}{8 \sigma_{\rm T} a T_{\rm CMB}^4 (1 - T_{\rm CMB}/T_{\rm e})}, \tag{18}$$

where $x_{\rm e} = n_{\rm e}/n_{\rm t}$, $n_{\rm e}$ is the electron number density, $n_{\rm t}$ is the number density of all atoms and ions, $T_{\rm CMB}$ is the CMB temperature and $T_{\rm e}$ is the electron temperature of the gas. Unlike the various atomic cooling processes described in Section refsec:CoolingAtomic, the Compton cooling rate per unit volume does not scale as the square of the particle density, since it involves an interaction between a particle and a cosmic microwave background photon. Since the CMB photon density is the same everywhere, independent of the local gas density, the Compton cooling rate scales linearly with density. As a result, the Compton cooling timescale is independent of gas density. Thus, if gas in a dark matter halo is able to cool via Compton cooling, it can do so at all radii (assuming that it is isothermal and has the same electron fraction everywhere).

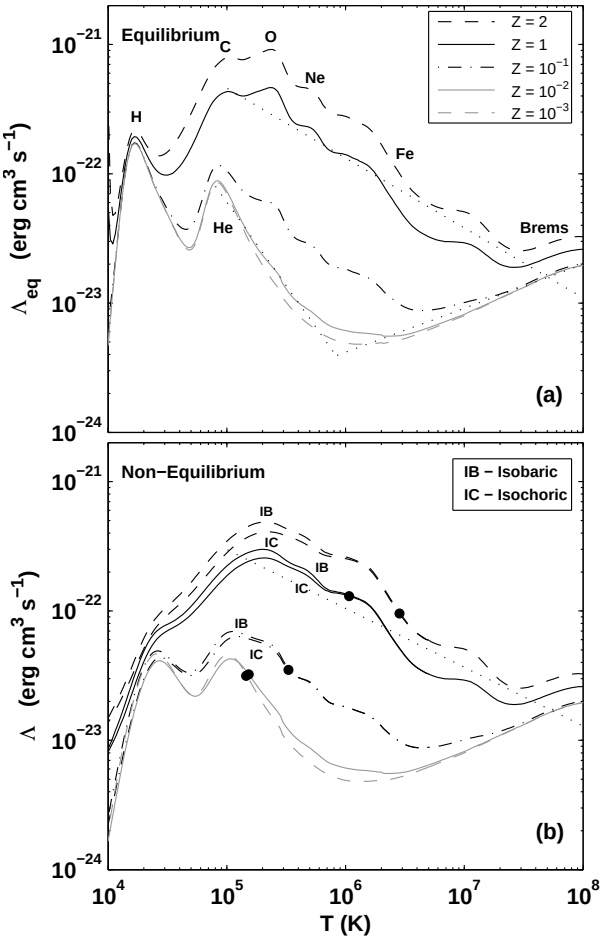

Figure 2: A comparison of cooling functions for gas in collisional ionization equilibrium (upper panel) with effective cooling functions for gas in which the time-dependent ionization state is computed throughout the cooling (lower panel). Line types indicate different metallicities (shown in the upper panel, values in units of Solar metallicity), while IB and IC labels indicate whether the gas was assumed to be cooling isobarically or isochorically. The primary coolant at each temperature is indicated in the upper panel.
Source: Reproduced with permission from Gnat and Sternberg 2007.

In a Universe with WMAP 5 yr cosmological parameters, the Compton cooling time is less than the age of the Universe above $z \approx 6$.

3.2.3. Molecular Hydrogen Cooling

Somewhat ironically, the gas in dark matter halos at the highest redshifts is too cold to cool any further. In halos with virial temperatures below 10^4K even shock heated gas (if shocks can occur) will be mostly neutral and therefore unable to cool via the usual atomic processes described in Section refsec:CoolingAtomic. Studies show that the dominant coolant in such cases becomes the small fraction of hydrogen in the form of molecular hydrogen (Abel et al. 1997). Cooling via molecular hydrogen is crucial for the formation of the first stars (Abel et al. 2002) and galaxies (Bromm et al. 2009) and, therefore, for the sources which cause the reionization of the Universe (Benson et al. 2006; Wise and Abel 2008a). The details of molecular hydrogen cooling are more complicated than those of atomic cooling: in addition to uncertainties in the molecular chemistry (Glover and Abel 2008), in many cases equilibrium is not reached and the photon background can lead to both negative (Wise and Abel 2007a) and positive (Ricotti et al. 2001) feedbacks.

Cosmologically, molecular hydrogen forms via the gas-phase reactions (McDowell 1961):

$$\begin{aligned} \mathrm{H} + \mathrm{e}^- &\rightarrow \mathrm{H}^-, +\gamma \\ \mathrm{H}^- + \mathrm{H} &\rightarrow \mathrm{H}_2 + \mathrm{e}^-, \end{aligned} \tag{19}$$

and

$$\begin{aligned} \mathrm{H}^+ + \mathrm{H} &\rightarrow \mathrm{H}_2^+ + \gamma, \\ \mathrm{H}_2^+ + \mathrm{H} &\rightarrow \mathrm{H}_2 + \mathrm{H}^+. \end{aligned} \tag{20}$$

Our discussion of molecular hydrogen cooling will mostly follow Yoshida et al. (2006).

The molecular hydrogen cooling timescale is found by first estimating the abundance, $f_{H_2,c}$, of molecular hydrogen that would be present if there is no background of H_2-dissociating radiation from stars. For gas with hydrogen number density n_H and temperature T_V the fraction is (Tegmark et al. 1997):

$$\begin{aligned} f_{\mathrm{H}_2,c} &= 3.5 \times 10^{-4} T_3^{1.52} [1 + (7.4 \times 10^8 (1+z)^{2.13} \\ &\quad \times \exp\{-3173/(1+z)\}/n_{\mathrm{H1}})]^{-1}, \end{aligned} \tag{21}$$

where T_3 is the temperature T_V in units of 1000K and n_{H1} is the hydrogen density in units of cm^{-3}. Using this initial abundance we calculate the final H_2 abundance, still in the absence of a photodissociating background, as

$$f_{\mathrm{H}_2} = f_{\mathrm{H}_2,c} \exp\left(\frac{-T_\mathrm{V}}{51920K}\right) \tag{22}$$

where the exponential cut-off is included to account for collisional dissociation of H_2, as in Benson et al. (2006).

Finally, the cooling timescale due to molecular hydrogen can be computed using (Galli and Palla 1998):

$$\tau_{\mathrm{H}_2} = 6.56419 \times 10^{-33} T_\mathrm{V} f_{\mathrm{H}_2}^{-1} n_{\mathrm{H1}}^{-1} \Lambda_{\mathrm{H}_2}^{-1}, \tag{23}$$

where

$$\Lambda_{\mathrm{H}_2} = \frac{\Lambda_{\mathrm{LTE}}}{1 + n_{\mathrm{cr}}/n_\mathrm{H}}, \tag{24}$$

$$\frac{n_{\mathrm{cr}}}{n_\mathrm{H}} = \frac{\Lambda_{\mathrm{H}_2}(\mathrm{LTE})}{\Lambda_{\mathrm{H}_2}[n_\mathrm{H} \rightarrow 0]} \tag{25}$$

and

$$\begin{aligned} \log_{10} \Lambda_{\mathrm{H}_2}[n_\mathrm{H} \rightarrow 0] &= -103 + 97.59 \ln(T) \\ &\quad -48.05 \ln(T)^2 + 10.8 \ln(T)^3 \\ &\quad -0.9032 \ln(T)^4 \end{aligned} \tag{26}$$

is the cooling function in the low density limit (independent of hydrogen density) and we have used the fit given by Galli and Palla (1998), and

$$\Lambda_{\rm LTE} = \Lambda_r + \Lambda_v \tag{27}$$

is the cooling function in local thermodynamic equilibrium and

$$\begin{aligned}\Lambda_r &= \frac{1}{n_{\rm H_1}}\left\{\frac{9.5\times10^{-22}T_3^{3.76}}{1+0.12T_3^{2.1}}\exp\left(-\left[\frac{0.13}{T_3}\right]^3\right)\right. \\ &\left.+3\times10^{-24}\exp\left(-\frac{0.51}{T_3}\right)\right\}\ {\rm ergs\ cm^3\ s^{-1}} \end{aligned}\tag{28}$$

$$\begin{aligned}\Lambda_v &= \frac{1}{n_{\rm H_1}}\left\{6.7\times10^{-19}\exp\left(-\frac{5.86}{T_3}\right)\right. \\ &\left.+1.6\times10^{-18}\exp\left(-\frac{11.7}{T_3}\right)\right\}\ {\rm ergs\ cm^3\ s^{-1}} \end{aligned}\tag{29}$$

are the cooling functions for rotational and vibrational transitions in H_2 (Hollenbach and McKee 1979).

It is also possible to estimate the rate of molecular hydrogen formation on dust grains using the approach of Cazaux and Spaans (2004), who find that the rate of H_2 formation via this route can be important in the high redshift Universe. In this case we have to modify equation (13) of Tegmark et al. (1997), which gives the rate of change of the H_2 fraction, to account for the dust grain growth path. The molecular hydrogen fraction growth rate becomes:

$$\dot{f} = k_{\rm d} f(1-x-2f) + k_{\rm m} n(1-x-2f)x, \tag{30}$$

where f is the fraction of H_2 by number, x is the ionization fraction of H which has total number density n,

$$k_{\rm d} = 3.025\times10^{-17}\frac{\xi_{\rm d}}{0.01}S_{\rm H}(T)\sqrt{\frac{T_{\rm g}}{100{\rm K}}}{\rm cm^3 s^{-1}} \tag{31}$$

is the dust formation rate coefficient (Cazaux and Spaans 2004; eqn. 4), and $k_{\rm m}$ is the effective rate coefficient for H_2 formation (Tegmark et al. 1997; eqn. 14). Adopting the expression given by Cazaux and Spaans (2004; eqn. 3) for the H sticking coefficient, $S_{\rm H}(T)$ and $\xi_{\rm d} = 0.53Z$ for the dust-to-gas mass ratio as suggested by Cazaux and Spaans (2004), results in $\xi_{\rm d} \approx 0.01$ for Solar metallicity. This must be solved simultaneously with the recombination equation governing the ionized fraction x. The solution, assuming $x(t) = x_0/(1+x_0 n k_1 t)$ and $1-x-2f \approx 1$ as do Tegmark et al. (1997), is

$$f(t) = f_0\frac{k_{\rm m}}{k_1}\exp\left[\frac{\tau_{\rm r}+t}{\tau_{\rm d}}\right]\left\{{\rm E_i}\left(\frac{\tau_{\rm r}}{\tau_{\rm d}}\right) - {\rm E_i}\left(\frac{\tau_{\rm r}+t}{\tau_{\rm d}}\right)\right\} \tag{32}$$

where $\tau_{\rm r} = 1/x_0/n_{\rm H}/k_1$, $\tau_{\rm d} = 1/n_{\rm H}/k_{\rm d}$, k_1 is the hydrogen recombination coefficient and E_i is the exponential integral.

3.3. Heating

While gas must cool in order to collapse and form a galaxy, there are several physical processes which instead heat the gas. In this subsection we review the nature and effects of those mechanisms.

3.3.1. Photoheating

Immediately after the epoch of cosmological recombination, the cosmological background light consists of just the blackbody radiation of the CMB. Once stars (and perhaps AGN) begin to form they emit photons over a range of energies, including some at energies greater than the ionization edges of important coolants such as hydrogen, helium and heavier elements. Such photons can, in principle, photoionize atoms and ions in dark matter halos. This changes the ionization balance in the halo and heats the gas (via the excess energy of the photon above the ionization edge), thereby altering the rate at which this gas can cool to form a galaxy.

The ionizing background at some wavelength, λ, and redshift, z, is given by

$$F_\lambda = \int_z^\infty \mathcal{E}\left(\frac{\lambda}{1+z'}, z'\right)\frac{\exp[-\tau(z,z',\lambda)]}{(1+z')^4}\frac{{\rm d}t}{{\rm d}z'}{\rm d}z, \tag{33}$$

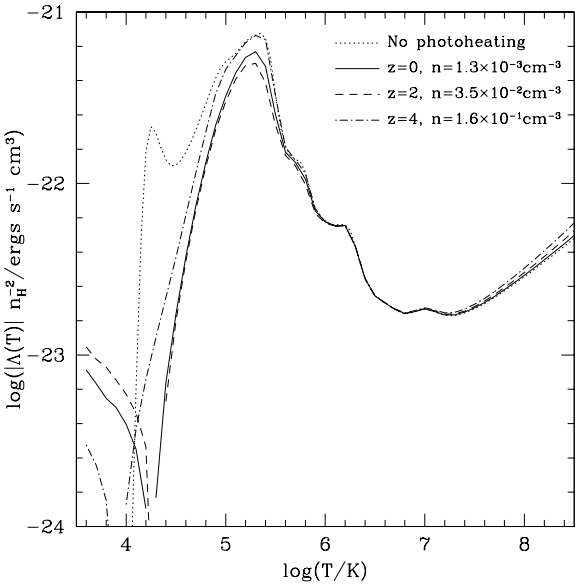

Figure 3: Cooling functions for gas at the mean density of cosmological halos at three different redshifts (as indicated in the figure). The dotted line shows the cooling function in the absence of any photoionizing background. Other lines show the net cooling/heating function in the presence of the photoionizing background self-consistently computed by Benson et al. (2002a). All calculations assume a metallicity of $0.3Z_\odot$. The discontinuity at low temperatures shows the transition from net heating to net cooling.

where $\mathcal{E}(\lambda, z)$ is the proper volume-averaged emissivity at redshift z and wavelength λ and $\tau(z_1, z_2, \lambda)$ is the optical depth between z_1 and z_2 for a photon with wavelength λ at z_1. Calculation of the background requires a knowledge of the emissivity history of the Universe and the optical depth (itself a function of the ionization state and density distribution in the IGM) as a function of redshift.

Detailed theoretical models of the ionizing background, using observational constraints on the emissivity history, together with models of the distribution of neutral gas and calculations of radiative transfer, have been developed by Haardt and Madau (1996; see also Madau and Haardt 2009) and allow the background to be computed for any redshift.

Once the background is known, its effects on gas in dark matter halos can be determined. Such calculations require the use of photoionization codes, such as CLOUDY (Ferland et al. 1998), to solve the complex set of coupled equations that describe the photoionization equilibrium and to determine the resulting net cooling or heating rates.

Figure 3 shows examples of net heating/cooling functions in the presence of a photoionizing background. These functions were calculated using the MAPPINGSIII code of Allen et al. (2008) with a photoionizing background computed self-consistently from the galaxy formation model of Benson et al. (2002a) and an assumed metallicity of $Z = 0.3Z_\odot$. Unlike collisional ionization equilibrium cooling functions, which are density independent[8], photoionization equilibrium cooling curves depend on the density of the gas. The curves shown are therefore computed for gas at densities typical of gas in dark matter halos at each redshift indicated. It can be seen that heating becomes important for temperatures $T \lesssim 3 \times 10^4$K.

3.3.2. Heating from Feedback

The overcooling problem has been a longstanding issue for galaxy formation theory. Simply put, in massive dark matter halos simple estimates suggest that gas can cool at a sufficiently large rate that, by the present day, galaxies much more massive than any observed will have formed (White and Rees 1978; White and Frenk 1991; Katz 1992; Benson et al. 2003). An obvious way to counteract this problem is to heat the cooling gas, thereby offsetting the

[8]Since the simple n^2 scaling is factored out of the cooling function by definition.

effects of cooling. Some sort of feedback loop is attractive here in order to couple the heating rate to the cooling rate and thereby balance the two.

In the massive halos where overcooling is a problem energy input from supernovae (see Section refsec:SNeFeedback) is insufficient to offset cooling[9]. Consequently, much interest has been recently given to the idea that heating caused by AGN may be responsible for solving the overcooling problem. The amount of energy available from AGN is up to a factor 20–50 higher than from supernovae (Benson et al. 2003). Semi-analytic models have demonstrated that such a scenario can work (see §6.3.2) — producing a significant reduction in the mass of gas able to cool in massive halos while simultaneously producing black holes with properties consistent with those observed — under the assumption that energy output from AGN can efficiently couple to the cooling atmosphere in the surrounding dark matter halo (Croton et al. 2006; Bower et al. 2006; Somerville et al. 2008b).

The mechanism by which energy output from the AGN is coupled to the surrounding atmosphere remains unclear. Several solutions have been proposed, from effervescent heating (in which AGN jets inflate bubbles which heat the intracluster medium (ICM) via $P\mathrm{d}V$ work; Roychowdhury et al. 2004; Vecchia et al. 2004; Ruszkowski et al. 2008, but see Vernaleo and Reynolds 2006) to heating by outflows driven by super-Eddington accretion (King 2009) and viscous dissipation of sound waves (Ruszkowski et al. 2004) with turbulence playing an important role (Brüggen and Scannapieco 2009).

3.3.3. Preheating

Heating that occurs prior to the collapse into a dark matter halo can also significantly affect the later evolution of baryons. Prior to virial collapse and any associated shock heating the gas evolves approximately adiabatically, maintaining a constant entropy. In cosmological studies the entropy is usually written as

$$K = k_\mathrm{B} T / \mu m_\mathrm{H} \rho_\mathrm{B}^{\gamma-1}, \tag{34}$$

where γ is a adiabatic index of the gas. An early period of heating (perhaps from the first generation of galaxies) can increase the entropy of the gas by raising its temperature. Since entropy is conserved this preheating will be "remembered" by the gas. We can consider what happens to such gas when it accretes into a halo, assuming for now that a shock forms close to the virial radius. A shock randomizes the ordered infall motion of the gas and therefore increases its entropy. At early times, when the shock is relatively weak, this entropy gain will be small compared to the preheated entropy of the gas. At late times, the shock entropy will dominate. The result is that the entropy distribution of preheated gas in a halo looks similar to that of non-preheated gas, except that there is a floor of minimum entropy.

The equation of hydrostatic equilibrium can be re-written in terms of entropy using the fact that $\rho = (P/K)^{1/\gamma}$ giving

$$\frac{\mathrm{d}P}{\mathrm{d}r} = -\frac{\mathrm{G}M(<r)}{r^2}\left(\frac{P}{K}\right)^{1/\gamma}, \tag{35}$$

and shows that the gas will arrange itself in the halo with the lowest entropy material in the center. The presence of an entropy floor leads to a density core in the halo center. This increases cooling times in the halo core and may therefore help prevent the formation of supermassive galaxies via the overcooling problem (see §3.3.2; Borgani et al. 2001; Voit et al. 2003; Younger and Bryan 2007). Additionally, X-ray observations of galaxy clusters seem to suggest the presence of entropy floors.

While preheating is an attractive way of explaining entropy floors in clusters and reducing the overcooling problem it is not clear whether it can consistently explain the abundance of galaxies in lower mass halos. If preheating occurred uniformly, it would drastically reduce the number of lower mass galaxies forming (Benson and Madau 2003). Preheating would need to occur preferentially in the sites of proto-clusters to avoid this problem—not inconceivable but not demonstrated either.

[9]The total binding energy of gas in a dark matter halo scales as $M^{5/3}$ while the energy available from supernovae, assuming 100% efficient conversion of gas into stars, scales as M. Consequently, in sufficiently massive halos, there will always be insufficient energy from supernovae to heat the entire halo.

3.3.4. Thermal Conduction

Shock heated gas in dark matter halos is an ionized plasma and is therefore expected to have a thermal conductivity given by (Spitzer 1962):

$$\kappa_{\rm S} = 32\left(\frac{2}{\pi}\right)^{1/2}\frac{n_{\rm e}}{\nu_0 m^{5/2}}T^{5/2}, \tag{36}$$

where $n_{\rm e}$ is the electron density and

$$\nu_0 = \frac{2\pi n_{\rm e} Z e^4 \ln\Lambda}{m^2}, \tag{37}$$

where Z is the atomic number of the ions. If cooling in the inner regions of the hot gas halo leads to a temperature gradient in the atmosphere then conduction will cause energy to be deposited at radius r at a rate per unit volume Σ given by:

$$\Sigma = 4\pi\frac{\rm d}{{\rm d}r}\left(\kappa_{\rm S} r^2 \frac{{\rm d}T}{{\rm d}r}\right), \tag{38}$$

where T is the temperature in the atmosphere. Thus, thermal conduction can, in principle, act as a heat source for the inner regions of the hot atmosphere—as they cool, heat is conducted inwards from the outer, hotter regions of the atmosphere. The actual conductivity may be substantially reduced below the Spitzer value if the hot atmosphere is threaded by tangled magnetic fields (such that electrons cannot directly transport heat but must effectively diffuse along field lines).

While thermal conduction is an attractive mechanism by which to solve the overcooling problem (since the conductivity is higher in more massive clusters due to the strong temperature dependence of $\kappa_{\rm S}$) it has been demonstrated that it cannot sufficiently offset cooling rates even with conductivities close to the Spizter value (Benson et al. 2003; Dolag et al. 2004; Pope et al. 2005), nor can it maintain a stable hot gas atmosphere over cosmological timescales (Conroy and Ostriker, 2008; Parrish et al., 2009).

3.4. Fate of Cooling Gas

In the simplest picture, gas which cools sufficiently below the virial temperature loses pressure support and flows smoothly towards the minimum of the gravitational potential well, settling there to form a galaxy. Such a picture is likely oversimplified, however.

Maller and Bullock (2004) consider the consequences of the thermal instability in cooling atmospheres. They find that cooling gas fragments into two phases: cold ($T \approx 10^4$), dense clouds in pressure equilibrium with a hot (approximately virial temperature), diffuse component which can persist for cosmological periods of time due to a long cooling time. The masses of the clouds are determined from the thermal conduction limit, known as the Field length[10] (Field 1965), and processes such as Kelvin-Helmholtz instabilities and conductive evaporation which act to destroy clouds. This significantly alters the manner in which fueling of galaxies occurs. The rate of gas supply to a forming galaxy now depends on the rate at which the dense gas clouds can infall, due to processes such a hydrodynamical drag and cloud-cloud collisions. The timescales for these two processes are given by

$$\tau_{\rm ram} = \frac{2m_{\rm cl}}{\pi C_{\rm d} r_{\rm cl}^2 \bar{\rho}_h v_{\rm cl}} \approx 2.6{\rm Gyr} \tag{39}$$

and

$$\tau_{\rm cc} = \frac{4m_{\rm cl}R_{\rm c}^3}{3M_{\rm cl}v_{\rm cl}r_{\rm cl}^2} \approx 2.4{\rm Gyr} \tag{40}$$

respectively, where $m_{\rm cl}$, $r_{\rm cl}$ and $v_{\rm cl}$ are the characteristic mass, radius and velocity of cold clouds respectively, $M_{\rm cl}$ is the total mass in clouds, $C_{\rm d}$ is a drag coefficient, $\bar{\rho}_{\rm h}$ is the mean density of hot gas in the halo and $R_{\rm c}$ is the radius within which gas is sufficiently dense that it has been able to radiate away all of its thermal energy (i.e. the "cooling radius"; Maller and Bullock 2004). The numerical values given in each equation are computed for typical cloud properties taken from Maller and Bullock (2004).

[10] Above this length scale thermal conduction can damp temperature perturbations in the intracluster medium and prevent cloud formation.

These timescales can significantly exceed the cooling time for gas in galactic scale dark matter halos. Consequently, Maller and Bullock (2004) find that considering the formation and infall of such clouds can significantly reduce the rate of gas supply to a forming galaxy (by factors of two or so), particularly in more massive halos. This picture has recently been confirmed in numerical experiments by Kaufmann et al. (2009).

4. Galaxy Interactions

The original concept of galaxies as "island universes" is, of course, the truth, but not the whole truth. While many galaxies do seem to be evolving in isolation there are clear indications that some galaxies are interacting strongly with other galaxies or their larger scale environment. We describe these interactions in the remainder of this section.

4.1. Galaxy Orbits

A consequence of the hierarchical nature of structure formation in a cold dark matter universe is that dark matter halos are built through the merging together of earlier generations of less massive halos. While for a long time numerical simulations indicated that all trace of earlier generations of halos was erased during the merging process (Katz and White 1993; Summers et al. 1995) it was understood on analytical grounds that this was likely a numerical artifact rather than a physical result (Moore et al. 1996a). Beginning in the late 1990's, N-body simulations clearly demonstrated that this was indeed the case (Tormen et al. 1998; Moore et al. 1999; Klypin et al. 1999). Unlike earlier generations of simulations, they found that halos can persist as *subhalos* within larger halos into which they merge. The current highest resolution simulations of individual halos (Kuhlen et al. 2008; Springel et al. 2008) show almost 300,000 subhalos[11] and even show multiple levels of subclustering (i.e. subhalos within subhalos within subhalos...). Each subhalo may, in principle, have acted as a site of galaxy formation and so may contain a galaxy which becomes a satellite in the host potential.

These subhalos are gravitationally bound to their host halo and, as such, will orbit within it. A subhalo's orbit can take it into regions where interactions affect the properties of any galaxy that it may contain. We begin, therefore, by considering the orbits of subhalos.

At the point of merging, which we will define as the time at which the center of mass of a subhalo-to-be first crosses the virial radius of its future host halo, we expect the orbital parameters (velocities, energy etc.) to be of order unity when expressed in units of the characteristic scales of the host halo. For example, Benson (2005) shows that the radial and tangential velocities of merging subhalos are distributed close to unity when expressed in units of the virial velocity of the host halo (Fig. 4). This distribution of velocities reflects the influence of the host halo (infall in its potential well) but also of the surrounding large scale structure which may have torqued the infalling subhalo.

Such orbits will typically carry subhalos into the inner regions of halos. Figure 5 shows the distribution of orbital pericenters assuming an NFW halo with concentration 10 and the orbital parameter distribution of Benson (2005). Most orbits initially reach to 40% of the virial radius, but a significant tail have orbits which carry them into the inner 10% of the halo.

4.2. Gravitational Interactions

4.2.1. Mergers

Orbiting subhalos are gravitationally bound to their host halos and, as such, rarely encounter other subhalos at velocities resulting in a bound interaction (Angulo et al. 2008; Somerville et al. 2008b; Wetzel et al. 2008).

To cause gravitationally bound interactions between subhalos and their galaxies typically requires a dissipative process to reduce their orbital energies. Dynamical friction fulfills this role and tends to drag subhalos down towards the center of their host halo, where they may merge with any other galaxy which finds itself there. The classic derivation of dynamical friction acceleration from Chandrasekhar (1943) has been used extensively to estimate dynamical

[11] This is a lower limit due to the limited resolution of the simulations. The earliest generations of cold dark matter halos may have masses as low as $10^{-12} M_\odot$ (depending on the particle nature of the dark matter) while state of the art simulations resolve only halos with masses greater than around $10^5 M_\odot$. The ability of even lower mass halos to survive is a subject of much debate (Berezinsky et al. 2006; Zhao et al. 2007; Goerdt et al. 2007; Angus and Zhao 2007; Elahi et al. 2009).

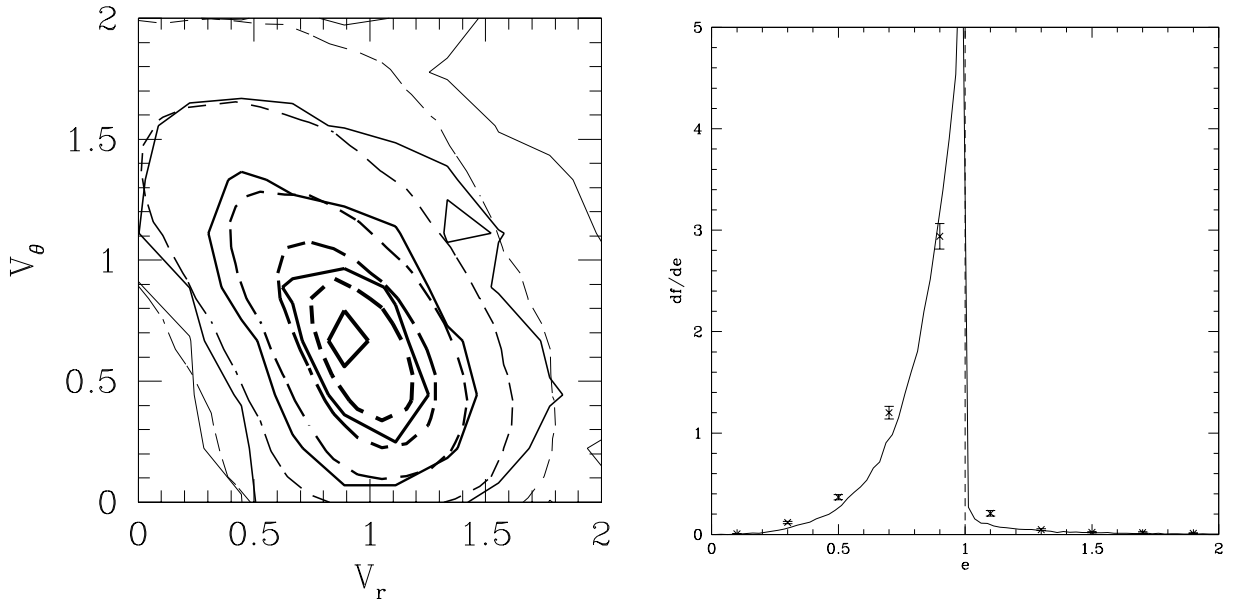

Figure 4: *Left-hand panel:* The joint distribution of radial and tangential velocities of infalling subhalos as they cross the virial radius of their host halo. Velocities are expressed in units of the virial velocity of the host halo. Solid contours indicate measurements from a compilation of N-body simulations while dashed lines indicate the fitting formula of Benson (2005). Contours are drawn at values of $\mathrm{d}^2 f/\mathrm{d}V_\theta \mathrm{d}V_r$ (the normalized distribution function) of 0.01, 0.1, 0.5, 1.0 and 1.4. *Right-hand panel:* The corresponding distribution of orbital eccentricities. The distribution peaks close to $e = 1$ (parabolic orbits) and it is apparent that some subhalos are on unbound ($e > 1$) orbits. Points indicate the distribution measured from a compilation of N-body simulations, while the solid line indicates the distribution found from the same fitting formula as used in the left-hand panel. Reproduced, with permission, from Benson (2005).

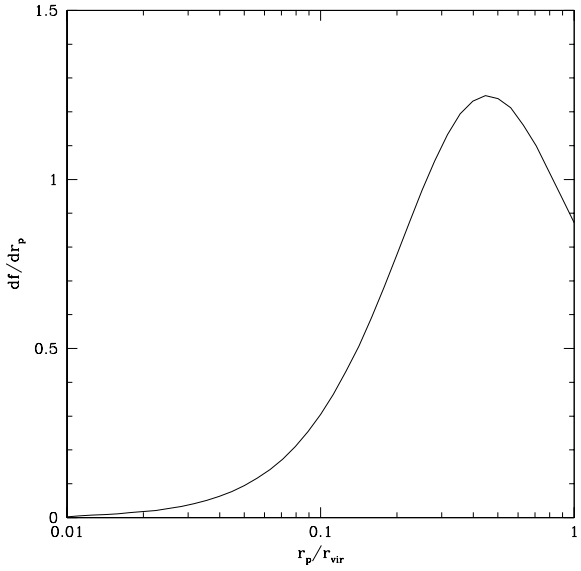

Figure 5: The distribution of orbital pericenters (in units of the virial radius) in an NFW halo having concentration parameter of 10, assuming the orbital parameter distribution of Benson (2005).

friction timescales within dark matter halos. For example, Lacey and Cole (1993) applied this formula to estimate merging timescales for subhalos in isothermal dark matter halos, finding:

$$T_{\rm df} = \frac{f(\epsilon)\tau_{\rm dyn}}{2B(1)\ln\Lambda}\left(\frac{r_c}{R_{\rm v}}\right)^2\left(\frac{M_{\rm v}}{m_{\rm v}}\right) \tag{41}$$

where $\tau_{\rm dyn} = R_{\rm v}/V_{\rm v}$ is the dynamical time of the halo, $m_{\rm v}$ the virial mass of the orbiting satellite,

$$B(x) = {\rm erf}(x) - \frac{2x}{\sqrt{\pi}}\exp(-x^2), \tag{42}$$

$\ln\Lambda \approx \ln(r_{\rm v}V_{\rm v}^2/{\rm G}m_{\rm v}) \equiv \ln(M_{\rm v}/m_{\rm v})$ is the Coulomb logarithm (treating the satellite as a point mass), $f(\epsilon)$ encapsulates the dependence on the orbital parameters through the quantity $\epsilon = J/J_{\rm c}(E)$ where J is the angular momentum of the satellite and $J_{\rm c}(E)$ is the angular momentum of a circular orbit with the same energy, E, as the actual orbit and $r_{\rm c}$ is the radius of that circular orbit. Lacey and Cole (1993) found that $f(\epsilon) = \epsilon^{0.78}$ was a good fit to numerical integrations of orbits experiencing dynamical friction.

Besides the fact the dark matter halos are not isothermal, there are a number of other reasons why this simple approach is inaccurate:

1. Chandrasekhar's derivation assumes an infinite, uniform medium, not a dark matter halo with a radially varying density profile;
2. There is the usual uncertainty in how to define the Coulomb logarithm (e.g. what is the maximum impact parameter for interactions between the satellite and dark matter particles);
3. Subhalos will experience mass loss as they orbit, changing the timescale;
4. The host halo itself is constantly evolving;
5. The host halo is non-spherical and has a non-isotropic velocity dispersion.

While some of these limitations can be overcome (e.g. mass loss can be modeled; (Benson et al., 2002a; Taylor and Babul, 2004); the Coulomb logarithm can be treated as a parameter to be fit to numerical results; results exists for dynamical friction in anisotropic velocity distributions; (Binney, 1977b; Benson et al., 2004)) others are more problematic. Recently, attempts have been made to find empirical formulae which describe the merging timescale. These usually begin with an expression similar to the one in eqn. (41) but add empirical dependencies on subhalo mass and orbital parameters which are constrained to match results from N-body simulations. Results from such studies (Jiang et al. 2008; Boylan-Kolchin et al. 2008) show that the simple formula in eqn. (41) tends to underestimate the timescale for low mass satellites (probably because it ignores mass loss from such systems) and overestimates the timescale for massive satellites (probably due to a failure of several of the assumptions made in this limit). Alternative fitting formulae have been derived from these studies. For example, Boylan-Kolchin et al. (2008) find

$$T_{\rm df} = \tau_{\rm dyn}A\frac{(M_{\rm V}/m_{\rm V})^b}{\ln(1+M_{\rm V}/m_{\rm V})}\exp\left[c\epsilon\right]\left[\frac{r_{\rm c}(E)}{r_{\rm V}}\right]^d, \tag{43}$$

with $A = 0.216$, $b = 1.3$, $c = 1.9$ and $d = 1.0$ while Jiang et al. (2008) finds

$$T_{\rm df} = \tau_{\rm dyn}\frac{0.94\epsilon^{0.60}+0.60}{2C}\frac{M_{\rm V}}{m_{\rm V}}\frac{1}{\ln(1+M_{\rm V}/m_{\rm V})}, \tag{44}$$

with $C = 0.43$. A comparison of the Boylan-Kolchin et al. (2008) fit, eqn. (41) and measurements from numerical simulations is shown in Fig. 6.

The consequences of merging for the galaxies involved are discussed in §5.2.1.

4.2.2. Tidal Destruction

An orbiting subhalo and its galaxy will experience tidal forces which may strip away the outer regions or, in extreme cases, entirely disrupt the galaxy resulting in a stellar stream (as seems to be happening with the Sagittarius dwarf galaxy in orbit around the Milky Way; Belokurov et al. 2006).

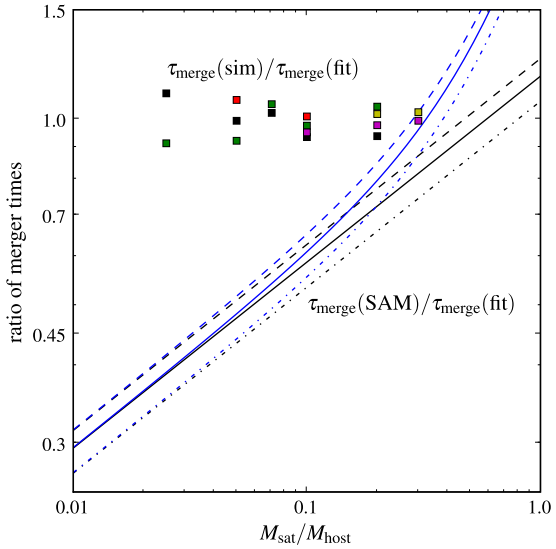

Figure 6: A comparison of dynamical friction timescales measured from N-body simulations, $\tau_{\rm merge}({\rm sim})$, with the fitting formula of Boylan-Kolchin et al. (2008), $\tau_{\rm merge}({\rm fit})$, is shown by the colored points, with colors coding for orbital circularity: $\epsilon = 0.33$ (red), 0.46 (green), 0.65 (black), 0.78 (magenta) and 1.0 (yellow). Lines compare $\tau_{\rm merge}({\rm fit})$ with the expectation from eqn. (41), labeled $\tau_{\rm merge}({\rm SAM})$. The different color curves correspond to different choices of Coulomb logarithms in eqn. (41): $\ln(1 + M_{\rm V}/m_{\rm V})$ (black curves) and $\frac{1}{2}\ln(1 + M_{\rm V}^2/m_{\rm V}^2)$ (blue curves). Reproduced, with permission, from Boylan-Kolchin et al. (2008).

In a rotating frame in which an orbiting satellite instantaneously has zero tangential velocity, the effective tidal field felt by the satellite is

$$\mathcal{D} = -\frac{\rm d}{{\rm d}r}\left(\frac{{\rm G}M_{\rm h}(r)}{r^2}\right) + \omega^2 r, \tag{45}$$

where $M_{\rm h}(r)$ is the mass enclosed within radius r in the host halo and ω is the instantaneous angular velocity of the satellite. An estimate of the radius, $r_{\rm t}$, in the satellite subhalo/galaxy system beyond which tidal forces become important can be made by equating the tidal force to the self-gravity of the subhalo

$$\mathcal{D}r_{\rm t} = \frac{{\rm G}M_{\rm s}(r_{\rm t})}{r_{\rm t}^2}. \tag{46}$$

Beyond this *tidal radius* material becomes unbound from the satellite, forming a stream of dark matter and, potentially, stars which continue to orbit in the host potential.

This simple estimate ignores the fact that particles currently residing in the inner regions of a subhalo may have orbits which carry them out to larger radii where they may be more easily stripped. As such, the degree of tidal mass loss should depend not only on the density profile of the satellite but also on the velocity distribution of the constituent particles. Attempts to account for this find that particles in an orbiting satellite that are on prograde orbits are more easily stripped than those on radial orbits which are in turn more easily stripped than those on retrograde orbits (Read et al. 2006). Additionally, some material will be stripped from within the classical tidal radius, as particles which contribute to the density inside that radius may be on orbits which carry them beyond it. This can lead to more extensive and continuous mass loss as the reduction in the inner potential of the satellite due to this mass loss makes it more susceptible to further tidal stripping. (Kampakoglou and Benson 2007).

4.2.3. Harassment

A less extreme form of tidal interaction arises when tidal forces are not strong enough to actually strip material from a galaxy. The tidal forces can, nevertheless, transfer energy from the orbit to internal motions of stars in

the galaxy, effectively heating the galaxy. The generic results of such heating are to cause the galaxy to expand and to destroy cold, ordered structures such as disks (Moore et al. 1996b, 1998; Mayer et al. 2001a,b; Gnedin 2003; Mastropietro et al. 2005a,b). The harassment process works via *tidal shocking* in which the stars in a galaxy experience a rapidly changing tidal field along its orbit and gain energy in the form of random motions, leading to the system expanding and becoming dynamically hotter. During such tidal shocks, the energy per unit mass of the galaxy changes by (Gnedin 2003)

$$\langle \Delta E \rangle = \frac{1}{6} I_{\rm tid} \langle r^2 \rangle, \tag{47}$$

where $\langle r^2 \rangle$ is the mean squared radius of the galaxy and

$$I_{\rm tid} = \sum_n \sum_{\alpha,\beta} \left(\int F_{\alpha\beta} {\rm d}t \right)_n^2 \left(1 + \frac{\tau_n^2}{t_{\rm dyn}^2} \right)^{-3/2}, \tag{48}$$

where the sums extend over all n peaks in the density field (i.e. the host halo and any other subhalos that it may contain) and over all components of the tidal tensor

$$F_{\alpha\beta} = -\frac{{\rm d}^2\Phi}{{\rm d}r_\alpha {\rm d}r_\beta}, \tag{49}$$

where Φ is the gravitational potential. Here, τ_n is the effective duration of the encounter with peak n and $t_{\rm dyn}$ is the dynamical time at the half-mass radius of the galaxy. The $(1 + \tau_n^2/t_{\rm dyn}^2)^{-3/2}$ term describes the transition from the impulsive to adiabatic shock regimes (Gnedin and Ostriker 1999; see also Murali and Weinberg 1997a,b,c).

4.3. Hydrodynamical Interactions

While the collisionless dark matter is affected only by gravity the baryonic content of galaxies (and their surrounding atmospheres of gas) can be strongly affected by hydrodyamical forces.

4.3.1. Ram pressure

The orbital motion of a subhalo through the hot atmosphere of a host halo leads to a large ram pressure. The characteristic magnitude of that pressure

$$P_{\rm ram} = \rho_{\rm host} V_{\rm orbit}^2 \tag{50}$$

can greatly exceed the binding energy per unit volume of both hot gas in subhalos and interstellar medium (ISM) gas in their galaxies. As such, ram pressure forces may be expected to quite efficiently remove the hot atmospheres of satellite galaxies, a process with several grim aliases including *strangulation* and *starvation*, and the ISM of the galaxy.

The first quantification of this process was made by Gunn and Gott (1972) who showed that the ram pressure force could remove material from a galactic disk if it exceeded the gravitational restoring force per unit area which itself cannot exceed

$$\mathcal{F} = 2\pi {\rm G} \Sigma_\star \Sigma_{\rm gas}. \tag{51}$$

For a disk of mass $M_{\rm d}$ with gas mass $M_{\rm g}$ having an exponential surface density profile for both gas and stars with scale length $r_{\rm d}$, the gravitational restoring force per unit area is given by (Abadi et al. 1999):

$$\mathcal{F} = \frac{{\rm G} M_{\rm d} M_{\rm g}}{4\pi r_{\rm d}^4} x {\rm e}^{-x} \left[I_0\left(\frac{x}{2}\right) K_1\left(\frac{x}{2}\right) - I_1\left(\frac{x}{2}\right) K_0\left(\frac{x}{2}\right) \right], \tag{52}$$

where $x = r/r_{\rm d}$ and I_0, I_1, K_0 and K_1 are Bessel functions.

The mass loss caused by this ram pressure can, in many cases, be further enhanced by related effects, such as turbulent viscous stripping (Nulsen 1982). This initial estimate has been revised and calibrated more accurately using numerical simulations (Abadi et al. 1999; McCarthy et al. 2008). The process of ram pressure stripping has been incorporated into some semi-analytic models of galaxy formation (Lanzoni et al. 2005; Font et al. 2008) where it plays an important role in mediating the transition of cluster galaxies from the blue cloud of star-forming galaxies to the red sequence of passively evolving galaxies (Font et al. 2008).

5. Galactic Structure

The preceding sections describe the path by which gas achieves sufficiently high density to allow a galaxy to form. The next significant question is what structure that galaxy will have. In the following section we will review the process of disk and spheroid formation and make quantitative estimates of the sizes of these structures.

5.1. Disk Formation

Disks are a common astrophysical phenomenon and galactic disks owe their origins to the same fundamental process as other astrophysical disks: conservation of angular momentum in a system collapsing under gravity eventually leading to arrest of the collapse by rotational support. Understanding the physical properties of galactic disks therefore requires knowledge of their angular momentum content and the gravitational potential in which they form.

The angular momentum of the gas which will eventually form a galactic disk arises in the same way as that of dark matter halos, namely from tidal torques from surrounding large scale structure Hoyle (1949)[12]. The magnitude of the angular momentum content of the baryonic component of a halo is close to being a scaled version of that of the dark matter—for example, van den Bosch et al. (2002) find that the distributions of spin parameters and angular momentum distributions within individual halos for dark matter and non-radiative gas are very similar. They find that there is, however, a significant (typically 30°) misalignment between the dark matter and gas angular momenta vectors[13]. Numerical hydrodynamical studies show that the angular momenta vectors of galactic disks *are* well aligned with the angular momenta of the inner regions of dark matter halos (Bett et al., 2009; Hahn et al., 2010).

The distribution of the angular momentum is less well studied but recent investigations (Sharma and Steinmetz 2005) using non-radiative hydrodynamical simulations have shown that the differential distribution of specific angular momenta, j, is given by

$$\frac{1}{M}\frac{\mathrm{d}M}{\mathrm{d}j} = \frac{1}{j_\mathrm{d}^\alpha \Gamma(\alpha)} j^{\alpha-1} \mathrm{e}^{-j/j_\mathrm{d}}, \tag{53}$$

where Γ is the gamma function, M is the total mass of gas, $j_\mathrm{d} = j_\mathrm{tot}/\alpha$ and j_tot is the mean specific angular momentum of the gas. Sharma and Steinmetz (2005) find that the simulated halos have a median value of $\alpha = 0.89$. The fraction of mass with specific angular momentum less than j is then given by

$$f(<j) = \gamma\left(\alpha, \frac{j}{j_\mathrm{d}}\right), \tag{54}$$

where γ is the incomplete gamma function.

We have assumed so far that the angular momentum of the pre-galactic gas is conserved during collapse. This may not be precisely true and indeed did not seem to be in earlier generations of hydrodynamical simulations which typically found that disk galaxies lost significant fractions of their angular momentum and, as a result, were too small (Navarro and Benz 1991; Navarro and White 1994; Navarro et al. 1995). However, more recent simulations (Thacker and Couchman 2001; Steinmetz and Navarro 2002) do show approximate conservation of angular momentum (most likely due to the inclusion of effective feedback in these later generations of simulations) and, furthermore, conservation of angular momentum leads to disks with sizes comparable to those observed—certainly the gas cannot lose a significant fraction of its angular momentum if it is to form a disk of comparable size to observed galactic disks. Confirmation of these ideas has recently been made by Zavala et al. (2008) who convincingly show in N-body+hydrodynamical simulations that the particular feedback prescription used can lead to the formation of a disk dominated or spheroid dominated galaxy in the same dark matter halo, with stronger feedback leading to a disk galaxy. The angular momentum of the mass in the disk galaxy tracks that of the dark matter halo as a whole, growing as expected during the linear regime and remaining nearly constant after halo collapse. With weaker feedback a spheroid forms instead. Its angular momentum also grows during the linear regime but then declines rapidly (as does that of the inner regions of the dark matter halo) due to angular momentum transfer from dense, progenitor blobs

[12] An alternative view of this process, although fundamentally based upon the same physics, involves considering the angular momentum supplied to a halo by accreting satellites and has been developed by Vitvitska et al. (2002), Maller et al. (2002) and Benson and Bower (2010).

[13] These authors note that a significant fraction (5–50%) of the gas in a halo can have a negative angular momentum relative to the total angular momentum of the halo, and suggest that this could lead to the formation of low angular momentum spheroids.

to the surrounding, diffuse dark matter. Feedback processes are clearly of crucial importance here—for example, Wise and Abel (2008b) show that feedback during the formation of protogalaxies at early times can effectively boost the angular momentum content of such systems by factors of three to five. This is achieved via forces associated with HII region and SNe blast waves which produce torques much stronger than the usual cosmological torques.

5.1.1. Sizes

The physics which determines the sizes of galaxy disks was originally described by Fall and Efstathiou (1980) and later expanded upon by many authors (see, in particular, Mo et al. 1998; Mao et al. 1998).

Once the angular momentum distribution of that part of the baryonic component of the halo which cools to form the galaxy is known, finding the structure of the resulting rotationally supported disk is reduced to solving the following equation

$$\frac{j^2(M)}{R^3(M)} = \frac{\partial}{\partial R}\Phi(R), \tag{55}$$

where $j(M)$ is the specific angular momentum enclosing mass M and this equation is solved for $R(M)$. The potential is a sum of the self-gravity of the disk and that of any external potential (dark matter halo and bulge for example) which may have responded adiabatically to the formation of the disk. For a thin disk, the potential is generically given by (Binney and Tremaine 2008)

$$\Phi(R,0) = -4\mathrm{G}\int_0^R \frac{\mathrm{d}a}{\sqrt{R^2-a^2}}\int_a^\infty \mathrm{d}R'\,\frac{R'\Sigma(R')}{\sqrt{R'^2-a^2}}, \tag{56}$$

which, for an exponential surface density profile[14]

$$\Sigma(R) = \Sigma_0 \exp\left(-\frac{R}{R_\mathrm{d}}\right), \tag{57}$$

simplifies to

$$\Phi(R,0) = \pi\mathrm{G}\Sigma_0 R[I_0(y)K_1(y) - I_1(y)K_0(y)], \tag{58}$$

where $y = R/2R_\mathrm{d}$ and I_0, I_1, K_0 and K_1 are Bessel functions. Knowing the functional form of $j(M)$ it is possible to solve for $R(M)$ and therefore the density profile of the disk. Often, for simplicity, a particular form for the density (e.g. exponential) is assumed which leaves a single free parameter (the scale length) to be solved for.

A significant complication to this picture arises from the fact that the external potential in which the disk forms is likely to change in response to the formation of the disk. If the disk forms slowly, such that the timescale for changes in the potential greatly exceeds the dynamical time of the dark matter halo, then we can use adiabatically invariant quantities (Binney and Tremaine 2008) to estimate the response of the halo to the forming disk. The original formulation of this argument for galaxies was given by Blumenthal et al. (1986) and has been used extensively ever since. In this simplified picture, the dark matter particles are considered to be on circular orbits in a spherical potential. In this case, the only adiabatic invariant whose corresponding angle variable has a non-infinite period is the magnitude of the angular momentum, L_ϕ. Prior to the formation of any galaxy, this angular momentum is given by

$$L_\phi^2 = (1-f_\mathrm{b})^{-1}\mathrm{G}M_\mathrm{DM}(r_0)r_0, \tag{59}$$

where $M_\mathrm{DM}(r)$ is the mass of dark matter within radius r, r_0 is the initial radius of the circular orbit and we have assumed that baryons are present in the halo at the universal fraction, $f_\mathrm{b}(\equiv \Omega_\mathrm{b}/[\Omega_\mathrm{b}+\Omega_\mathrm{CDM}])$ and distributed as the dark matter. If L_ϕ is conserved during the formation of a galaxy, then, at any point after galaxy formation has begun we have

$$L_\phi^2 = (1-f_\mathrm{b}')^{-1}\mathrm{G}[M'_\mathrm{DM}(r_\mathrm{f}) + M_\mathrm{gal}(r_\mathrm{f})]r_\mathrm{f}, \tag{60}$$

[14]These equations assume a razor thin disk. For a thickened disk a density distribution $\rho(R,z) = \rho_0\exp(-R/R_\mathrm{d})\mathrm{sech}^2(2/2z_0)$, with z_0 being the scale height of the disk, is often assumed as it is the self-consistent distribution for an isothermal population of stars (Spitzer 1942). The resulting gravitational potential can be found (e.g. Kuijken and Gilmore 1989) although the calculation is significantly more involved.

where $M'(r)$ is the mass of dark matter enclosed within radius r after responding to the forming galaxy, $M_{\rm gal}(r)$ is the mass of the galaxy within that same radius[15], $f'_{\rm b}$ is the baryon fraction remaining uncondensed into the galactic phase and $r_{\rm f}$ is the radius of the new circular orbit for this dark matter particle. If we assume no shell crossing, then $M'_{\rm DM}(r_{\rm f}) = M_{\rm DM}(r_0)$. Given a knowledge of the mass and density distribution of the galaxy this allows us to solve for $r_{\rm f}$ as a function of the initial radius r_0.

This approach makes several simplifying assumptions, including adiabatic growth, a spherical halo and circular orbits for dark matter particles. Many of these assumptions have yet to be adequately tested. However, recent work has attempted to address the last of these. With a more realistic distribution function for the dark matter, the particles will occupy a range of orbital eccentricities. In a spherical potential, the angular momentum is joined by a second adiabatic invariant, the radial action:

$$L_r = \frac{1}{\pi}\int_{r_{\rm min}}^{r_{\rm max}} v_r(r){\rm d}r, \tag{61}$$

where the integral is taken along the orbit of a particle from its pericenter to apocenter. The effects of taking into account this second invariant and a physically reasonable orbital distribution have been explored by Gnedin et al. (2004). Gnedin et al. (2004) find that the simple model described above systematically overpredicts the degree of contraction of the halo. However, they find that a simple modification in which the combination $M(r)r$ in the above is replaced with $M(\overline{r})r$, where $\overline{r}$ is the orbit-averaged radius, approximately accounts for the orbital eccentricities and gives good agreement with numerical simulations. Gnedin et al. (2004) further find that the orbit-averaged radius in cosmological halos can be well fit by the relation $\overline{r}/r_{\rm vir} = A(r/r_{\rm vir})^w$ with $A = 0.85 \pm 0.05$ and $w = 0.8 \pm 0.02$. More recent simulations (Gustafsson et al. 2006) support this picture, but show that the optimal values of A and w vary from galaxy to galaxy and seem to depend on the formation history (i.e. on the adopted rules for star formation and feedback; see also Abadi et al. 2009). This suggests that the process of halo response to galaxy growth is more complicated than is captured by these simple models, perhaps because the assumed invariants are not precisely invariant in non-spherical potentials or perhaps because galaxy growth is not sufficiently slow to be truly adiabatic.

Galaxy disks are, of course, not razor thin. The origins of the vertical extent of galaxy disks remain a topic of active research but various possibilities are currently considered seriously:

1. External origins (accretion):
   (a) The hierarchical nature of galaxy formation implies that a galactic disk can expect to accrete pre-existing, smaller stellar systems frequently during its life. The stars from these smaller galaxies are often found in numerical simulations to form a thickened disk structure, in the same plane as the pre-existing disk of the galaxy (Abadi et al. 2003; Villalobos and Helmi 2008). This is to be expected as dynamical friction will tend to drag orbiting satellites into the plane of the disk where tidal forces will proceed to shred the satellite, leaving its stars orbiting in the plane of the disk.
   (b) Early, chaotic gas accretion: In a slightly different scenario, Brook et al. (2004) find, in numerical simulations of a forming galaxy, that many of the thick disk stars form from accreted gaseous systems during an early, chaotic period of merging.
2. Internal origins (dynamical heating):
   (a) Dark matter substructure: Building upon earlier works (Toth and Ostriker 1992; Quinn et al. 1993; Sellwood et al. 1998; Velazquez and White 1999), in recent years there have been numerous studies focused on the question of whether relatively thin galactic disks can survive in the rather violent environment of a hierarchically formed dark matter halo (Font et al. 2001; Benson et al. 2004; Kazantzidis et al. 2008; Read et al. 2008; Kazantzidis et al. 2009; Purcell et al. 2009). A careful treatment of dark matter substructure orbital evolution and the build-up of the substructure population over time is required to address this problem. The consensus conclusion from these studies is that galactic disks can survive in the currently accepted cold dark matter cosmogony, but that interactions with orbiting dark matter substructure must be a significant contribution to the thickening of galaxy disks. The heating is dominated by the most massive dark matter substructures and so is a rather stochastic process, depending on the details of the merger history of each galaxy's dark matter halo and the orbital properties of those massive substructures.

[15]Note that we are approximating the galaxy as a spherical mass distribution here.

(b) Molecular clouds: Massive molecular clouds can gravitationally scatter stars that happen to pass by them, effectively transforming some of their orbital energy in the plane of the galaxy disk into motion perpendicular to that plane, thereby effectively thickening the disk (Spitzer and Schwarzschild 1953; Lacey 1984).
(c) Spiral arms: Spiral density waves can also act as scatterers of stars, but predominantly increase the stellar velocity dispersion in the plane of the galaxy, resulting in little thickening (Jenkins and Binney 1990; Minchev and Quillen 2006).

Most likely, a combination of these processes is at work. A recent review of these mechanisms is given by Wen and Zhao (2004).

5.1.2. Stability

Spiral arms and other non-axisymmetric features such as bars in galactic disks are a visually impressive reminder that these systems possess interesting dynamics. The basic theory of spiral arms, that they are density waves, was first proposed by Lin and Shu (1964; see also Marochnik and Suchkov 1996; Binney and Tremaine 2008) and has come to be widely accepted. From our current standpoint, the question in which we are interested in is whether these perturbations to an otherwise smooth disk are stable or unstable and, if unstable, how they affect the evolution of the galaxy as a whole.

Toomre (1964; see also Goldreich and Lynden-Bell 1965) derived an expression for the local stability of thin disks to axisymmetric modes in the tight-winding approximation which turns out to be extremely useful (and often approximately correct even in regimes where its assumptions fail). Disks will be unstable to axisymmetric modes if $Q < 1$ where

$$Q = \frac{\kappa\sigma_{\rm gas}}{\pi {\rm G}\Sigma_{\rm gas}}, \tag{62}$$

where

$$\kappa = \left(R\frac{{\rm d}\Omega^2}{{\rm d}R} + 4\Omega^2\right)^{1/2} \tag{63}$$

is the epicyclic frequency and Ω is the angular frequency of the disk, for a gaseous disk of surface density $\Sigma_{\rm gas}$ and velocity dispersion $\sigma_{\rm gas}$, and

$$Q = \frac{\kappa\sigma_\star}{3.36{\rm G}\Sigma_\star} \tag{64}$$

for a stellar disk of surface density $\Sigma_\star$ and velocity dispersion $\sigma_\star$. For a disk consisting of two components, gas and stars, a joint stability analysis was carried out by Jog and Solomon (1984). Efstathiou (2000; see also Bertin and Romeo 1988) solves the resulting cubic equation for the most unstable mode and finds a criterion

$$Q = \frac{\kappa\sigma_{\rm gas}}{\pi {\rm G}\Sigma_{\rm gas} g(\alpha,\beta)}, \tag{65}$$

where α and β are the ratio of stellar to gas velocity dispersions and surface densities respectively and the function $g(\alpha,\beta)$ is as given by Efstathiou (2000) and is shown in Fig. 7. Wang and Silk (1994) also show that the stability of a two-component disk can be approximated by

$$Q = (Q_\star^{-1} + Q_{\rm gas}^{-1})^{-1}, \tag{66}$$

while a more general criterion taking into account the thickness of the disk was found by Romeo (1992) and Romeo (1994).

Toomre's criterion applies to local perturbations. Perturbations on the scale of the disk can occur also. Study of these global instabilities is less amenable to analytic treatment (since one can no longer ignore contributions from distant parts of the disk). Significant work on this subject began in the 1970's. The classic result from that time is due to Ostriker and Peebles (1973) who found that rapidly rotating, self-gravitating stellar systems would become violently unstable to non-axisymmetric $m = 2$ modes if $T/|W| \gtrsim 0.14$ (for a stellar system) or 0.27 (for a fluid system) where T and W are the kinetic and potential energies of the system. Such systems can be unstable to global perturbations even if they satisfy Toomre's stability criterion. These values were approximately confirmed by numerous numerical studies, but also challenged by others (see Christodoulou et al. (1995b) for a discussion of this). Later work

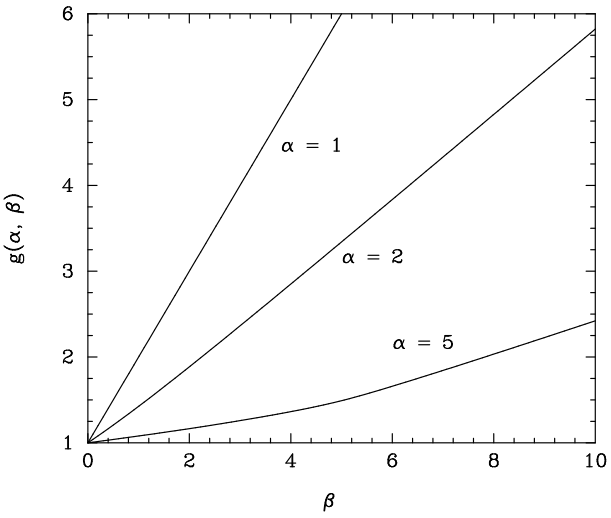

Figure 7: The function $g(\alpha,\beta)$ appearing in eqn. (65). $g(\alpha,\beta)$ is shown as a function of β (the ratio of stellar to gas velocity dispersions) for various values of α (the ratio of stellar to gas surface density). Reproduced, with permission, from Efstathiou (2000).

(Christodoulou et al. 1995a) has demonstrated that $T/|W|$ is not a sufficiently general parameter to determine stability in all systems. More recent studies have proposed improved stability criteria. For example Christodoulou et al. (1995b) find that

$$\alpha = \frac{T/|W|}{\Omega/\Omega_{\rm J}}, \tag{67}$$

where $\Omega_{\rm J}$ is the Jeans frequency in the radial direction and Ω is the mean angular velocity of the system, is a much better indicator of stability. This can be approximated by

$$\alpha = T_J/|W|, \tag{68}$$

where $T_J = L\Omega_J/2$ and L is the total angular momentum of the system. Christodoulou et al. (1995b) found that $\alpha \leq 0.254$–0.258 is required for stability in stellar systems while $\alpha \leq 0.341$–0.354 is required for gaseous systems. Christodoulou et al. (1995b) also demonstrate that this criterion is approximately equivalent to the alternative form found by Efstathiou et al. (1982) on the basis of numerical simulations of exponential stellar disks:

$$\epsilon_m \equiv \frac{v_m}{(GM_{\rm D}/R_{\rm S})^{1/2}} \gtrsim 1.1, \tag{69}$$

and show that an equivalent result for gaseous disks would replace the 1.1 with 0.9. A much more extensive review of disk stability is given by Sellwood (2010).

Global instabilities most likely lead to the formation of a very strong bar which effectively disrupts the disk leaving, after a few dynamical times, a boxy/peanut bulge or a disky bulge (Athanassoula 2008). This may therefore be a possible formation scenario for pseudo-bulges (Kormendy and Kennicutt 2004), i.e. bulges formed through secular processes in the disk (see §5.2.2) rather than as the result of a merger event (see §5.2.1).

5.1.3. Bars/Spiral Arms

The presence of perturbations in the disk can also affect its structure in less dramatic but still significant ways. (Once again, the work by Sellwood (2010) gives a more in depth review of these subjects and is highly recommended.) For example, numerical simulations by Roskar et al. (2008b; see also Roskar et al. 2008a) show that a significant fraction of stars in galaxy disks undergo large migrations in radius (as shown in Fig. 9) due to resonant scattering from spiral arms. The resonant scattering of a star initially on an approximately circular orbit tends to change its energy and angular momentum in such a way as to keep it in a circular orbit, but to change the radius of that orbit. In a frame

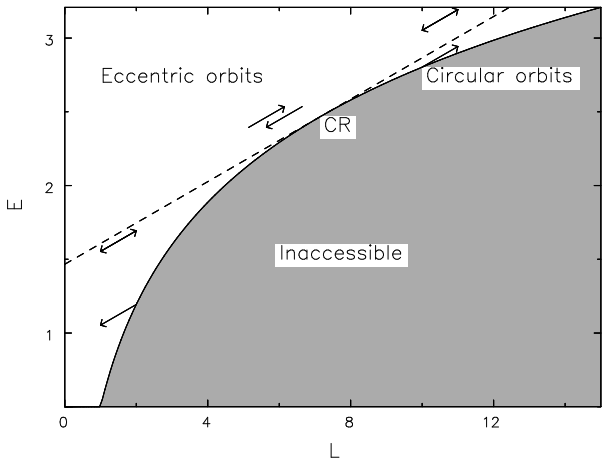

Figure 8: The Lindblad diagram showing allowed regions of the energy–angular momentum plane (white, with forbidden regions shaded gray) bounded by the curve corresponding to circular orbits. Arrows indicate how scattering from spiral density waves moves stars in this diagram. At the corotation resonance (CR) this motion parallels the circular orbit curve, implying that scattering at corotation of stars initially on circular orbits leaves those stars on approximately circular orbits. Reproduced, with permission, from Sellwood and Binney (2002).

corotating with the spiral perturbation there is an energy-like invariant quantity know as Jacobi's integral, E_J, defined as (Binney and Tremaine 2008)

$$E_J = E - \Omega_p L, \tag{70}$$

where E and L are the energy and angular momentum of an orbit respectively and Ω_p is the pattern speed of the perturbation. This implies that changes in energy and angular momentum are related by

$$\Delta E = \Omega_p \Delta L. \tag{71}$$

As shown in Fig. 8 the slope of the E–L relation for circular orbits at the corotation resonance is Ω_p. As such, stars initially on circular orbits near the corotation resonance will tend to be scattered into approximately circular orbits. Roskar et al. (2008b) show that this phenomenon can lead to the formation of an outer stellar disk with a steeper exponential decline than the inner disk and formed entirely of stars scattered from the inner regions of the galaxy. This process also smooths out age and metallicity gradients in disks that otherwise form inside out and so tend to be older and less metal rich in the center.

5.2. Spheroid Formation

The formation of galactic spheroids (which we take here to mean both the bulges of disk galaxies and isolated elliptical galaxies) can proceed via two distinct routes. The first, through the destruction of pre-existing stellar systems in violent mergers, is a natural consequence of hierarchical galaxy formation. The second, secular evolution of galactic disks, is a natural consequence of the dynamics of self-gravitating disk systems. It is worth noting that, observationally, it has been proposed that bulges be divided into two broad classes (Kormendy and Kennicutt 2004): "classical" bulges (those which look like ellipticals in terms of their light distribution and kinematics but happen to live inside a disk) and "pseudo-bulges" (those which do not look like ellipticals[16]). There is good evidence (see §4.2.1) that ellipticals (and therefore presumably classical bulges also) form through major mergers, and suggestions that pseudo-bulges are the result of secular evolution of galactic disks.

[16]Typically, pseudo-bulges are better fit by a Sersic (1968) profile with index $n \approx 1$ (as opposed to the $n = 4$ profiles of classical bulges), have significant rotation and may show signs of disk phenomena such as bars or spiral features.

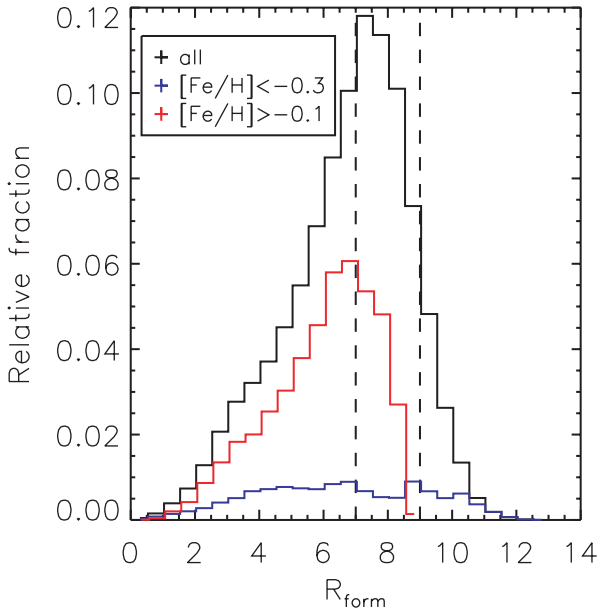

Figure 9: The distribution of formation radii, $R_{\rm form}$ (in kpc), for stars in the Solar neighborhood. The black histogram shows the distribution from all stars while the red and blue histograms show the contributions from high and low metallicity stars respectively. Reproduced, with permission, from Roskar et al. (2008b).

5.2.1. Major Mergers

As was discussed in §4.2.1, dissipative processes can lead to gravitationally bound interactions between galaxies. When the masses of the galaxies in question are comparable we may expect significant changes in their structure and the formation of a merger remnant which is very different from either of the merging galaxies. Such *major mergers* are thought to be responsible for the formation of spheroidal (i.e. elliptical) galaxies from pre-existing galaxies (which could be, in principle, disk galaxies, other spheroidals or something intermediate).

The process of violent relaxation (Lynden-Bell 1967; see also Tremaine et al. 1986), in which the energy of orbits undergoes order unity changes due to signficant time-variable fluctuations in the gravitational potential, leads to a randomization of the orbits leading to a Maxwellian distribution of energies but with temperature proportional to stellar mass. This can turn the ordered motions of disks into the random motions seen in spheroids. This process is, however, rather poorly understood—it seeks an equilibrium state which maximizes the entropy of the system, but the usual entropy is unbounded in gravitating systems implying no equilibrium state exists. Arad and Lynden-Bell (2005) demonstrate this problem by showing hysteresis effects in violently relaxed systems (i.e. the final state depends on how the system goes from the initial to final states).

The remnants of major mergers of purely stellar disk systems, while spheroidal, do not look like elliptical galaxies. As shown by Hernquist et al. (1993) their phase space densities are too low in the central regions compared to observed ellipticals. This implies that mergers between reasonably gas rich (gas fractions of around 25%) galaxies are required—the presence of gas allows for dissipation and the formation of higher phase-space density cores. Robertson et al. (2006b) find that similar gas fractions and the subsequent dissipation are required to produce the observed tilt in the fundamental plane of elliptical galaxies—mergers of purely stellar systems instead follow the expected virial scalings.

Mergers are often separated into *major* (mergers between galaxies of comparable mass) and *minor* (mergers in which one galaxy is significantly less massive than the other). Numerical simulations (e.g. Bournaud et al. 2005) show that mergers with a mass ratio $\mu \equiv M_2/M_1 \gtrsim 0.25$ are able to destroy any disks in the ingoing galaxies and leave a spheroidal remnant, while mergers with lower mass ratio tend to leave disks in place (although somewhat thickened).

As this transition is unlikely to be a sharp one, Somerville et al. (2008b) propose a more gradual transition[17], with a fraction

$$f_{\rm sph} = 1 - \left[1 + \left(\frac{\mu}{f_{\rm ellip}}\right)^8\right]^{-1}, \tag{72}$$

where $f_{\rm ellip} \approx 0.25$–$0.30$, of the disk stellar mass being put into the spheroid component of the merger remnant.

Mergers are expected to trigger a, possibly very large, enhancement in the star formation rate in the merging system. The strengths of such *bursts* of star formation depend upon the properties of the merging galaxies. Cox et al. (2008) have calibrated this enhancement against a large suite of N-body+hydrodynamics merger simulations. They define the "burst efficiency", e, to be the fraction of gas consumed during the interaction above that which would have been consumed by the constituent galaxies in isolation during the same time period. They find that the burst efficiency is well fit by[18]

$$e = \begin{cases} e_{1:1}\left(\frac{M_{\rm sat}}{M_{\rm primary}} - e_0\right)^{\gamma} & \text{if } M_{\rm sat}/M_{\rm primary} > e_0 \\ 0 & \text{if } M_{\rm sat}/M_{\rm primary} \leq e_0, \end{cases} \tag{73}$$

where $e_{1:1} = 0.56$, $\gamma = 0.50$ and $e_0 = 0.09$.

It has recently become clear that not all major mergers lead to the formation of a spheroid. Under certain conditions, major mergers of very gas rich systems can lead to the reformation of a disk after the merger is over (Barnes 2002; Springel and Hernquist 2005; Robertson et al. 2006a). This requires a high gas fraction (greater than about 50%) just prior to the final coalescence of the merging galaxies and therefore may preferentially occur under conditions which prevent the rapid depletion of gas after the first passage of the galaxies.

5.2.2. Secular Evolution

Major mergers are not the only way to form a spheroid. Internal, secular processes[19] in galaxies can also disrupt the cold and relatively fragile disks (Kormendy and Kennicutt 2004). In particular, bars (a disk phenomenon) can efficiently redistribute mass and angular momentum and lead to the build-up of dense central mass concentrations, reminiscent in many ways of bulges formed through mergers. To distinguish such secularly formed bulges from their merger-formed (or "classical") counterparts, they are referred to as "pseudo-bulges" (Kormendy and Kennicutt 2004).

Such secular processes are the result of quite generic dynamical considerations[20] and so most likely operate in all galaxies. Whether or not they are important depends upon their timescale. For example, relaxation due to star-star encounters in a galaxy operates on a timescale many orders of magnitude longer than the age of the Universe and so can be safely neglected. Instead, most relevant secular processes involve the interaction of stars (or gas elements) with collective phenomena such as bars or spiral arms.

A general picture of how secular evolution leads to the formation of pseudo-bulges has emerged. As a bar spontaneously begins to form[21] it transfers angular momentum to the outer disk and increases in amplitude. The response of gas to this bar is crucial—gas accelerates as it enters the bar potential and decelerates as it leaves. This leads to shocks forming in the gas which lie approximately along the ridge line of the bar. These shocks lead to dissipation of orbital energy and, consequently, inflow of the gas. The enhancement in the gas density as it is concentrated towards

[17] Somerville et al. (2008b) give no justification for this particular functional form, it is merely intended to give a smooth but rapid transition.

[18] The equation in Cox et al. (2008) is missing the coefficient of $e_{1:1}$ (Cox, private communication).

[19] Generically, any internal dynamical process operating on a timescale significantly longer than the dynamical time.

[20] As pointed out by Kormendy and Kennicutt (2004) disks are fundamentally prone to spreading in the presence of any dissipative process, where mass is transported inwards and angular momentum outwards, because this lowers the energy of the system while conserving angular momentum (Lynden-Bell and Kalnajs 1972). This result can be traced back to the negative specific heat of gravitating systems, and is analogous to the process of core collapse in three dimensional systems (Lynden-Bell and Kalnajs 1972; Binney and Tremaine 2008).

[21] The bar instability in galactic disks involves some fascinating dynamics. Binney and Tremaine (2008) give a clear explanation of the physics involved. Briefly, the bar instability involves the joint actions of the swing amplifier and a feedback mechanism. A randomly occurring leading spiral density wave in a disk will unwind and, as it does so, will rotate faster. As it swings from leading to trailing it reaches a maximum rotation speed which is close to the average orbital speed of stars in the disk. This leads to a resonance condition, in which the wave can strongly perturb the orbits of those stars, the self-gravity of which enhances the bar further, leading to an amplification of the wave. If there is some mechanism to convert the amplified trailing wave that results into a leading wave once more (e.g. if the wave can pass through the center of the galaxy and emerge as a leading wave, or if nonlinear couplings of waves can generate leading waves) the whole process can repeat and the wave will grow stronger and stronger.

the galactic center inevitably leads to star formation and the build-up of a pseudo-bulge. Bars eventually destroy themselves in this way—the increase in the central mass of the galaxy effectively prevents the bar instability from working.

While this general picture seems to be incontrovertible, many of the details (e.g. the redshift evolution of bars, the importance of the dark matter halo and the cosmological evolution of the disk) remain poorly understood, but actively studied (Friedli and Benz 1993; Shlosman and Noguchi 1993; El-Zant and Shlosman 2002; Athanassoula 2002; Bournaud and Combes 2002; Shen and Sellwood 2004).

5.2.3. Sizes

The sizes of spheroidal galaxies formed through major mergers can be determined given the properties of the progenitor galaxies and their orbit and some knowledge of the extent to which mass and energy is conserved through the merging process. If the galaxies are dissipationless, purely stellar systems (a so-called *dry merger*) then energy is at least approximately conserved[22] In a gas rich (or *wet*) merger the gaseous component is likely to radiate significant amounts of energy prior to forming stars.

A simple model to compute the size of a galaxy formed via a major merger was described by Cole et al. (2000), who assumed perfect conservation of mass and energy. The size of the merger remnant, $r_{\rm f}$, is then given by

$$\begin{aligned}\frac{c_f \mathrm{G}(M_1+M_2)^2}{r_{\rm f}} &= \frac{c_1 \mathrm{G} M_1^2}{r_1} + \frac{c_2 \mathrm{G} M_2^2}{r_2} \\ &\quad + \frac{f_{\rm orbit} \mathrm{G} M_1 M_2}{r_1 + r_2}. \end{aligned} \tag{74}$$

The left-hand side represents the gravitational binding energy of the final system while the first two terms on the right represent the gravitational binding energy of the two merging galaxies, which have masses M_1 and M_2 respectively and half-mass radii r_1 and r_2 respectively. The "c" coefficients relate the actual binding energy to the characteristic value of $\mathrm{G}M^2/r$ and depend on the density distribution of the galaxy[23]. Cole et al. (2000) find $c = 0.45$ for a de Vaucouler's spheroid and $c = 0.49$ for an exponential disk and so adopt $c = 0.5$ for all galaxies (which may be composite systems consisting of both a disk and a spheroid) for simplicity. The final term in eqn. (74) represents the orbital energy of the two merging galaxies just prior to merging and is parameterized in terms of their gravitational binding energy when separated by the sum of the half-mass radii. Cole et al. (2000) adopt $f_{\rm orbit} = 1$ so that this orbital term corresponds to a circular orbit. According to this approach, a merger of two identical galaxies of radii r_1 results in a remnant of size $r_{\rm f} = (4/3)r_1$.

More recently, Covington et al. (2008) performed numerical simulations of merging galaxies including gaseous components, and found significant deviations from the simple model of Cole et al. (2000) as a result of energy loss due to radiative processes in merging galaxies containing gas. Covington et al. (2008) propose an improved model which accounts for this energy loss and results in a merger remnant size given by

$$E_{\rm int,f} = E_{\rm int,i} + E_{\rm rad} + E_{\rm orb}, \tag{75}$$

where

$$E_{\rm int,f} = -\frac{c \mathrm{G} M_{\rm f}^2}{r_{\rm f}} \tag{76}$$

is the internal binding energy of the final galaxy,

$$E_{\rm int,i} = -\frac{c \mathrm{G} M_1^2}{r_1} - \frac{c \mathrm{G} M_2^2}{r_2} \tag{77}$$

[22] In principle, energy may be lost from the stellar system by being transferred to the dark matter, or high energy stars may be flung out beyond the escape velocity, removing both mass and energy from the system.

[23] In principle, the binding energy terms should also account for the stellar–dark matter binding energy. Cole et al. (2000) ignore the dark matter contribution of the binding energy, effectively assuming that its contribution to each term in eqn. (74) scales in proportion to the stellar masses of the galaxies.

is the internal binding energy of the initial galaxies,

$$E_{\rm orb} = -\frac{{\rm G}M_1M_2}{r_{\rm sep}} + \frac{1}{2}M_1V_1^2 + \frac{1}{2}M_2v_2^2 \tag{78}$$

is the orbital energy of the galaxies just prior to the merger when their separation is $r_{\rm sep}$ and their center of mass velocities are V_1 and V_2, and

$$E_{\rm rad} = -c_{\rm rad}\sum_{i=1}^{2} K_i f_{{\rm g},i} f_{{\rm k},i}(1 + f_{{\rm k},i}) \tag{79}$$

is the radiative energy loss where K_i and $f_{{\rm g},i}$ are the initial internal kinetic energy and gas fraction for progenitor i. The impulse, $f_{{\rm k},i}$ is defined to be $f_{\rm k} = \Delta E/K_{\rm tot}$ where $K_{\rm tot}$ is the total initial internal kinetic energy of the galaxy and

$$\Delta E = \frac{A{\rm G}^2M_{1,{\rm tot}}^2M_{2,{\rm tot}}}{V_{\rm peri}^2(r_{\rm peri}^2 + Br_{1,{\rm tot}}r_{\rm peri} + Cr_{1,{\rm tot}}^2)}, \tag{80}$$

where $M_{1,{\rm tot}}$ and $M_{2,{\rm tot}}$ are the total masses of the galaxies (baryonic plus dark matter), $r_{1,{\rm tot}}$ is the total half-mass radius of the primary galaxy and $r_{\rm peri}$ is the pericentric distance of the first passage of the two galaxies, treating them as point masses from their initial orbit. Covington et al. (2008) find that values $A = 1.6$, $B = 1.0$, $C = 0.006$ and $c_{\rm rad} = 1$ best fit their simulation results.

Similar arguments have been applied to the formation of spheroids through secular processes (e.g. Cole et al. 2000), but the assumptions of this approach are far less well tested in such cases.

6. Star Formation, AGN and Feedback

So far, we have not considered how a galaxy converts its available gas into stars and what effect those stars, and associated supernovae explosions, may have on the evolution of the galaxy. Additionally, observational evidence suggests that all galaxies contain a supermassive black hole at their center, which may play a key role in limiting the process of galaxy formation. We will discuss these aspects of galaxy formation theory below. We do not explore in detail the role of the associated galactic winds in galaxy evolution, but refer the reader to Veilleux et al. (2005) for a thorough review.

6.1. Star Formation

Star formation theory warrants an entire review to itself (for a recent example see McKee and Ostriker 2007) and so we will summarize only those aspects most pertinent to galaxy formation theory. The past decade has seen a greatly improved understanding of how the key processes of turbulence, magnetic fields and self-gravity interact to form molecular clouds and stars. Nevertheless, there remain numerous unsolved problems in star formation theory. These problems propagate into galaxy formation theory if we wish to understand the rate at which stars form in a galaxy and any consequences that may have for further galactic evolution. This problem is somewhat mitigated by the fact that, for galaxy formation theory, we do not necessarily care about the details of how stars form. Instead, we would simply like to know, given the large scale properties of a galaxy (e.g. mass, size, density, dynamical time, gas fraction, chemical composition), what is the resulting rate of star formation.

Traditionally, this question has been answered by appealing to empirical rules or dimensional analysis. For example, much use has been made of the empirically derived scaling relations of Schmidt (1959) and Kennicutt (1989, 1998). The Schmidt-Kennicutt law states that the rate of star formation per unit surface area, $\dot{\Sigma}_\star$, depends on the surface density of gas, $\Sigma_{\rm gas}$ as

$$\dot{\Sigma}_\star \propto \Sigma_{\rm gas}^n, \tag{81}$$

where n is measured to be approximately 1.4. While this relation is practically useful for galaxy formation theory, insofar as it allows one to bypass the question of star formation and move directly to a star formation rate, it suffers from the same issue as all empirical relations used in theoretical models: there is no way to be sure that it is valid beyond the regimes where it was originally measured.

Recently, new observations have suggested a relatively simple model for star formation (Krumholz and Tan 2007). Stars form in molecular clouds and so it is natural that it would be the density of molecular gas (rather than total) gas which matters. Furthermore, it is observed that a constant fraction (around 2%) of molecular gas turns into stars per free-fall timescale. This implies $\dot{\rho}_\star = \epsilon_{\rm ff} f_{\rm H_2} \rho_{\rm gas}/t_{\rm ff}$ where $\epsilon_{\rm ff}$ is the fraction of molecular gas turned into stars per free-fall time, $f_{\rm H_2}$ is the molecular fraction and $t_{\rm ff}$ is the local free-fall timescale.

In the model of Robertson and Kravtsov (2008, see also Krumholz et al. 2009) the star formation rate is given by

$$\dot{\Sigma}_\star \propto f_{\rm H_2} h_{\rm SFR} h_{\rm gas}^{-1.5} \Sigma_{\rm gas}^{1.5}, \tag{82}$$

where $f_{\rm H_2}$ is the fraction of hydrogen in molecular form, $h_{\rm SFR}$ is the scale height of the star-forming gas and $h_{\rm gas}$ is the scale height of the interstellar medium. Robertson and Kravtsov (2008) compute $f_{\rm H_2}$ and the scale height self-consistently in the presence of the interstellar radiation field produced by earlier generations of stars. This results in a net scaling with total gas surface density of

$$\dot{\Sigma}_\star \propto \Sigma_{\rm gas}^{n_{\rm tot}}, \tag{83}$$

where $n_{\rm tot} \approx 2$ for massive galaxies and $n_{\rm tot} \gtrsim 4$ for dwarf galaxies. When expressed in terms of the molecular hydrogen gas surface density a scaling

$$\dot{\Sigma}_\star \propto \Sigma_{\rm H_2}^{n_{\rm mol}}, \tag{84}$$

with $n_{\rm mol} \approx 1.3$ is found for all galaxies. These scalings are consistent with a broad range of observations of star formation in different galaxies.

Similarly, Krumholz et al. (2009) find that the following expression encapsulates the complex physics of star formation:

$$\begin{aligned} \dot{\Sigma}_\star &= f_{\rm H_2}(\Sigma_{\rm g}, c, Z') \frac{\Sigma_{\rm g}}{2.6\ {\rm Gyr}} \\ &\times \begin{cases} \left(\frac{\Sigma_{\rm g}}{85 M_\odot {\rm pc}^{-2}}\right)^{-0.33}, & \text{if } \frac{\Sigma_{\rm g}}{85 M_\odot {\rm pc}^{-2}} < 1 \\ \left(\frac{\Sigma_{\rm g}}{85 M_\odot {\rm pc}^{-2}}\right)^{0.33}, & \text{if } \frac{\Sigma_{\rm g}}{85 M_\odot {\rm pc}^{-2}} > 1, \end{cases} \end{aligned} \tag{85}$$

where the molecular hydrogen fraction is

$$f_{\rm H_2}(\Sigma_{\rm g}, c, Z') \approx 1 - \left[1 + \left(\frac{3}{4}\frac{s}{1+\delta}\right)^{-5}\right]^{-1/5}, \tag{86}$$

and $s = \ln(1+0.6\chi)/(0.04\Sigma_{\rm comp,0} Z')$, $\chi = 0.77(1+3.1 Z'^{0.365})$, $\delta = 0.0712(0.1 s^{-1}+0.675)^{-2.8}$, $\Sigma_{\rm comp,0} = \Sigma_{\rm comp}/(1 M_\odot {\rm pc}^{-2})$ and Z' is the metallicity normalized to the Solar value. The transition at gas surface densities of $85 M_\odot {\rm pc}^{-2}$ corresponds to the point at which the ambient pressure becomes comparable to the internal pressure in molecular clouds (and therefore influences the properties of those molecular clouds). Here, $\Sigma_{\rm comp}$ is the surface density of a ~ 100 pc-sized atomic–molecular complex. Since simulations and semi-analytic models typically only predict the gas distribution on scales significantly larger than this we can write $\Sigma_{\rm comp} = c\Sigma_{\rm g}$ where c is a clumping factor that accounts for structures which are unresolved in the simulation. This clumping factor should approach unity as the resolution approaches 100 pc at which point molecular cloud complexes should be adequately resolved.

6.2. Black Hole Formation

Over the past ten years it has become possible to measure the masses of supermassive black holes residing at the centers of galaxies for relatively large samples. The existence of strong correlations between the masses of these black holes and the properties of their host galaxy — such as spheroid mass (Magorrian et al. 1998), velocity dispersion (Ferrarese and Merritt 2000; Gebhardt et al. 2000a,b), number of globular clusters (Burkert and Tremaine 2010) or even host dark matter halo (Ferrarese 2002) — is suggestive of some interaction between forming galaxies and supermassive black holes. Of course, correlation does not imply causation (Munroe 2009) and Jahnke and Maccio (2010) show that a black hole–host galaxy mass relation can arise from uncorrelated initial conditions via simple merging, but the theoretical need for large amounts of energy to inhibit galaxy formation in massive halos naturally

leads to the idea that supermassive black holes (SMBH) and galaxy formation are connected (Benson et al. 2003). In addition, understanding the formation of these most massive of black holes is interesting in its own right and has important observational consequences for both studies of active galactic nuclei and gravitational wave detection experiments such as the *Laser Interferometer Space Antenna*[24].

In light of these reasons, several studies have attempted to follow the process of SMBH formation within forming galaxies (Silk and Rees 1998; Monaco et al. 2000; Kauffmann and Haehnelt 2000; King 2003; Wyithe and Loeb 2003; Matteo et al. 2003; Volonteri et al. 2003; King 2005; Begelman and Nath 2005; Malbon et al. 2007; Matteo et al. 2008; Volonteri et al. 2008; Sijacki et al. 2009; Volonteri and Natarajan 2009). We will not review all details of this process here. Instead, we will focus on the basic formation mechanisms and, in §6.3.2, on the interaction between SMBHs and galaxy.

Before supermassive black holes can grow via accretion or merging, there must be some pre-existing (probably not supermassive) *seed* black holes. Most plausibly, these seeds form at high redshifts as the remnants of the earliest generation of Population III stars which have reached the end of their stellar lifetimes. Details of the formation of these first stars remain incompletely understood, but hydrodynamical simulations suggest that they have masses in the range of a few hundred Solar masses (Abel et al. 2002; Bromm et al. 2002), leaving intermediate mass black hole remnants.

To determine the rate at which gas accretes onto a black hole (or, more precisely, the black hole and any associated accretion disk system) we must consider how the black hole affects the gas through which it is moving. The gravity of a fast moving black hole will deflect gas that passes by it, focusing it into a wake behind the black hole which will then accrete onto the black hole. This problem, and the equivalent for a slowly (subsonically) moving black hole, was first studied by Hoyle and Lyttleton (1939) and Bondi and Hoyle (1944). This leads to an accretion rate of

$$\dot{M}_{\rm BHL} = \frac{4\pi {\rm G}^2 M_\bullet^2 \rho}{(c_{\rm s}^2 + v^2)^{3/2}}, \tag{87}$$

where $M_\bullet$ is the mass of the black hole, $c_{\rm s}$ is the sound speed and v the relative velocity of black hole and gas. The accretion occurs from a characteristic radius of

$$r_{\rm BHL} = \frac{{\rm G}M_\bullet}{c_{\rm s}^2}. \tag{88}$$

An in-depth review of Bondi-Hoyle-Lyttleton accretion is given by Edgar (2004). The growth of black holes will be enhanced by any process which increases the density in the central regions of the galaxy in which they reside. At early times, this may occur due to gravitationally unstable disks forming bars and driving gas towards the center (Volonteri et al. 2008), while at later times galaxy-galaxy mergers can results in dissipation and gas flows to the center (Matteo et al. 2005). Other mechanisms for delivering gas to the centers of galaxies are also possible, for example McKernan et al. (2010) show that warm clouds from the surrounding halo occasionally impact galactic centers, potentially delivering 10^4–$10^6 M_\odot$ of gas.

Bondi-Hoyle-Lyttleton accretion causes gas to flow towards the black hole. At some point, the angular momentum of the gas will become important and the accreting gas must form a disk. The final stage of accretion is then governed by this accretion disk, which may be a geometrically thin, radiative (Shakura and Sunyaev 1973) or a geometrically thick, radiatively inefficient (e.g. ADAF) flow (Narayan and Yi 1994). The details of the flow may be important for determining the spin of the black hole (see below) and the effects of feedback from any nuclear activity (see §6.3.2).

Galaxy-galaxy mergers can also lead to galaxies containing two (or potentially more) SMBHs, resulting in the potential for black hole mergers. The process of bringing two SMBHs together begins by dynamical friction against the background of dark matter (the same process which is causing the black hole host galaxies to merge). The subsequent merging process was originally outlined by Begelman et al. (1980) and assumes that the two black holes form a binary system at an initial separation of

$$a_{\rm b} = \frac{{\rm G}(M_1 + M_2)}{2\sigma^2}, \tag{89}$$

[24] `http://lisa.nasa.gov/`

where $M_1 > M_2$ are the masses of the black holes and σ is the velocity dispersion of the host galaxy, such that the binary orbit contains a mass in stars and dark matter comparable to the sum of the black holes masses. Around this binary, the stellar distribution is expected to form a cusp with density profile $\rho_\star \propto r^{-7/4}$ (Bahcall and Wolf 1976). Initially, the binary hardens due to dynamical friction against the stellar background acting on each black hole individually. As the binary hardens this process becomes less effective as perturbations from distant stars tend to perturb the center of mass of the binary without changing its semi-major axis. However, once the binary becomes sufficiently hard, at a separation of (Quinlan 1996)

$$a_{\rm h} = \frac{{\rm G}M_2}{4\sigma^2}, \tag{90}$$

it can harden further by three-body interactions in which a passing star is captured and then ejected at high velocity. The timescale, $a/\dot{a}$, for hardening in this regime is (Quinlan 1996)

$$t_{\rm h} = \frac{\sigma}{{\rm G}\rho_\star a H}, \tag{91}$$

where the dimensionless hardening rate $H \approx 15$. If hardening continues long enough, the binary eventually becomes sufficiently hard that gravitational radiation dominates the evolution of the system which then coalesces on a timescale of (Peters 1964)

$$t_{\rm GR} = \frac{5{\rm c}^4 a^4}{256{\rm G}^3 M_1 M_2 (M_1 + M_2)}. \tag{92}$$

The fly in the ointment of this neat picture is that the above estimates for the rate of hardening by stellar encounters assumes a fixed stellar background. In reality, as stars are ejected in three-body encounters the parts of phase-space containing stars that can be captured becomes depleted (so-called "loss cone depletion"). This inevitably slows the hardening process. The past ten years have seen numerous studies of this process and examination of various mechanisms by which the loss cone may be refilled. For example, Yu (2002) finds that in triaxial potentials scattering of stars can efficiently refill the loss cone while Gould and Rix (2000) suggest that the presence of a gaseous disk surrounding the black holes can help harden the binary. Numerical and analytical works have also indicated that the random walking of the binary center of mass may help mitigate loss cone depletion (Quinlan and Hernquist 1997; Milosavljevic and Merritt 2001), while the effective refilling of the loss cone by ejected stars returning on eccentric orbits (Milosavljevic and Merritt 2003; Sesana et al. 2007) and interactions with stars bound to the binary (Sesana et al. 2008) may enhance the rate of hardening. While the details remain uncertain it seems that this basic process can lead to black holes merging in less than 10 Gyr.

In addition to their mass, cosmological black holes are characterized by one other parameter, their angular momentum[25]. The spin of a black hole can have a strong influence on the radiative efficiency and jet power of black holes (see §6.3.2) and so the cosmological evolution of this quantity is important to understand. There are fundamentally two mechanisms which change the spin of a black hole: merging with another hole and accretion of material.

The outcomes of binary black hole mergers have proven very difficult to simulate numerically. However, recent advances in numerical techniques have allowed for successful simulation of the entire merging process (e.g. Tichy and Marronetti 2007) and, therefore, determination of the final spin of the merger product. While the number of simulations carried out to date is small, Boyle et al. (2008) exploit symmetries of the problem to construct simple fitting formula which accurately predict the spin of the final black hole as a function of the incoming black hole masses, spins and orbital properties.

As first considered by Bardeen (1970), material accreted from an accretion disk carries with it some angular momentum (approximately equal to its angular momentum at the latest stable circular orbit, before it began its plunge into the black hole). Defining a dimensionless spin parameter for a black hole through

$$j = J{\rm c}/{\rm G}M_\bullet^2, \tag{93}$$

[25]They will not possess any significant charge, as this would be quickly neutralized by accretion of oppositely charged material.

where J is the angular momentum of the hole of mass $M_\bullet$, such that $0 \leq j \leq 1$, then Shapiro (2005) defines a dimensionless spin-up function $s(j)$ by

$$s(j) = \frac{\mathrm{d}j}{\mathrm{d}t}\frac{M_\bullet}{\dot{M}_{\bullet,0}}, \tag{94}$$

where $\dot{M}_{\bullet,0}$ is the rate of rest mass accretion. For a standard, relativistic, Keplerian thin disk accretion flow with no magnetic fields, the expected spin-up function due to accretion is given by (Shapiro 2005)

$$s(j) = \mathcal{L}_{\mathrm{ISCO}} - 2jE_{\mathrm{ISCO}}, \tag{95}$$

where

$$\mathcal{L}_{\mathrm{ISCO}}(j) = \frac{\sqrt{r_{\mathrm{ISCO}}}(r_{\mathrm{ISCO}}^2 - 2j\sqrt{r_{\mathrm{ISCO}}} + j^2)}{r_{\mathrm{ISCO}}\sqrt{r_{\mathrm{ISCO}}^2 - 3r_{\mathrm{ISCO}} + 2j\sqrt{r_{\mathrm{ISCO}}}}}, \tag{96}$$

and

$$E_{\mathrm{ISCO}}(j) = \frac{r_{\mathrm{ISCO}}^2 - 2r_{\mathrm{ISCO}} + j\sqrt{r_{\mathrm{ISCO}}}}{r_{\mathrm{ISCO}}\sqrt{r_{\mathrm{ISCO}}^2 - 3r_{\mathrm{ISCO}} + 2j\sqrt{r_{\mathrm{ISCO}}}}}, \tag{97}$$

are the (dimensionless) specific angular momentum and specific energy of the innermost stable circular orbit (ISCO) of the black hole respectively. The radius of the ISCO orbit (in units of the gravitational radius $GM_\bullet/c^2$) is

$$\begin{aligned} r_{\mathrm{ISCO}} &= -\sqrt{[3 - A_1(j)][3 + A_1(j) + 2A_2(j)]} \\ &\quad +3 + A_2(j) \end{aligned} \tag{98}$$

where

$$\begin{aligned} A_1(j) &= 1 + [(1-j^2)^{1/3}] \\ &\quad \times[(1+j)^{1/3} + (1-j)^{1/3}], \end{aligned} \tag{99}$$

$$A_2(j) = \sqrt{3j^2 + A_1(j)^2}. \tag{100}$$

Thorne (1974) found a small correction to this formula due to the fact that the hole preferentially swallows negative angular momentum photons resulting in a spin-up function for the standard thin disk that is positive for all $j < 0.998$, and therefore lets the black hole spin up to $j \approx 0.998$ in finite time as noted by Shapiro (2005). For a thick accretion flow the result is somewhat different (since the flow is no longer supported against gravity by its rotation alone as it has significant thermal and magnetic pressure). Benson and Babul (2009) compute the spin-up function for ADAF models. Additionally, Benson and Babul (2009) compute how the magnetic torques which allow black holes to drive jets (via the Blandford-Znajek and/or Blandford-Payne mechanisms; Blandford and Znajek 1977; Blandford and Payne 1982) result in a braking torque on the black hole, spinning it down and resulting in an equilibrium spin of $j \approx 0.93$ for a hole accreting from an ADAF.

The relative importance of mergers and accretion for determining the spins of cosmological black holes depends upon the rate of galaxy mergers, the supply of gas to the black hole and additional factors such as the alignment of accretion disks and black hole spins and merging black hole spins and orbits. Many of these factors are not too well understood. However, cosmological calculations (Berti and Volonteri 2008; see also Volonteri et al. 2005) suggest that accretion dominates over mergers in terms of determining the spins of supermassive black holes, with the consequence that most such holes are predicted to be rapidly spinning.

One additional consequence of black hole mergers is that the gravitational waves emitted during the final inspiral carry away linear momentum resulting in the black hole recoiling in the opposite direction with a velocity potentially large enough to unbind it from the galaxy (Fitchett 1983; Favata et al. 2004; Merritt et al. 2004; Blanchet et al. 2005). Studies of this effect within a cosmological framework suggest that such ejected black holes (wandering through intergalactic space) can make up 2–3% of the total mass density of supermassive black holes, while in individual cases they can account for up to half of the total black hole mass associated with a galaxy (Libeskind et al. 2006).

6.3. Feedback

As early as 1974 (Larson 1974; see also White and Rees 1978; Dekel and Silk 1986) it was realized that star formation could not proceed with 100% efficiency in all dark matter halos. Evidence for this comes from multiple observed facts, but the two crucial ones are:

1. The total mass density in stars is $\Omega_\star = (2.3 \pm 0.34) \times 10^{-3}$ (Cole et al. 2001), much less than the total baryonic mass density of the Universe $\Omega_b = 0.0462 \pm 0.0015$ (Dunkley et al. 2009). Therefore, only a small fraction of all baryons have been able to turn into stars.
2. The distribution of galaxy luminosities (as described by the luminosity function) is very different from the distribution of dark matter halo masses. In particular there are many fewer faint galaxies relative to bright galaxies than there are low mass to high mass dark matter halos. If each halo contained baryons at the universal mix and turned all of them into stars we would expect these two ratios to be equal (Benson et al. 2003).

This second point can be made even stronger: if all dark matter halos turned a constant fraction of their mass into stars we would still have too many faint relative to bright galaxies. There are a wealth of other observational constraints which indicate that the efficiency of galaxy formation must depend strongly upon halo mass—a useful summary of these constraints is given by Behroozi et al. (2010).

Clearly what is needed is some process which preferentially suppresses the formation of stars in lower mass dark matter halos. The usual suspect for this process is energy/momentum input from supernovae explosions, perhaps augmented by stellar winds.

A similar problem occurs in the most massive dark matter halos. Although cooling is relatively inefficient in such halos they can nevertheless cool significant mass of gas over cosmic time. Unchecked, this leads to the formation of galaxies significantly more luminous than any that are observed. The energetic requirements of this problem suggest that AGN are a possible solution.

6.3.1. Supernovae/Stellar Winds

Energy input from SNe due to a single stellar population are shown in Fig. 10. If we assume that a fraction ϵ of this energy is coupled into an outflow of ISM gas which leaves the galaxy at the escape velocity (so that we do not waste energy by giving the gas a velocity at infinity) this results in an outflow rate $\dot{M}_{\rm out}$ given by

$$\begin{aligned} \frac{1}{2}\dot{M}_{\rm out}V_{\rm esc}^2 &= \epsilon \int_0^t \dot{M}_\star(t')\dot{E}_{\rm SNe+winds}(t-t')\mathrm{d}t' \\ &\approx \dot{M}_\star(t)E_{\rm SN+winds}, \end{aligned} \tag{101}$$

where in the last step we have approximated energy input from SNe and winds as occurring instantaneously after star formation. This implies an outflow rate of

$$\dot{M}_{\rm out} = \dot{M}_\star(t)\frac{2\epsilon E_{\rm SN+winds}}{V_{\rm esc}^2}. \tag{102}$$

This has the required features: given some initial mass of cold gas, a fraction $1/(1+\beta)$ where $\beta \equiv 2\epsilon E_{\rm SN+winds}/V_{\rm esc}^2$ will be turned into stars, resulting in much lower star formation efficiencies in low mass galaxies.

Figure 10 shows the cumulative energy input[26] into the interstellar medium as a function of time from a $1M_\odot$ burst of star formation with a Chabrier (2003) initial mass function.

Similar arguments can be made using the momentum of supernovae explosions to drive the wind, which may be more relevant if energy is efficiently radiated from expanding SNe bubbles[27] (Murray et al. 2005). The rate of momentum injection from supernovae is given by (Murray et al. 2005)

$$\dot{P}_{\rm SN} \approx 2 \times 10^{28}\left(\frac{\dot{M}_\star}{1M_\odot\ \mathrm{yr}^{-1}}\right)\ \mathrm{kg\ m\ s}^{-2}. \tag{103}$$

[26] We assume that a Type II supernovae releases 10^{51} ergs of usable energy. We express the energy input in units of 10^{51}ergs so that it can be interpreted as the equivalent number of supernovae.

[27] The momentum, of course, cannot be radiated away.

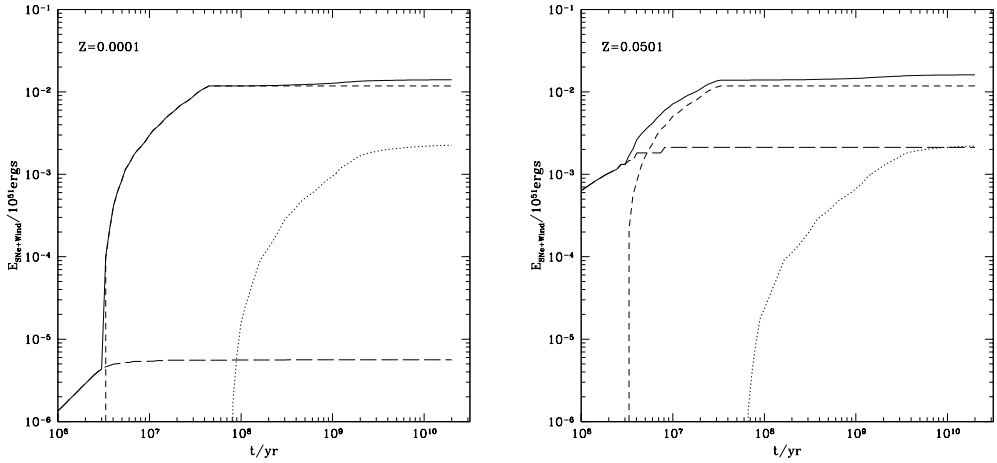

Figure 10: Cumulative energy input into the interstellar medium, expressed as the number of equivalent supernovae, per unit mass of stars formed as a function of time for a Chabrier initial mass function. The two panels show results for two different metallicities as indicated in the panels. The long dashed line indicates the contribution from stellar winds, the dotted line the contribution from Type Ia supernovae and the short dashed line the contribution from Type II supernovae. The solid line shows the sum total of all contributions.

Since the momentum in any wind driven by this momentum input must satisfy $\dot{P}_{\rm W} = \dot{M}_{\rm out} V_\infty$, where V_∞ is the wind velocity at infinity we have that

$$\dot{M}_{\rm out} \approx \frac{\dot{P}_{\rm SN}}{V_{\rm esc}}, \tag{104}$$

where we have assumed that $V_\infty \approx V_{\rm esc}$ (Murray et al. 2005). This gives a different scaling with the galaxy escape velocity compared to energy driven winds.

The details of how supernovae feedback actually operates remain somewhat unclear, and is complicated by the necessity to understand how an expanding supernovae remnant interacts with a complex, multiphase interstellar medium. Our discussion below will mostly follow Efstathiou (2000; see also McKee and Ostriker 1977).

The basic picture considered involves a two phase interstellar medium consisting of hot, diffuse material (which fills most of the volume) and cold, dense clouds (which contain most of the mass). Evaporation of cold clouds by supernovae moves gas from the cold phase into the hot phase. Outflows, and suppression of star formation, from the hot phase will result if the hot phase:

1. fills most of the volume;
2. is sufficiently low density that radiative cooling times are long, and;
3. its temperature exceeds the virial temperature of galaxy (so that the gas may climb out of the potential).

The effectiveness of feedback in such a model can be examined by considering the mass of cold clouds swept up and evaporated by an expanding supernovae remnant, $M_{\rm ev}$. Efstathiou (2000) finds

$$M_{\rm ev} \approx 1390 E_{51}^{6/5} f_\Sigma^{-3/5} \phi_\kappa^{3/5} n_{\rm h-2}^{-4/5} M_\odot, \tag{105}$$

where E_{51} is the energy released by a supernovae in units of 10^{51} ergs, $n_{\rm h-2}$ is the number density of hydrogen in units of 10^{-2} cm^{-3}, and the evaporation parameter as defined by McKee and Ostriker (1977) is

$$\Sigma = \frac{\gamma}{4\pi a_1 N_{\rm cl} \phi_\kappa} \equiv f_\Sigma \Sigma_\odot, \tag{106}$$

where $\gamma = v_{\rm h}/c_{\rm h} \approx 2.5$ relates the blast wave velocity, $v_{\rm h}$, to the isothermal sound speed, $c_{\rm h}$, a_1 is a typical cloud radius, $N_{\rm cl}$ is the number of clouds per unit volume, ϕ_κ relates the effective conductivity, $\kappa_{\rm eff}$, to the classical thermal

conductivity, κ, via $\kappa_{\rm eff} = \phi_\kappa \kappa$ and $\Sigma_\odot \approx 95$ pc^2 is the value of the evaporation parameter in the Solar neighborhood. (Units are chosen so that all variables have values of order unity in a typical galaxy.)

Since $M_{\rm ev}$ is significantly larger than the mass of stars formed per supernovae then we may expect that if a significant fraction of this evaporated gas can escape as a wind then star formation may be efficiently suppressed.

Gas in the hot phase will escape the galaxy if its specific enthalpy

$$\frac{1}{2}v^2 + \frac{5}{2}\frac{p}{\rho} \tag{107}$$

exceeds its specific gravitational binding energy. This therefore requires that we determine the thermodynamic properties of the hot phase. Efstathiou (2000) does this by assuming that supernovae remnants have a porosity of unity (i.e. the total volume of remnants equals the volume of the galaxy, thereby creating an overlapping network of remnants). Given a model for the expanding supernovae remnant this allows the thermodynamic properties of the hot phase to be determined.

Efstathiou (2000) shows that such a model of feedback can indeed produce self-regulated star formation in a galaxy disk that is quiescently forming stars (bursts are not required) and that both negative and positive (due to pressure-enhanced star formation) feedback can work simultaneously.

6.3.2. AGN

Very simple energetic arguments suggest that the energy output involved in building a black hole in a galaxy can have significant effects on the formation of the galaxy itself (Benson et al. 2003). To order of magnitude, let us assume that each galaxy contains a supermassive black hole with a mass equal to 0.1% of its stellar mass. The energy released by the formation of the black hole per unit mass of stars formed is then

$$\mathcal{E}_\bullet = 10^{-3}\frac{\epsilon}{1-\epsilon}{\rm c}^2, \tag{108}$$

where ϵ is the efficiency of conversion of rest mass into energy output (either in radiation or mechanical outflow). For typical values of $\epsilon \sim 0.1$ this implies $\mathcal{E} = 1.8 \times 10^{50}$ ergs $M_\odot^{-1}$, which is an order of magnitude greater than that released by supernova explosions and stellar winds and is comparable to the energy released by cooling gas in forming some of the most massive galaxies.

Feedback from AGN has the potential to directly link the properties of supermassive black holes and their host galaxies. As such, it may be a natural explanation for the observed correlations between supermassive black hole mass and galaxy mass or velocity dispersion. The first study of how AGN feedback can lead to such correlations[28] was described by Silk and Rees (1998). They showed that, on quite general grounds, coupling of the energy released by the formation of the supermassive black hole to the surrounding forming galaxy would lead to a relationship close to the observed $M_\bullet$–σ relation. The generality of these arguments imply that this result may be reasonably independent of the details of any more specific feedback model.

The physical mechanism through which AGN feedback operates remains somewhat unclear. AGN likely radiatively heat cooling gas in the atmosphere surrounding galaxies, reducing the rate at which that gas can cool. Additionally, radiatively driven winds originating from the broad line region surrounding the black hole may result in mechanical feedback on the galaxy itself. Finally, in low accretion states, AGN may drive highly collimated and powerful jets which can reach out well into the surrounding halo. Plausibly all of these mechanisms could be active during galaxy formation.

Ciotti et al. (2009) examined the roles of radiative and mechanical feedback modes. They find that radiative feedback alone, while able to forestall the "cooling catastrophe" (see §8.3), is unable to sufficiently limit the growth of black holes, resulting in them being too massive for a given galaxy (by a factor of around four). Mechanical feedback is found to be successful in limiting the growth of black holes. This is in agreement with other numerical simulations, such as Springel et al. 2005a; Matteo et al. 2005; Sijacki et al. 2007, 2009; Booth and Schaye 2009, which incorporate energy injection from quasars (typically triggered by major mergers) and show that AGN activity can effectively expel gas from a galaxy and can establish the observed correlations between supermassive black hole and galaxy

[28] Once again, assuming that any causative process is needed at all (Jahnke and Maccio 2010).

properties. However, Ciotti et al. (2009) find that mechanical feedback of high efficiency (as is required to match the scaling relations) is too effective, depleting galaxies of gas to a degree greater than is observed, while low efficiency mechanical feedback allows too much star formation to occur at late times, resulting in blue cores in elliptical galaxies that are inconsistent with observations. Precisely how efficiently jets from an AGN can couple their energy to the surrounding hot gas remains a topic of intense study. The general picture that is emerging is that the jets inflate bubbles or cavities in the hot atmosphere. For example, Omma et al. (2004) use numerical simulations to show that jets inflate cavities in the hot gas that can excite g modes in the cluster atmosphere and heat the gas, while Roychowdhury et al. (2004) explore a model in which the bubbles are buoyant and heat the atmosphere by doing $p\mathrm{d}V$ work as they rise.

Recent years have seen numerous implementations of detailed models of galaxy formation incorporating AGN feedback (Scannapieco and Oh 2004; Croton et al. 2006; Bower et al. 2006; Cattaneo et al. 2006; Somerville et al. 2008b). These have shown that AGN feedback can explain the long standing issue of the exponential break in the galaxy luminosity function (without AGN feedback such models tend to produce far too many bright galaxies; Benson et al. 2003) and helps produce a bimodal distribution of galaxy colors (as AGN feedback makes massive galaxies "red and dead"). These models typically assume a "radio mode" feedback in which the AGN drives jets out of the galaxy while in a radiatively quiet state. Benson and Babul (2009) give an expression for the jet power produced by a spinning black hole accreting from a geometrically thick accretion flow[29] relevant to this situation. As a result this type of AGN feedback is effective only when there is a quasi-hydrostatic atmosphere of hot gas in a dark matter halo for it to couple to. Therefore, AGN feedback only works in the virial shocking regime, resulting in it being important above a critical halo mass of order $10^{12}M_\odot$ (with a weak redshift dependence).

6.4. Chemical Enrichment

The first generation of stars (known as Population III) and galaxies must have formed from primordial gas which is (almost) metal free. Stellar nucleosynthesis and subsequent pollution of the ISM and IGM (through stellar winds and supernovae explosions) with heavy elements has a significant impact on later generations of galaxies. In particular, the presence of heavy elements significantly alters the rate at which gas can cool (see §3.2) and leads to the formation of dust which both attenuates optical and UV light from galaxies and re-emits that light at longer wavelengths. To accurately model the properties of galaxies therefore requires a treatment of chemical enrichment.

The fraction of material returned to the ISM by a stellar population as a function of time is given by

$$R(t) = \int_{M(t;Z)}^{M_\mathrm{u}} [M - M_\mathrm{r}(M;Z)]\phi(M)\frac{\mathrm{d}M}{M} \tag{109}$$

where $\phi(M)$ is the initial mass function normalized to unit stellar mass and $M_\mathrm{r}(M)$ is the remnant mass of a star of initial mass M. Here, $M(t)$ is the mass of a star with lifetime t. Figure 11 shows the fraction of material recycled to the interstellar medium from a single stellar population as a function of time, t, since the birth of that population. Typical Pop. II initial mass functions (e.g. Salpeter 1955; Chabrier 2003) lead to around 40% of mass being recycled after 10 Gyr, dropping to around 30% at 1 Gyr. A Pop. III initial mass function recycles much more mass (since it consists of much more massive stars), recycling 70% of the mass within a few tens of millions of years.

Similarly, the yield of element i is given by

$$y_i(t) = \int_{M(t;Z)}^{M_\mathrm{u}} M_i(M_0;Z)\phi(M_0)\frac{\mathrm{d}M_0}{M_0} \tag{110}$$

where $M_i(M_0;Z)$ is the mass of metals produced by stars of initial mass M_0. For a specified IMF we can compute $y_i(t;Z)$ for all times and elements of interest. Figure 12 shows examples of the total metal yield for Pop. II and Pop. III initial mass functions. Typical total metal yields for Pop. II are around 0.04 increasing to 0.1 for the Pop. III initial mass function shown here. Stellar data are taken from Portinari et al. (1998) for low and intermediate mass stars and Marigo (2001) for high mass stars.

In many cases, the process of chemical enrichment has been simplified by adopting the instantaneous recycling approximation, in which mass and metals are assumed to be returned to the interstellar medium instantaneously after

[29] The jet power from a hole accreting from a thin accretion disk is much lower, due to the much weaker magnetic field in such a disk.

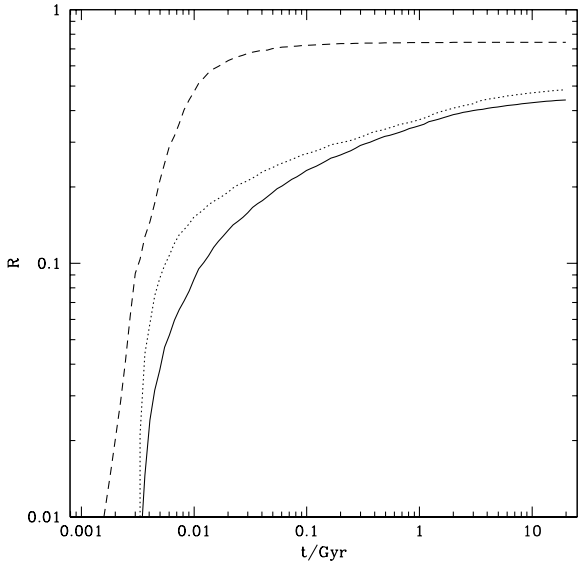

Figure 11: The fraction of mass from a single stellar population born at time, $t = 0$, recycled to the interstellar medium after time t. Solid and dotted lines show results for a Chabrier initial mass function with zero and Solar metallicity respectively, while the dashed line shows results for zero metallicity (Pop. III) stars with a lognormal IMF (case A from Tumlinson 2006).

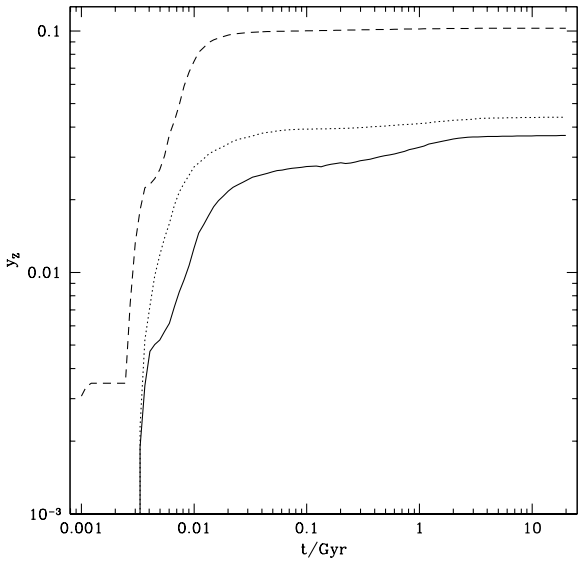

Figure 12: The total metal yield from a single stellar population born at time, $t = 0$, after time t. Solid and dotted lines show results for a Chabrier initial mass function with zero and Solar metallicity respectively, while the dashed line shows results for zero metallicity (Pop. III) stars with a lognormal IMF (case A from Tumlinson 2006).

the formation of a population of stars (essentially assuming that stellar evolution happens instantaneously). Typically, the recycled fractions and yields are evaluated at some time, t, of order the age of the Universe. This approximation is reasonable at late times, when the ages of typical stellar populations in galaxies is several Gyr. For example, Fig. 12 shows that the metal yield is approximately constant after about 0.1 Gyr, although the recycled fraction (see Fig. 11) does not converge so rapidly. The advantage of the instantaneous recycling approximation is that it greatly simplifies the equations governing chemical enrichment such that we have

$$R(t) = \int_{M(t_{\rm ira};Z)}^{M_{\rm u}} [M - M_{\rm r}(M;Z)]\phi(M)\frac{{\rm d}M}{M} \equiv R \tag{111}$$

with a similar result for yields. The normal convolution integral to determine the rate of return of mass to the interstellar medium,

$$\dot{M}_{\rm R}(t) = \int_0^t \dot{R}(t-t')\dot{M}_\star(t'){\rm d}t', \tag{112}$$

then simplifies to

$$\dot{M}_{\rm R}(t) = R\dot{M}_\star(t). \tag{113}$$

This removes the need for knowledge of the entire star formation history of a galaxy to determine the rate of recycling (which can greatly reduce computational demand in numerical models of galaxy formation).

While the instantaneous recycling approximation has its advantages, it is, of course, an approximation and one which breaks down in regimes of rapid star formation and at high redshifts where stars are much less than 10 Gyr old (since the Universe itself is very young). Detailed models of chemical evolution are well established within the monolithic collapse scenario (Matteucci and Greggio 1986; Matteucci and Gibson 1995; Timmes et al. 1995; François et al. 2004; Pipino and Matteucci 2004, 2006; Romano et al. 2005), but have only received limited study within the physically motivated context of hierarchical galaxy formation. Numerous hydrodynamical simulation codes now contain implementations of chemical enrichment (Scannapieco et al. 2005; Kobayashi et al. 2007; Pontzen et al. 2008; Gnedin et al. 2009). Semi-analytic models of galaxy formation are beginning[30] to implement detailed chemical enrichment models also (Nagashima et al. 2005a,b; Pipino et al. 2008; Arrigoni et al. 2009). Within the context of hierarchical structure formation models such chemical enrichment modeling has been shown to be in agreement with measurements of the intracluster medium metallicities of individual elements (Nagashima et al. 2005a), to reproduce the observed trend of metallicity and [α/Fe] with stellar mass in elliptical galaxies (Arrigoni et al. 2009) and to reproduce the measured distribution of metallicities in damped Lyman-α systems (Pontzen et al. 2008).

6.5. Stellar Populations

Observational studies of galaxies make use of radiation emitted by them (or, sometimes, the lack of radiation due to absorption by galaxies) to infer their physical properties. As such, it is often crucial to be able to compute the emergent spectrum from each galaxy in a theoretical model. This is two-step process, involving first computing the spectrum of light emitted by all of the stars (and possibly the AGN) in the galaxy and, secondly, computing how this light is reprocessed by the gas and dust in the galaxy and along the line of sight from the galaxy to the observer.

6.5.1. Steller Population Synthesis

In the absence of absorbing dust or gas, the luminosity as a function of frequency for a galaxy, the spectral energy distribution (SED), is simply a sum over the SEDs of its constituent stars. We can imagine a galaxy as consisting of

[30] Implementation of chemical enrichment models of this type is, in many ways, significantly easier in N-body simulations than in semi-analytic models. N-body simulations that include star formation typically spawn new star particles during each timestep to represent the stars formed at that time. Each particle can therefore be trivially tagged with a formation time and metallicity. On subsequent timesteps the rate of mass and metal return from that particle is easily computed and applied to surrounding gas particles for example. Semi-analytic models on the other hand have traditionally not recorded the full star formation history of each galaxy (due to computational resource requirements) as is needed to compute the chemical enrichment at each timestep. This can, of course, be done, as we are now seeing.

numerous "simple stellar populations"—populations of stars of the same age, metallicity and initial mass function. The luminosity, $L_\nu^{(\mathrm{galaxy})}$, of a galaxy at frequency ν is then simply given by the following convolution integral

$$\begin{aligned} L_\nu^{(\mathrm{galaxy})} &= \int_0^t \mathrm{d}t' \int_0^\infty \mathrm{d}Z' \dot{M}_\star(t', Z') \\ &\quad \times L_\nu^{(\mathrm{SSP})}(t - t', Z', \phi) \end{aligned} \tag{114}$$

where $\dot{M}_\star(t, Z)$ is the rate of formation of stars of metallicity Z in the galaxy at time t and $L_\nu^{(\mathrm{SSP})}(t, Z, \phi)$ is the luminosity of a simple stellar population of age t, metallicity Z and with initial mass function $\phi(M)$. Given a model which predicts the rate of star formation in a galaxy as a function of time and metallicity (which is the galaxy formation aspect of this calculation), the problem is reduced to determining suitable $L_\nu^{(\mathrm{SSP})}$ (the stellar astrophysics aspect of the calculation). This, in turn depends upon the spectra of individual stars, $L_\nu^{(\mathrm{star})}(t, Z)$, and the stellar initial mass function, $\phi(M)$, such that

$$L_\nu^{(\mathrm{SSP})}(t, Z, \phi) = \int_{M_{\mathrm{min}}}^{M_{\mathrm{max}}} \phi(M') L_\nu^{(\mathrm{star})}(t, Z) \mathrm{d}M', \tag{115}$$

where M_{min} and M_{max} are the minimum and maximum masses for stars respectively.

Several libraries exist which provide $L_\nu^{(\mathrm{SSP})}(t, Z, \phi)$ for several different ages, metallicities and initial mass functions (Bruzual and Charlot 2003; Maraston 2005; Dotter et al. 2007; Conroy et al. 2008; Lee et al. 2009). These are constructed using a combination of theoretical stellar evolution models, observations of stars of known age and metallicity and theoretical models of stellar atmospheres where no good observations exist. While enormous progress has been made in understanding the spectra of stars significant uncertainties remain. For example, Conroy et al. (2008), who performed a study of how uncertainties in such models propagate into constraints derived from galaxy observations, find that current models do not fully characterize the metallicity dependence of the thermally pulsating asymptotic giant branch phase and that uncertainties in the slope of the initial mass function[31] lead to an uncertainty in the evolution of the K-band magnitude of a stellar population of around 0.4 magnitudes per unit redshift (which leads to significant uncertainty when trying to interpret or predict the evolution of galaxy populations).

6.5.2. Dust Absorption and Re-emission

The presence of dust in galaxies has been known for a long time, and the effects of this dust on the observed properties of galaxies have been extensively studied. Simply put, dust absorbs light emitted by stars (and AGN), particularly at short wavelengths, is heated by this light and therefore re-emits it at longer wavelengths (typically in the infrared and sub-mm). The presence of dust in galaxies can therefore significantly affect their observed luminosities at optical and UV wavelengths. Models of galaxy formation must therefore take into account the effects of dust before comparing their predictions to observational data. The simplest such approach, adopted by many early models, is a "obscuring screen" or "slab" geometry, in which a plane of dust is placed in front of the model galaxy, given an extinction curve measured from the Milky Way (for example) and normalized to have an optical depth at optical wavelengths based on properties of the model galaxy (gas content and metallicity). This provides a simple estimate of the amount of extinction, but clearly does not reflect the true geometry of the dust (which is distributed throughout the galaxy) or the fact that stars may preferentially form in dense, dust regions.

Cole et al. (2000) introduced a model for dust extinction in galaxies which significantly improved upon earlier "slab" models. In Cole et al. (2000) the mass of dust is assumed to be proportional to the mass and metallicity of the ISM and to be mixed homogeneously with the ISM (possibly with a different scale height from the stars) and to have properties consistent with the extinction law observed in the Milky Way. To compute the extinction of any galaxy, a random inclination angle is selected and the extinction computed using the results of radiative transfer calculations carried out by Ferrara et al. (1999).

Beyond these relatively simple models of dust extinction it has recently become possible to employ much more realistic ray tracing techniques to compute the effects of dust on galaxy spectra. For example, the Grasil software

[31] See Kroupa (2001) for a recent discussion of the difficulties associated with determining the local initial mass function. Kroupa (2001), along with Chary (2008) and van Dokkum (2008), also discuss evidence for the non-universality of the initial mass function, although no definitive evidence for such yet exists.

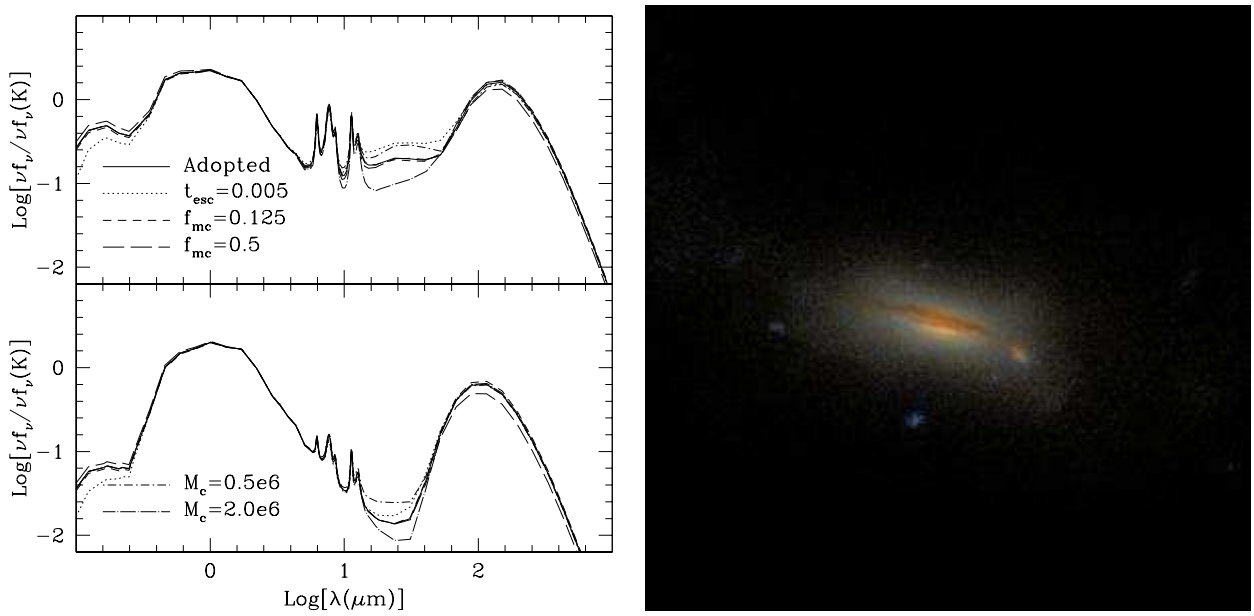

Figure 13: *Left-hand panel:* An example of the spectral energy distributions from two face-on spiral galaxies as computed by GRASIL (Granato et al. 2000). The SED shows direct emission from stars at short wavelengths, with reprocessed light emitted from dust at long wavelengths. In the intermediate region lines associated with PAHs are visible. Reproduced, with permission, from Granato et al. (2000). *Right-hand panel:* An image of a post-merger galaxy from a simulation by Cox et al. (2008) as computed by SUNRISE (Jonsson 2006). A complex dust morphology, including a strong dust lane, is clearly visible. Reproduced, with permission, from Cox et al. (2008).

(Silva et al. 1998) is designed to compute the radiative transfer of star light through an idealized galactic geometry consisting of a disk and a bulge each of which may contain both diffuse and clumpy gas and dust. GRASIL takes an input galactic SED together with physical parameters of a galaxy (size of each component, metallicity and mass of gas present) and computes the resulting SED including absorption, scattering and remission from the dust, taking into account a realistic distribution of grains and polycyclic aromatic hydrocarbons (PAHs) the temperature distribution of which are computed self-consistently, and assuming that stars are born in the dense molecular clouds and escape from these on some timescale (leading to enhanced absorption in the UV which is produced primarily by young stars) (Fig. 13). This code is therefore ideal for (semi-)analytic studies of galaxies and has been employed to examine the expected properties of submillimeter and infrared galaxies in hierarchical cosmologies (Granato et al. 2000; Baugh et al. 2004, 2005; Lacey et al. 2008; Swinbank et al. 2008).

Similarly, the SUNRISE code of Jonsson (2006) and RADISHE by Chakrabarti and Whitney (2009) solve essentially the same problem (radiative transfer through a dusty medium) but work for arbitrary geometry using Monte Carlo, polychromatic algorithms and so are particularly well suited to hydrodynamical simulations of galaxy formation, allowing realistic images of simulated galaxies to be made at any wavelength. SUNRISE has been applied to studies of luminous infrared galaxies (Younger et al. 2009), quantitative morphology of merger remnants (Lotz et al. 2008), physical models to infer star formation rates from molecular indicators (Narayanan et al. 2010) and tests of our ability to recover physical parameters of galaxies from their broadband SEDs (Wuyts et al. 2009).

Since these ray tracing methods are computationally expensive they cannot yet be applied to large samples of model galaxies. Therefore, attempts have been made to construct simpler algorithms which capture most of their results. For example, Gonzalez-Perez et al. (2008) extended the model of Cole et al. (2000) by assuming that some fraction, $f_{\rm cloud}$, of the dust is in the form of dense molecular clouds where the stars form (see Baugh et al. 2005). Stars were assumed to form in these clouds and to escape on a timescale of $\tau_{\rm quies}$ (for quiescent star formation in disks) or $\tau_{\rm burst}$ (for star formation in bursts), which is a parameter of the dust model (Granato et al. 2000). Since massive, short-lived stars dominate the UV emission of a galaxy this enhances the extinction at short wavelengths, so these stars spend a significant fraction of their lifetime inside the clouds.

To compute emission from dust they assumed a far infrared opacity of

$$\kappa = \begin{cases} \kappa_1(\lambda/\lambda_1)^{-\beta_1} & \text{for } \lambda < \lambda_{\rm break} \\ \kappa_1(\lambda_{\rm break}/\lambda_1)^{-\beta_1}(\lambda/\lambda_{\rm break})^{-\beta_2} & \text{for } \lambda > \lambda_{\rm break}, \end{cases} \tag{116}$$

where the opacity normalization at $\lambda_1 = 30\ \mu$m is chosen to be $\kappa_1 = 140{\rm cm}^2/{\rm g}$ to reproduce the dust opacity model used in Grasil, as described in Silva et al. (1998). The dust grain model in Grasil is a slightly modified version of that proposed by Draine and Lee (1984). Both the Draine and Lee (1984) and Grasil dust models have been adjusted to fit data on dust extinction and emission in the local ISM (with much more extensive ISM dust emission data being used by Silva et al. 1998). The normalization is set at 30μm because the dust opacity in the Draine and Lee (1984) and Grasil models is well fit by a power-law longwards of that wavelength, but not shortwards. The dust luminosity is then assumed to be

$$L_\nu = 4\pi\kappa(\nu)B_\nu(T)M_{\rm Z,gas}, \tag{117}$$

where $B_\nu(T) = [2{\rm h}\nu^3/{\rm c}^2]/[\exp({\rm h}\nu/{\rm k}T) - 1]$ is the Planck blackbody spectrum and $M_{\rm Z,gas}$ is the mass of metals in gas. The dust temperature, T, is chosen such that the bolometric dust luminosity equals the luminosity absorbed by dust.

This extended dust model, including diffuse and molecular cloud dust components, provides a better match to the detailed results of Grasil while being orders of magnitude faster, although it does not capture details such as PAH features.

Fontanot et al. (2009b) have explored similar models which aim to reproduce the results of Grasil using simple, analytic prescriptions. They found that by fitting the results from Grasil they were able to obtain a better match to the extinction in galaxies than previous, simplistic models of dust extinction had been able to attain.

6.6. Absorption by the Intergalactic Medium

In addition to having to pass through the internal gas and dust in each galaxy, light emitted from a galaxy must pass through the entire intervening intergalactic medium between it and ourselves before we can observe it. The intergalactic medium contains significant amounts of neutral hydrogen (even at relatively low redshifts, long after reionization) which is known to be clumped into clouds by virtue of observations of the Lyman-α forest of absorption systems in quasar spectra. Light emitted at redshift $z_{\rm em}$ at some wavelength $\lambda_{\rm em}$, shortwards of the Lyman-α wavelength of 1216Å, will eventually be redshifted into the Lyman-α line and so will be absorbed by any clouds of neutral hydrogen at redshift $1 + z_{\rm abs} = (1 + z_{\rm em})[\lambda_{\rm em}/1216{\rm Å}]$. Light emitted at even shorter wavelengths may be additionally absorbed by higher lines in the Lyman series, or by the Lyman continuum shortwards of 912Å.

Models of the effective optical depth due to this absorption (based upon the observed distribution of Lyman-α forest absorber properties) have been described by Madau (1995) and Meiksin (2006). The resulting absorption of starlight shortwards of Lyman-α is so severe that galaxies appear essentially dark at wavelengths shorter than $\lambda_{\rm obs} = 1216{\rm Å}(1 + z_{\rm em})$. This forms the basis of the "dropout" techniques for identifying high redshift galaxies and quasars on the basis of their broadband colors (Madau et al. 1996; Fan et al. 2001).

7. Computational Techniques

The process of galaxy formation involves nonlinear physics and a wide variety of physical processes. As such, it is impossible to treat in full detail using analytic techniques. There are two major approaches that have been developed to circumvent this problem. The first, numerical N-body simulation, attempts to directly and numerically solve the fully nonlinear equations governing the physical processes inherent to galaxy formation. The second, semi-analytic modeling, attempts to construct a coherent set of analytic approximations which describe these same physics. Each has its strengths and weaknesses, as will be discussed below. As a result of this and of our ignorance of how some key processes work, both approaches contain a little of each other (rather like yin yang). A different, more empirical approach, utilizing so-called "halo occupation distributions" has become widely used in the past ten years and will be discussed briefly below.

7.1. N-body/Hydro

The most accurate computational method for solving the physics of galaxy formation is via direct simulation, in which the fundamental equations of gravitation, hydrodynamics and perhaps radiative cooling and transfer are solved far a large number of points (arranged either on a grid or following the trajectories of the fluid flow). I will not attempt to review the numerical methods utilized in this approach in any detail here (recent treatments of this can be found in Bertschinger 1998; Agertz et al. 2007; Rosswog 2009), but will instead merely highlight some of the approaches used.

Collisionless dark matter is (relatively) simple to model in this way, since it responds only to the gravitational force. For the velocities and gravitational fields occurring during structure and galaxy formation non-relativistic Newtonian dynamics is more than adequate and so solving the evolution of some initial distribution of dark matter (usually a Gaussian random field of density perturbations consistent with the power spectrum of the CMB) reduces to summing large numbers of $1/r^2$ forces between pairs of particles. In practice, clever numerical techniques (such as particle–mesh, tree algorithms etc.) are usually used to reduce this N^2 problem into something more manageable (Kravtsov et al. 1997; Springel 2005). The largest pure dark matter simulations carried out to date contain around 10 billion particles (Springel et al. 2005b). Dark matter only simulations of this type (carried out primarily for the cold dark matter scenario, but see White et al. 1984; Klypin et al. 1993; Bode et al. 2001; Davé et al. 2001; Colín et al. 2002; Ahn and Shapiro 2005) have been highly successful in determining the large scale structure of the Universe, as embodied in the so-called "cosmic web". As a result, the spatial and velocity correlation properties of dark matter and dark matter halos (Davis et al. 1985; White et al. 1987a,b; Efstathiou et al. 1988; Eke et al. 1996; Jenkins et al. 1998; Padilla and Baugh 2002; Bahcall et al. 2004; Kravtsov et al. 2004; Reed et al. 2009), together with the density profiles (Navarro et al. 1997; Bullock et al. 2001b; Navarro et al. 2004; Merritt et al. 2005; Prada et al. 2006), angular momenta (Barnes and Efstathiou 1987; Efstathiou et al. 1988; Warren et al. 1992; Cole and Lacey 1996; Lemson and Kauffmann 1999; Bullock et al. 2001a; van den Bosch et al. 2002; Bett et al. 2007; Gao et al. 2008) and internal structure (Moore et al. 1999; Klypin et al. 1999; Kuhlen et al. 2008; Springel et al. 2008) of dark matter halos are known to very high accuracy.

Of course, to study galaxy formation dark matter alone is insufficient, and baryonic material must be added in to the mix. This makes the problem much more difficult since, at the very least, pressure forces must be computed and the internal energy of the baryonic fluid tracked. Particle-based methods (most prominently smoothed particle hydrodynamics; Springel 2005) have been successful in this area, as have Eulerian grid methods (Ricker et al. 2000; Fryxell et al. 2000; Plewa and Müller 2001; Quilis 2004). The addition of radiative cooling is relatively straightforward (at least while the gas remains optically thin to its own radiation) by simply tabulating the rate at which gas of given density and temperature radiates energy.

Going beyond this level of detail becomes extremely challenging. Numerous simulation codes are now able to include star formation and feedback from supernovae explosions, while some even attempt to follow the formation of supermassive black holes in galactic centers. It should be kept in mind though that for galaxy scale simulations the real physics of these processes is happening on scales well below the resolution of the simulation and so the treatment of the physics is often at the "subgrid" level, which essentially means that it is put in by hand using a semi-analytic approach (Thacker and Couchman 2000; Kay et al. 2002; Marri and White 2003; White 2004; Stinson et al. 2006; Cox et al. 2006; Scannapieco et al. 2006a; Tasker and Bryan 2006; Stinson 2007; Vecchia and Schaye 2008; Oppenheimer and Davé 2008; Okamoto et al. 2008b; Booth and Schaye 2009; Ciotti 2009).

Beyond this, problems such as the inclusion of radiative transfer or magnetic fields complicate the problem further by introducing new sets of equations to be solved and the requirement to follow additional fields. For example, in radiative transfer one must follow photons (or photon packets) which have a position, direction of travel and wavelength, and determine the absorption of these photons as they traverse the baryonic material of the simulation, while simultaneously accounting for the re-emission of absorbed photons at other wavelengths. Despite these complexities, progress has been made on these issues using a variety of ingenious numerical techniques (Abel et al. 1999; Ciardi et al. 2001; Gnedin and Abel 2001; Ricotti et al. 2002; Petkova and Springel 2009; Li et al. 2008; Aubert and Teyssier 2008; Collins et al. 2009; Dolag and Stasyszyn 2008; Finlator et al. 2009; Laursen et al. 2009). Providing Moore's Law continues to hold true, the ability of simulations to provide ever more accurate pictures of galaxy formation should hold strong. A brief survey of current cosmological hydrodynamical codes and their functionalities is given in Table 1.

Table 1: A survey of physical processes included in several of the major hydrodynamical codes. The primary reference is indicated next to the name of the code. Where implementations of major physical processes are described elsewhere the reference is given next to the entry in the relevant row.

Feature	GADGET-3[1]	GASOLINE[2]	HART[3]	ENZO(ZEUS)[4]	FLASH[5]
Gravity	Tree	Tree	AMR[6] PM[7]	AMR[6] PM[7]	Multi-grid
Hydrodynamics	SPH[8]	SPH[8]	AMR[6]	AMR[6]	AMR[6]
→ Multiphase subgrid model[9]	✓[10]	×	N/A	N/A	N/A
Radiative Cooling	✓	✓	✓	✓	✓[11]
→ Metal dependent	✓[12]	×	✓[13]	✓[14]	✓[11]
→ Molecular chemistry	✓[15]	×	✓[13,16]	✓[17]	×
Thermal Conduction	✓[18]	×	×	×	✓
Star formation	✓[19]	✓[20]	✓[13]	✓[21]	×
→ SNe feedback	✓[19]	✓[20]	✓[13]	✓[21]	×
→ Chemical enrichment	✓[19]	✓[20]	✓[13]	✓[21]	×
Black hole formation	✓[22]	×	×	×	✓[23]
→ AGN feedback	✓[22]	×	×	×	×
Radiative transfer	OTVET[24,25]	×	OTVET[24]	✓[26]	✓[27]
Magnetic fields	✓[28]	×	×	✓[29]	✓[30]

Notes

[1]"GAlaxies with Dark matter and Gas intEracT" (Springel, 2005);
[2]Wadsley et al. (2004);
[3]Hydrodynamic Adaptive Refinement Tree (Kravtsov et al., 2002);
[4]O'Shea et al. (2004);
[5]`http://flash.uchicago.edu` (Fryxell et al., 2000);
[6]Adaptive Mesh Refinement;
[7]Particle–mesh;
[8]Smoothed Particle Hydrodynamics;
[9]Applicable only to SPH codes—used correctly, AMR codes naturally resolve multiphase media;
[10]Scannapieco et al. (2006a);
[11]Banerjee et al. (2006);
[12]Scannapieco et al. (2005);
[13]Tassis et al. (2008);
[14]Smith et al. (2009);
[15]Yoshida et al. (2003);
[16]Equilibrium only;
[17]Turk (2009);
[18]Jubelgas et al. (2004);
[19]Scannapieco et al. (2005);
[20]Governato et al. (2007);
[21]Tasker and Bryan (2008);
[22]Matteo et al. (2005);
[23]Federrath et al. (2010);
[24]Optically Thin Variable Eddington Tensor;
[25]Petkova and Springel (2009);
[26]Flux-limited diffusion approximation (Norman et al. 2009; see also Wise and Abel 2008b);
[27]Rijkhorst et al. (2006); Peters et al. (2010);
[28]Dolag and Stasyszyn (2008);
[29]Collins et al. (2009; see also Wang and Abel 2009);
[30]Robinson et al. (2004);

7.2. Semi-Analytic

The technique of "semi-analytic modeling" or, perhaps, "phenomenological galaxy formation modeling" takes the approach of treating the various physical processes associated with galaxy formation using approximate, analytic techniques. As with N-body/hydro simulations, the degree of approximation varies considerably with the complexity of the physics being treated, ranging from precision-calibrated estimates of dark matter merger rates to empirically motivated scaling functions with large parameter uncertainty (e.g. in the case of star formation and feedback—just as in N-body/hydro simulations).

The primary advantage of the semi-analytic approach is that it is computationally inexpensive compared to N-body/hydro simulations. This facilitates the construction of samples of galaxies orders of magnitude larger than possible with N-body techniques and for the rapid exploration of parameter space (Henriques et al. 2009) and model space (i.e. adding in new physics and assessing the effects). The primary disadvantage is that they involve a larger degree of approximation. The extent to which this actually matters has not yet been well assessed. Comparison studies of semi-analytic vs. N-body/hydro calculations have shown overall quite good agreement (at least on mass scales well above the resolution limit of the simulation) but have been limited to either simplified physics (e.g. hydrodynamics and cooling only; Benson et al. 2001b; Yoshida et al. 2002; Helly et al. 2003b) or to simulations of individual galaxies (Stringer et al. 2010).

Some of the earliest attempts to construct a self-consistent semi-analytic model of galaxy formation began with White and Frenk (1991), Cole (1991) and Lacey and Silk (1991), drawing on earlier work by Rees and Ostriker (1977) and White and Rees (1978). Since then numerous studies (Kauffmann et al. 1993; Baugh et al. 1999b, 1998; Somerville and Primack 1999; Cole et al. 2000; Benson et al. 2002a; Hatton et al. 2003; Monaco et al. 2007) have extended and improved this original framework. A recent review of semi-analytic techniques is given by Baugh (2006). Semi-analytic models have been used to investigate many aspects of galaxy formation including:

- galaxy counts (Kauffmann et al. 1994; Devriendt and Guiderdoni 2000);
- galaxy clustering (Diaferio et al. 1999; Kauffmann et al. 1999a,b; Baugh et al. 1999a; Benson et al. 2000c,a; Wechsler et al. 2001; Blaizot et al. 2006);
- galaxy colors and metallicities (Kauffmann and Charlot 1998; Springel et al. 2001; Lanzoni et al. 2005; Nagashima et al. 2005b; Font et al. 2008);
- sub-mm and infrared galaxies (Guiderdoni et al. 1998; Granato et al. 2000; Baugh et al. 2005; Lacey et al. 2008);
- abundance and properties of Local Group galaxies (Benson et al. 2002b; Somerville 2002; Li et al. 2010);
- the reionization of the Universe (Devriendt et al. 1998; Benson et al. 2001a; Somerville and Livio 2003; Benson et al. 2006);
- the heating of galactic disks (Benson et al. 2004);
- the properties of Lyman-break galaxies (Governato et al. 1998; Blaizot et al. 2003, 2004; Lacey et al. 2010);
- supermassive black hole formation and AGN feedback (Kauffmann and Haehnelt 2000; Croton et al. 2006; Bower et al. 2006; Malbon et al. 2007; Somerville et al. 2008b; Fontanot et al. 2009a);
- damped Lyman-α systems (Maller et al. 2001, 2003);
- the X-ray properties of galaxy clusters (Bower et al. 2001, 2008);
- chemical enrichment of the ICM and IGM (Lucia et al. 2004; Nagashima et al. 2005a);
- the formation histories and morphological evolution of galaxies (Kauffmann 1996; Lucia et al. 2006; Fontanot et al. 2007; Somerville et al. 2008a).

The term "semi-analytic" model has become somewhat insufficient, since this name now encompasses such a diverse range of models that the name alone does not convey enough information. Semi-analytic models in the literature contain a widely disparate range of physical phenomena and implementations. Table 2 is an attempt to assess in detail the physics included in currently implemented semi-analytic models[32].

7.3. Halo Occupation Distributions

Given the complexity of galaxy formation it is sometimes desirable to take a more empirical approach to the problem. This can be advantageous both to relate observations to the assumed underlying physical structure of the Universe (e.g. Zheng et al. 2007; Tinker et al. 2010), and to make predictions based on extrapolations from current data and which have a cosmological underpinning. "Halo occupation distributions", first described by Neyman and Scott (1952) and used to study galaxy clustering (see, for example, Benson et al. 2000c; Peacock and Smith 2000) in their simplest form specify the probability of finding N galaxies of some prescribed type in a dark matter halo of mass M, $P(N|M)$. Given this probability distribution, knowledge of the distribution of dark matter halo masses and their spatial distribution plus some assumptions about the locations of galaxies within halos, one can construct (statistically or within an N-body simulation) the distribution of galaxies. This allows, for example, the abundance and clustering properties of those galaxies to be inferred. A detailed discussion of the use of halo occupation distributions in studying galaxy clustering is given by Cooray and Sheth (2002).

This approach has recently been extended by incorporating simple prescriptions relating, for example, star formation rates or quasar activity to halo mass and redshift. Several authors have demonstrated that such empirical models, while simple, can fit a wide variety of galaxy data and can be used to gain insight into phenomena such as "downsizing" (Yang et al., 2003; Conroy and Wechsler, 2009; Croton, 2009). At a fundamental level, the success of simple, empirical models such as these suggests that, despite the complexity of galaxy formation physics, its outcome is relatively simple.

8. Topics of Current Interest

Having reviewed the major inputs to our current theory of galaxy formation and explored some of the tools employed to solve them, in this section we briefly explore five topics of particular interest in contemporary galaxy formation theory.

8.1. The First Galaxies

After the initial excitement of the Big Bang, inflation, nucleosynthesis and the recombination the Universe enters a protracted period of relative quiescence, known as the "Dark Ages", during which there are no luminous sources and structure grows primarily only in the dark sector. The end of the Dark Ages is thought to occur when the first star forms. The formation of these first stars is an unusual problem in astrophysics in that it represents a clean, well-defined problem that can be tackled numerically—the initial conditions are simply those of an expanding Universe containing small perturbations in the dark matter and baryonic components which is a simple mixture of hydrogen and helium. As such, this problem has been examined and explored in significant detail (Abel et al. 2002; Yoshida et al. 2006; Gao et al. 2007). The consensus picture that has emerged from this work is that the first star will form due to gas collapse and cooling (via the gas-phase formation of molecular hydrogen) in a halo of mass around $10^6 M_\odot$ at a redshift of $z \approx 50$. The first star is likely to be very massive (current simulations cannot follow the evolution of the proto-star beyond the point at which it becomes optically thick in various lines of molecular hydrogen due to a lack of treatment of the necessary radiative transfer, but at this stage the collapsing core typically has an accretion rate that is expected to lead to the formation of a star with a mass of several tens of Solar masses) and, therefore, short lived. What happens after this first star forms rapidly becomes a much more complicated problem, involving the poorly understood physics of supernovae explosions and the numerically challenging problem of radiative transfer.

[32] One component missing from Table 2 is the specific implementation of stellar population synthesis used by each code. We have chosen to not include this because all the models listed treat this calculation in precisely the same way (see §6.5.1), differing only in which compilation of stellar spectra they choose to employ. Since it is trivial to replace one compilation of stellar spectra with another we do not consider this a fundamental difference between the models. Nevertheless, the choice of which stellar spectra to use can have important consequences for the predicted properties of galaxies (Conroy and Gunn, 2010) and so should not be overlooked.

Table 2: A survey of physical processes included in major semi-analytic models of galaxy formation. In each case we indicate how this process is implemented and give references where relevant. In many cases a single model has implemented a given physical process at different levels of complexity/realism. In such cases, we list the most "advanced" implementation that the model is capable of.

	Model				
Feature	DURHAM[1]	MUNICH[2]	SANTA-CRUZ[3]	MORGANA[4]	GALICS[5]
Merger Trees					
→ Analytic	Modified ePS[6]	ePS[7]	ePS	PINOCCHIO[8]	×
→ N-body	✓[9]	✓	✓	×	✓
Halo Profiles	Einasto[10]	Isothermal	NFW	NFW	Empirical[11]
Cooling Model					
→ Metal-dependent	✓	✓	✓	✓	✓
Star Formation	✓	✓	✓	✓	✓
Feedbacks					
→ SNe	✓	✓	✓	✓	✓
→ AGN	✓[12]	✓	✓	✓	✓[13]
→ Reionization	✓[10]	×	✓	✓[14]	✓[15]
Merging					
→ Substructure[16]	N-body[17]	N-body[17]	DF[18]	DF[18]	N-body[17]
→ Substructure–Substructure[19]	✓[20,10]	×	✓[21,22]	×	✓[21]
Environments					
→ Ram Pressure Stripping	✓[23]	✓[24]	×	×	✓[25]
→ Tidal Stripping	✓[10]	×	✓	✓	✓
→ Harassment	×	×	×	×	×
Disks					
→ Disk Stability	✓	✓	✓[26]	✓	✓
→ Dynamical Friction[27]	✓[28]	×	×	×	×
→ Thickness	✓[28]	×	×	×	×
Sizes					
→ Adiabatic contraction	✓	×	✓	✓	×
Chemical Enrichment	✓ [delayed[10]]	✓ [instant[29]]	✓ [delayed[30]]	✓ [instant]	✓ [delayed[31]]
Dust	GRASIL[32]	Screen[33]	Slab[34]	GRASIL[32,35]	Slab[34]

Notes

[1]Cole et al. (2000);
[2]Croton et al. (2006);
[3]Somerville et al. (2008b);
[4]Monaco et al. (2007);
[5]Hatton et al. (2003);
[6]Parkinson et al. (2008);
[7]Kauffmann and White (1993);
[8]Monaco et al. (2002);
[9]Helly et al. (2003a);
[10]Benson and Bower (2010);
[11]A "dark matter" core is included in calculations of disk sizes with an empirically selected dark matter fraction;
[12]Bower et al. (2006);
[13]Cattaneo et al. (2006);
[14]Macció et al. (2009);
[15]Lanzoni et al. (2005);
[16]How does the model track substructures within halos?;
[17]Substructure orbits and merging times are determined from N-body simulations;
[18]Dynamical Friction: substructure merging times are computed from analytic estimates of dynamical friction timescales;
[19]Does the model allow merging between pairs of subhalos orbiting in the same host halo?;
[20]Using hierarchically nested substructures;
[21]Using random collisions of subhalos;
[22]Somerville and Primack (1999);
[23]Font et al. (2008);
[24]Brüggen and Lucia (2008);
[25]Lanzoni et al. (2005);
[26]Somerville et al. (2008a);
[27]Does the model include dynamical friction forces exerted by a galaxy disk on orbiting satellites?;
[28]Benson et al. (2004);
[29]Lucia et al. (2004);
[30]Arrigoni et al. (2009);
[31]Pipino et al. (2008);
[32]Silva et al. (1998);

Needless to say then, studying the formation of the first galaxies is more complicated still, although no more complicated than modeling the formation of later generations. In the next decade new facilities such as JWST and thirty meter class telescopes will begin to open a window on the earliest generations of galaxies and, as such, there is a need for theoretical understanding and predictions for this epoch of cosmic history. In particular, this represents a real opportunity to make testable predictions from galaxy formation theory which can be confronted with data in the near future.

In considering the earliest generations of galaxies there are various physical processes which, while often neglected at lower redshifts, are of potentially crucial importance. For example, understanding the properties of Population III stars, their various feedback processes (both positive and negative) and initial mass function (Glover and Abel 2008; Trenti and Stiavelli 2009; Ohkubo et al. 2009; Machida et al. 2008; Lawlor et al. 2008; O'Shea and Norman 2007, 2008; Harris et al. 2007; Stacy and Bromm 2007) may be crucial for understanding how this population of galaxies grows (Tegmark et al. 1997; Ricotti et al. 2001; Wise and Abel 2007a,b; Greif et al. 2008; Wise and Abel 2008b; Wise et al. 2008; Bromm et al. 2009). Additionally, connecting these galaxies to later generations involves understanding how they evolve through (and cause) the epoch of cosmic reionization (Benson et al. 2002a; Alvarez et al. 2008), modeling non-local feedbacks (i.e. interactions between neighboring galaxies or the galaxy population as a while) and feedbacks in general (Busha et al. 2009).

Various interesting questions await definitive answers. For example, how long is the period of Population III star formation? This seemingly simple question depends on how we define Population III—theoretical reasoning suggests that we may expect a significant shift in the initial mass function once gas is raised above a critical metallicity of $10^{-4}Z_{\odot}$ (Santoro and Shull 2006) and the ability of Population III stars to enrich their surroundings (and, therefore, future generations of star formation). Since Population III stars are likely to produce many more hydrogen ionizing photons per unit mass than their Population II counterparts this question may have important consequences for the reionization history of the Universe.

Reionization itself remains an interesting problem. While it has been convincingly demonstrated theoretically (Chiu and Ostriker 2000; Ciardi et al. 2003; Somerville et al. 2003; Benson et al. 2006) that the universe could be reionized by galaxies sufficiently early to match constraints on the optical depth to the CMB (Dunkley et al. 2009) these calculations are currently forced to make assumptions about the distribution of mass and ionized regions in the IGM and about the ionizing photon escape probability from high redshift galaxies (Dove et al. 2000; Ricotti and Shull 2000; Razoumov and Sommer-Larsen 2006; Gnedin et al. 2008; Yajima et al. 2009; Wise and Cen 2009) which are still poorly understood.

In addition to observing high redshift galaxies directly, it may be possible to learn much about them from the study of their present day remnants. "Galactic archeology" of this sort has been investigated quite extensively (Freeman and Bland-Hawthorn 2002; Scannapieco et al. 2006b; Brook et al. 2007).

The conclusions are that Population III stars (usually taken as a convenient proxy for "first galaxies") that formed in progenitor galaxies of the Milky Way likely formed over a fairly broad range of redshifts, with the formation rate peaking at $z \approx 10$ but continuing until $z \approx 4$–5 (in chemically isolated halos which have not been contaminated by metals produced by star formation in earlier forming halos). As such, any remnants of these stars are probably spread over most of the nearby Galactic halo. The lack of detection of such metal-free stars therefore places constraints on their initial mass function—they must have been sufficiently massive to have evolved off of the main sequence by the present day. Currently, this suggests that such stars must have been more massive then about $0.8M_{\odot}$ (Brook et al. 2007). If we examine truly old stars, however, the situation is rather different. Simulations suggest that these formed in halos close to the high density peak that eventually formed the final system, and therefore are preferentially located in the central regions (typically the bulge) of the Milky Way.

8.2. The Formation and Sizes of Galaxy Disks

Galactic disks are, perhaps, the most prominent feature of galaxies in the local Universe. Additionally, recent observations (Law et al. 2009; Schreiber et al. 2009) have demonstrated that massive disks are already in place as long ago as $z = 2$. Understanding the details of how disks form and grow is therefore of crucial importance for galaxy formation theory (Silk 2001).

The basic picture has been in place for a long time (Fall and Efstathiou 1980). Collapsing systems of dark matter and gas are imparted some small amount of angular momentum as a result of tidal torques from inhomogeneities

in the surrounding matter distribution (Hoyle 1949; Barnes and Efstathiou 1987). While gas can radiate energy and thereby collapse to form a galaxy it cannot radiate angular momentum. As such, angular momentum is conserved[33] during the collapse and is eventually responsible for halting that collapse when the proto-galaxy reaches a radius at which its angular momentum is sufficient to provide support against the gravitational potential in which it resides. Back of the envelope type estimates of the resulting sizes of disks show that this picture produces disks with sizes comparable to those that are observed (Fall and Efstathiou 1980; Mo et al. 1998). However, this basic picture makes several simplifying assumptions, some of them difficult to justify. A careful analysis of these assumptions is therefore warranted to understand the process of disk formation in greater detail.

It has been convincingly established that the distribution of angular momentum of gas in halos prior to any cooling and galaxy formation is similar to that of the dark matter (van den Bosch et al. 2002, 2003) in so far as the distribution of spin parameters is very similar (the directions of the angular momenta vectors of dark matter and gas are often misaligned; van den Bosch et al. 2002). The distribution of the angular momentum of gas within an individual halo is less well studied, but recent hydrodynamical simulations (Sharma and Steinmetz 2005) have demonstrated that the distribution of the specific angular momentum, j, can be well described by a simple form:

$$\frac{1}{M}\frac{\mathrm{d}M}{\mathrm{d}j} = \frac{1}{j_{\rm d}^{\alpha_j}\Gamma(\alpha_j)} j^{\alpha_j-1}\mathrm{e}^{-j/j_{\rm d}}, \tag{118}$$

where Γ is the gamma function, M is the total mass of gas, $j_{\rm d} = j_{\rm tot}/\alpha$ and $j_{\rm tot}$ is the mean specific angular momentum of the gas. The parameter α_j takes on different values in different halos, with a median value of 0.89. The fraction of mass with specific angular momentum less than j is then given by

$$f(<j) = \gamma\left(\alpha_j, \frac{j}{j_{\rm d}}\right), \tag{119}$$

where γ is the incomplete gamma function. Despite this knowledge of the initial distribution of angular momentum in the baryonic component, the question of how well angular momentum is conserved during the process of cooling and collapse is less clear. However, recent simulation studies have begun to shed some light on this issue. Zavala et al. (2008) describe high resolution SPH simulations in which the baryonic physics (particularly the star formation and feedback from supernovae) is varied such that one simulation results in the formation of a disk galaxy and another in the formation of a spheroidal galaxy. They show that, in the case of the disk galaxy the angular momentum of the baryonic material that will eventually form the galaxy tracks the behavior of the dark matter angular momentum: growing as predicted by linear theory at early times and then remaining constant. In the case of the spheroidal galaxy, the angular momentum still grows initially as expected from linear theory, but then 90% is rapidly lost as pre-galactic fragments undergo mergers which transfer their angular momentum to the dark matter. In the disk galaxy case, strong feedback prevents gas from cooling into these small halos at early times, and so avoids angular momentum loss to the dark halo.

In addition to macroscopic quantities such as the size of a disk, the picture described above can predict the radial density profiles of disks. This is interesting since observed disks typically follow an exponential radial profile (at least out to some radius, beyond which the stellar light profile typically truncates—gaseous disks typically extend out further beyond this stellar truncation radius). In a hierarchical Universe, in which dark matter halos and their gas content grow in mass and size with time, the angular momentum of material accreting onto a galaxy will, on average, increase with time also. As a result, disk formation is an "inside out" process, with early infall leading to the formation of the inner regions of the disk and later infall adding primarily to the outer regions. Knowing the distribution of specific angular momenta of the gas from which the disk formed it is possible to determine the distribution of radii at which that gas will settle and, consequently, the radial density profile. Of course, this assumes that the angular momenta of gas elements are unchanged after they arrive in the disk. In reality this may not be the case—viscosity in a gaseous disk may redistribute angular momentum and even in a purely stellar disk stars can scatter from perturbations such as spiral density waves and thereby change their angular momentum and may help to establish the exponential radial

[33] It is conserved if we ignore the possibility of torques between baryons and dark matter which could transfer angular momentum from the gas to the dark halo. We will review this assumption later.

profile if the viscous timescale is of order the star formation timescale (Silk and Norman 1981; Lin and Pringle 1987; Clarke 1989, 1991; Firmani et al. 1996). Current results suggest that exponential disks can plausibly arise given our present understanding of the initial distribution of angular momentum, star formation efficiency and supernovae feedback without the need for viscous redistribution of angular momentum (Dutton 2009; Stringer et al. 2010), although the detailed properties (e.g. scale length distributions) of the disks do not necessarily agree perfectly with what is observed (Dutton et al. 2007). Of course, comparison with measurements of stellar disks requires determination of not just the mass density profile but the stellar density profile. Star formation will proceed most rapidly where the gas is densest (i.e. in the inner regions of the disk) and may be inhibited altogether at larger radii where the background radiation can prevent the formation of molecular hydrogen and where the disk may become stable to perturbations and so unable to form molecular cloud complexes (Martin and Kennicutt 2001; Schaye 2004).

The assumption that the angular momentum distribution of the disk remains constant after formation is not precisely correct even in the absence of hydrodynamical effects such as viscosity. Stars in a disk can interact with perturbations such as spiral density waves, exchanging energy and angular momentum with them. Sellwood and Binney (2002) show that interactions between stars and spiral waves at the corotation resonance lead to an exchange of energy and angular momentum that changes the radius of a star's orbit while keeping it circular. A star can, in principle, interact with multiple spiral waves and thereby migrate over a significant radial range. The question of how much radial mixing occurs due to this effect has been examined recently by Roskar et al. (2008a) and Roskar et al. (2008b). They find that this is a significant process which can lead to the formation of a population of stars beyond the star formation truncation radius in a disk, and which also flattens metallicity gradients (particularly in older stellar populations).

Disks are dynamically rather fragile systems and so not only must they form but they must survive across cosmological spans of time. This requires that the disk be stable to the growth of large scale perturbations which could destroy it. Additionally, in a hierarchical universe, survival is a non-trivial feat as the disk must survive frequent merging with other galaxies and constant bombardment by dark matter substructures orbiting within its own dark matter halo. Significant work has gone into studying the effects of dark matter substructures on galactic disks[34] (Toth and Ostriker 1992; Velazquez and White 1999; Font et al. 2001; Benson et al. 2004; Kazantzidis et al. 2008; Read et al. 2008; Kazantzidis et al. 2009; Purcell et al. 2009). The current consensus seems to be that the cold dark matter model is consistent with the presence of thin galactic disks, but only just so, and some fraction of disks have probably been significantly thickened or destroyed by interactions with dark matter substructures.

8.3. The Overcooling Problem

White and Rees (1978) proposed that galaxies would form as gas cools inside of dark matter halos and demonstrated that this provided a reasonable estimate of the typical mass scale of galaxies. This simple picture has a long standing problem however. The mass function of dark matter halos rises steeply (approximately as $M^{-1.9}$; Reed et al. 2007) at low masses. Since cooling is very efficient in these low mass halos we might expect the galaxy mass and/or luminosity function to show a similar slope at the low mass/luminosity end. In fact, measured slopes are much shallower (typically around -1; e.g. Cole et al. 2001). Rectifying this discrepancy is usually achieved by postulating some form of feedback, typically from supernovae, which can inhibit star formation in these low mass systems (e.g. by driving a wind out of the galaxy). However, as shown by Benson et al. (2003) this causes another problem—too much gas is now left over to accrete into massive halos (group and cluster mass objects) at late time wherein it cools and forms over-massive galaxies (much more massive than any galaxy observed).

This "overcooling" problem is not easy to solve, for the simple reason that the energy scales involved are much larger than for lower mass systems (the characteristic potential well depth of a dark matter halos scales as $M^{2/3}$ for halos of the same mean density). Several possible solutions have been proposed however, ranging from thermal conduction (Benson et al. 2003; Dolag et al. 2004; Pope et al. 2005), massive outflows (Benson et al. 2003), multiphase cooling (in which gas cools but is locked up into clouds which are inefficiently transferred to the galaxy; Maller and Bullock 2004; Kaufmann et al. 2009) and feedback from active galactic nuclei.

The AGN feedback scenario has gained considerable favor in the past few years for a variety of reasons. Firstly, observations have indicated that all galaxies seem to contain a central supermassive black hole with a mass that scales

[34] Primarily because this is potentially a means by which to rule our the cold dark matter scenario: if the predicted abundance of substructure was sufficient to destroy galactic disks, the model could be ruled out.

roughly in proportion to the mass of the galaxy (Magorrian et al. 1998; Gebhardt et al. 2000a; Ferrarese and Merritt 2000; Gebhardt et al. 2000b; Tremaine et al. 2002). The formation of these black holes must have involved the liberation of large amounts of energy and material sinks deep into the potential well of the black hole in some form of accretion flow (Benson et al. 2003). If this energy can be successfully utilized to counteract the overly rapid cooling of gas onto the galaxy it would provide a natural source of sufficient energy available in every galaxy. Additionally, some feedback loop connection between supermassive black hole and galaxy formation of this type is attractive as it provides a means to explain the correlation between galaxy and black hole properties.

Feedback from AGN can be divided into two categories: quasar mode and radio mode. The quasar mode is triggered when large amounts of gas are funneled into the circumnuclear disk from much larger scales by, for example, a merger between two galaxies in which torques act to transfer angular momentum from the gas, causing it to flow inwards. This is likely the dominant mechanism for black hole mass growth and results in a high (relative to Eddington) accretion rate — most likely through a thin accretion disk — and significant optical luminosity. In contrast, radio mode feedback occurs when the black hole is accreting at a more modest rate due to Bondi accretion from a diffuse hot atmosphere of gas and is in an optically dim but radio loud phase. In this phase, the black hole is thought to drive powerful jets (Meier 1999, 2001; Villiers et al. 2005; Nemmen et al. 2007; Komissarov et al. 2007; Benson and Babul 2009) which can reach to large distances and have been seen to have a significant impact on their surroundings (Birzan et al. 2004). The mechanism via which energy from the jets is efficiently coupled to the hot atmosphere of gas remains poorly understood: a combination of observational evidence (e.g. Owen et al. 2000) and theoretical insights suggest that jets inflate bubbles or cavities in the hot atmosphere (see §6.3.2). Despite these uncertainties, semi-analytic treatments which simply assume an efficient coupling have demonstrated that this can effectively shut down cooling in massive halos, resulting in a reduction in the masses of the largest galaxies and good agreement with luminosity functions and the bimodal distribution of galaxy colors (Croton et al. 2006; Bower et al. 2006; Somerville et al. 2008b). Observational evidence in support of AGN feedback is beginning to emerge (Schawinski et al. 2007) and seems to favor a radio mode scenario (Schawinski 2009).

8.4. Local Group Dwarf Satellites

As with any theory, galaxy formation theory is often best tested by exploring its predictions in extremes of physical conditions. For example, while our current theory may do well at explaining the properties of galaxies of average luminosity, it may perform less well in explaining the properties of the lowest mass galaxies that can form. Unfortunately, low mass galaxies are also low luminosity and so are difficult to observe. Fortunately, our own privileged position within the Milky Way and the Local Group means that there exists a population of faint, dwarf galaxies much closer by than we might otherwise expect. Study of the population of Local Group galaxies therefore has the potential to teach us much about galaxy formation at the lowest mass scales (and therefore, in a hierarchical Universe, at the earliest times). We must be cautious, however, of over-interpreting conclusions drawn from the Local Group which is, after all, just one small patch of the Universe.

Until the advent of the Sloan Digital Sky Survey around 11 satellite galaxies were known to exist within the virial radius of the Milky Way's halo[35] (Mateo 1998). The deep and uniform photometry of the SDSS has allowed many new such galaxies to be found by searching for overdensities in the stellar distribution in both position and color (Willman et al. 2005). The current roster of dwarf satellites within the Milky Way's halo amounts to 24 (Tollerud et al. 2008). However, the SDSS covers only around one fifth of the sky and detection algorithms are imperfect. Recent estimates of the total number of dwarf satellites in the Milky Way's halo alone are of the order a few hundred (Tollerud et al. 2008). The faintest galaxy currently known, Segue 1, has a luminosity of only 340 times that of the Sun (Belokurov et al. 2007).

These dwarf galaxies are interesting from a theoretical perspective for several reasons. Firstly, their low mass makes them highly sensitive to feedback effects, both internal (from supernovae for example; Font et al. 2010) and external (photoheating of the IGM by the entire population of galaxies can, in principle, inhibit the formation of these satellites; Gnedin 2000; Okamoto et al. 2008a). Furthermore, they may have gained at least some of their mass as a result of molecular hydrogen cooling, and have very low metallicities which may provide insight into the process

[35] We are following the definition of virial radius given by Benson et al. (2002a) here. Under this definition, 9 Local Group satellites are within the virial radius of M31, while a further 19 lie outside of the virial radii of the halos of both the Milky Way and M31.

of chemical enrichment. Beyond these galaxy-related aspects, the dwarf satellites appear to be highly dark matter dominated (Strigari et al. 2008), making them excellent systems in which to explore the properties of dark matter and, therefore, to place interesting constraints on the behavior of dark matter on small scales.

Consequently, these galaxies have attracted significant theoretical attention over the past few years. In particular, when simulations demonstrated that dark matter substructure could survive within a host halo for significant periods of time, it became clear that the Milky Way's halo should contain thousands of small dark matter halos that could potentially have formed a dwarf galaxy within them (Moore et al. 1999; Kuhlen et al. 2008; Springel et al. 2008). This was in stark contrast to the 10 or so satellites known at that time. This "missing satellites" problem appears to have been largely solved. Theoretical models have demonstrated that a combination of supernovae feedback, suppression of galaxy formation by a photoionizing background and tidal plus ram pressure stripping (Bullock et al. 2000; Somerville 2002; Benson et al. 2002a; Busha et al. 2009; Macció et al. 2009; Wadepuhl and Springel 2010; Font et al. 2010) can reduce the number of satellites significantly (leaving a population of truly dark subhalos; Kormendy and Freeman 2004), while the discovery of new satellites (and accounting for ones as yet undetected) has raised the observational target closer to the theoretical predictions.

Beyond this first order question though, there are many other interesting aspects to the Local Group satellites. For example, while they all contain populations of old stars, many of them show evidence of periodic star formation at much more recent times (Tolstoy et al. 2009). What triggers this star formation? Given that feedback can strongly affect these systems, it is interesting to ask if we can gain insight into the feedback mechanism by studying these galaxies (e.g. their metallicities are highly sensitive to the strength of feedback so may place useful constraints on any feedback model; Font et al. 2010). Finally, some of these galaxies must have been torn apart by the tidal field of the Milky Way (the Sagittarius dwarf is currently suffering this fate)—the dwarf satellite population may therefore have contributed to the build-up of the Milky Way's stellar halo (Cooper et al. 2009), and there may be remnant tidal streams which could provide information about the hierarchical growth of the Milky Way's halo (Bullock and Johnston 2005; Robertson et al. 2005; Font et al. 2006a,b; Johnston et al. 2008).

8.5. The Origins of the Hubble Sequence

The variety of morphologies of galaxies is, perhaps, the most obvious observed characteristic of galaxies. Traditionally, morphology has been measured "by eye" by a trained observer who classifies each galaxy into a different morphological class based upon (amongst other things) the prominence of any central bulge, how concentrated the light distribution is and the presence or otherwise of dust lanes. Hubble (1936; see also de Vaucouleurs 1959) placed galaxies into a morphological classification scheme using such an approach, and this basic morphological classification has persisted to the present (de Vaucouleurs et al. 1991). Applying this type of morphological classification to today's large datasets is difficult, but has been achieved by utilizing "crowdsourcing" techniques (Lintott et al. 2008). A key observational goal is to assess how the Hubble sequence evolves over time, as this should place strong constraints on theoretical models. This is observationally challenging, but progress is being made (e.g. Kriek et al. 2009).

Theoretically, morphological evolution is inevitable in a hierarchical universe in which galaxies interact with each other. Early work demonstrated that major mergers between galaxies could transform disks into spheroids leading to morphological evolution (Barnes and Hernquist 1992), but it is clear that the picture is more complicated, with secular evolution playing an important role in transforming disks into spheroids (Kormendy and Kennicutt 2004) and major mergers of very gas rich systems can lead to the reformation of a disk after the merger is over (Barnes 2002; Springel and Hernquist 2005; Robertson et al. 2006a).

A fundamental difficulty in assessing the ability of any given theoretical model to explain the morphological properties of galaxies is that the definition of morphology itself is very complicated, and somewhat nebulously defined. This problem is beginning to be circumvented, both by the ability of numerical simulations of galaxy formation to produce realistic "mock images" of galaxies (Jonsson 2006) which can, in principle, be classified by eye just as a real galaxy, and by the use of more quantitative morphological measures such as bulge–disk decomposition (Schade et al., 1996; Ratnatunga et al., 1999; Simard et al., 2002; Benson et al., 2007), Gini-M20 (Lotz et al., 2004), concentration-asymmetry-smoothness (Watanabe et al., 1985; Abraham et al., 1996; Bell et al., 2003) and so on.

Understanding the build-up and evolution of the Hubble sequence of morphologies is, nevertheless, an important task for galaxy formation theory. The morphological structure of a galaxy clearly tells us something about its

formation history and therefore captures information which its stellar population, for example, does not. Several studies have explored this aspect of galaxy formation theory (Baugh et al. 1996a,b; Kauffmann 1996; Governato et al. 1999; Firmani and Avila-Reese 2003; Lucia et al. 2006; Lucia and Blaizot 2007; Governato et al. 2007; Parry et al. 2009; Benson and Devereux 2009) with the general conclusion that hierarchical cosmologies can plausibly give rise to the observed mix of morphological types, although with significant uncertainties remaining in both the modeling of morphological transformation and in the comparison with observed morphologies. The consensus opinion is that massive elliptical galaxies form most of their stars in smaller progenitor galaxies and only assemble them into a single galaxy significantly later, while spiral galaxies are dominated by in situ star formation. Secular evolution of disks into spheroids also seems to be a crucial ingredient, particularly in the production of lower mass spheroidal systems (Parry et al. 2009; Kormendy et al. 2009).

9. Future Directions

The fundamental goal of galaxy formation studies is to comprehend how the laws of nature turned a Gaussian random distribution of density fluctuations laid down by inflation into a complex population of galaxies seen at the present day. At this time, this author does not see any convincing evidence that any new physics is needed to explain the phenomena of galaxies[36]. The problem is more one of complexity: can we tease out the underlying mechanisms that drive different aspects of galaxy formation and evolution. The key here then is "understanding". One can easily comprehend how a $1/r^2$ force works and can, by extrapolation, understand how this force applies to the billions of particles of dark matter in an N-body simulation. However, it is not directly obvious (at least not to this author) how a $1/r^2$ force leads to the formation of complex filamentary structures and collapsed virialized objects. Instead, we have developed simplified analytic models (e.g. the Zel'dovich approximation, spherical top-hat collapse models etc.) which explain these phenomena in terms more accessible to the human intellect. It seems that this is what we must strive for in galaxy formation theory—a set of analytic models that we can comprehend and which allow us to understand the physics and a complementary set of precision numerical tools to allow us to determine the quantitative outcomes of that physics (in order to make precision tests of our understanding).

The division of galaxy formation models into N-body/hydro and semi-analytic is rather idealized. In reality there is significant overlap between the two—many semi-analytic models make use of dark matter halo merger trees drawn from N-body simulations while many hydrodynamics simulations include recipes for star formation and feedback which are semi-analytic in nature. It seems most likely that these two techniques will continue to develop and may, in fact, grow less distinguishable, incorporating aspects of each other into each other (once again, yin yang).

Galaxy formation benefits from a wealth of observational data, often to the degree that it is an observationally lead field in which theory plays the role of trying to explain observed phenomena. This deluge of data is unlikely to cease any time soon — we can expect more and higher quality data on local galaxies and also the arrival of usefully sized datasets of galaxies at the highest redshifts. Galaxy formation theory should continue to attempt to develop our comprehension of these observed phenomena but should also strive to move into the regime of making true predictions for as-yet-unobserved regions of parameter space (e.g. the high redshift, $z \gtrsim 6$, Universe; e.g. Finlator et al. 2010; Lacey et al. 2010). Only in this way can we grow our confidence that we have truly understood the physics of galaxy formation.

10. Summary

Our theory of galaxy formation is gradually becoming more and more complete, but it is clear that large gaps in our understanding remain. This is, perhaps, not suprising — galaxy formation incorporates a wide array of physical processes, many of which we can currently observe the consequences of only indirectly. Most of the physics of galaxy formation is inherently nonlinear, making it difficult to obtain accurate solutions. Finally, what we observe from galaxies is usually several steps removed from the underlying physical properties (mass, density etc.) that we would ideally like to know about. Despite all of these difficulties, rapid progress is being made. The next decade

[36]By "new physics" here I mean modifications to established physical laws, new forces or fields etc. Of course, dark matter and dark energy probably require "new physics" of one type or another, but I will leave those as a problem for cosmology…

should see this trend continuing via a combination of ever better observational datasets (both low and high redshift) and the continued development of novel theoretical tools.

Acknowledgments

The author acknowledges the support of the Gordon & Betty Moore Foundation. This work has benefited greatly from discussions with the Durham galaxy formation Group (Carlos Frenk, Shaun Cole, Richard Bower, Carlton Baugh, Cedric Lacey, Martin Stringer, Andreea Font and John Helly) and with Juna Kollmeier, Alyson Brooks, Annika Peter, Brant Robertson, TJ Cox, Dan Grin, Laura Book and Elisabeth Krause. The author would particularly like to thank Carlos Frenk for carefully reading through this manuscript and the anonymous referee for numerous valuable suggestions.

References

Abadi, M.G., Moore, B., Bower, R.G., 1999. MNRAS 308, 947–954.
Abadi, M.G., Navarro, J.F., Fardal, M., Babul, A., Steinmetz, M., 2009.
Abadi, M.G., Navarro, J.F., Steinmetz, M., Eke, V.R., 2003. Astrophysical Journal 597, 21–34.
Abel, T., Anninos, P., Zhang, Y., Norman, M.L., 1997. New Astronomy 2, 181–207.
Abel, T., Bryan, G.L., Norman, M.L., 2002. Science 295, 93–98.
Abel, T., Norman, M.L., Madau, P., 1999. Astrophysical Journal 523, 66–71.
Abraham, R.G., Tanvir, N.R., Santiago, B.X., Ellis, R.S., Glazebrook, K., van den Bergh, S., 1996. Monthly Notices of the Royal Astronomical Society 279, L47.
Agertz, O., Moore, B., Stadel, J., Potter, D., Miniati, F., Read, J., Mayer, L., Gawryszczak, A., Kravtsov, A., Nordlund, Åke., Pearce, F., Quilis, V., Rudd, D., Springel, V., Stone, J., Tasker, E., Teyssier, R., Wadsley, J., Walder, R., 2007. Monthly Notices of the Royal Astronomical Society 380, 963–978.
Ahn, K., Shapiro, P.R., 2005. Monthly Notices of the Royal Astronomical Society 363, 1092–1110.
Allen, M.G., Groves, B.A., Dopita, M.A., Sutherland, R.S., Kewley, L.J., 2008. Astrophysical Journal Supplement Series 178, 20–55.
Alvarez, M.A., Busha, M.T., Abel, T., Wechsler, R.H., 2008.
Angulo, R.E., Lacey, C.G., Baugh, C.M., Frenk, C.S., 2008.
Angus, G.W., Zhao, H., 2007. Monthly Notices of the Royal Astronomical Society 375, 1146–1156.
Arad, I., Lynden-Bell, D., 2005. Monthly Notices of the Royal Astronomical Society 361, 385–395.
Arons, J., Silk, J., 1968. Monthly Notices of the Royal Astronomical Society 140, 331.
Arrigoni, M., Trager, S.C., Somerville, R.S., Gibson, B.K., 2009.
Athanassoula, E., 2002. Astrophysical Journal 569, L83–L86.
Athanassoula, E., 2008. Monthly Notices of the Royal Astronomical Society 390, L69–L72.
Aubert, D., Teyssier, R., 2008. Monthly Notices of the Royal Astronomical Society 387, 295–307.
Bahcall, J.N., Wolf, R.A., 1976. Astrophysical Journal 209, 214–232.
Bahcall, N.A., Hao, L., Bode, P., Dong, F., 2004. Astrophysical Journal 603, 1–6.
Banerjee, R., Pudritz, R.E., Anderson, D.W., 2006. Monthly Notices of the Royal Astronomical Society 373, 1091–1106.
Bardeen, J.M., 1970. Nature 226, 64.
Barnes, J., Efstathiou, G., 1987. ApJ 319, 575–600.
Barnes, J.E., 2002. Monthly Notices of the Royal Astronomical Society 333, 481–494.
Barnes, J.E., Hernquist, L., 1992. Annual Review of Astronomy and Astrophysics 30, 705–742.
Baugh, C.M., 2006. Reports on Progress in Physics 69, 3101–3156.
Baugh, C.M., Benson, A.J., Cole, S., Frenk, C.S., Lacey, C.G., 1999a. MNRAS 305, L21–L25.
Baugh, C.M., Cole, S., Frenk, C.S., 1996a. Monthly Notices of the Royal Astronomical Society 282, L27–L32.
Baugh, C.M., Cole, S., Frenk, C.S., 1996b. Monthly Notices of the Royal Astronomical Society 283, 1361–1378.
Baugh, C.M., Cole, S., Frenk, C.S., Lacey, C.G., 1998. ApJ 498, 504.
Baugh, C.M., Lacey, C.G., Cole, S., Frenk, C.S., 1999b. in: The Most Distant Radio Galaxies, Royal Netherlands Academy of Arts and Science, Amsterdam. p. 265.
Baugh, C.M., Lacey, C.G., Frenk, C.S., Benson, A.J., Cole, S., Granato, G.L., Silva, L., Bressan, A., 2004. New Astronomy Review 48, 1239–1246.
Baugh, C.M., Lacey, C.G., Frenk, C.S., Granato, G.L., Silva, L., Bressan, A., Benson, A.J., Cole, S., 2005. MNRAS 356, 1191–1200.
Begelman, M.C., Blandford, R.D., Rees, M.J., 1980. Nature 287, 307–309.
Begelman, M.C., Nath, B.B., 2005. Monthly Notices of the Royal Astronomical Society 361, 1387–1392.
Behroozi, P.S., Conroy, C., Wechsler, R.H., 2010. http://adsabs.harvard.edu/abs/2010arXiv1001.0015B.
Bell, E.F., McIntosh, D.H., Katz, N., Weinberg, M.D., 2003. Astrophysical Journal Supplement Series 149, 289–312.
Belokurov, V., Zucker, D.B., Evans, N.W., Gilmore, G., Vidrih, S., Bramich, D.M., Newberg, H.J., Wyse, R.F.G., Irwin, M.J., Fellhauer, M., Hewett, P.C., Walton, N.A., Wilkinson, M.I., Cole, N., Yanny, B., Rockosi, C.M., Beers, T.C., Bell, E.F., Brinkmann, J., Ivezić, Å., Lupton, R., 2006. The Astrophysical Journal 642, L137–L140.
Belokurov, V., Zucker, D.B., Evans, N.W., Kleyna, J.T., Koposov, S., Hodgkin, S.T., Irwin, M.J., Gilmore, G., Wilkinson, M.I., Fellhauer, M., Bramich, D.M., Hewett, P.C., Vidrih, S., Jong, J.T.A.D., Smith, J.A., Rix, H., Bell, E.F., Wyse, R.F.G., Newberg, H.J., Mayeur, P.A., Yanny,

B., Rockosi, C.M., Gnedin, O.Y., Schneider, D.P., Beers, T.C., Barentine, J.C., Brewington, H., Brinkmann, J., Harvanek, M., Kleinman, S.J., Krzesinski, J., Long, D., Nitta, A., Snedden, S.A., 2007. Astrophysical Journal 654, 897–906.
Benson, A., Devereux, N.A., 2009. Monthly Notices of the Royal Astronomical Society 402, 2321–2334.
Benson, A.J., 2005. MNRAS 358, 551–562.
Benson, A.J., 2008. Monthly Notices of the Royal Astronomical Society 388, 1361–1371.
Benson, A.J., Babul, A., 2009.
Benson, A.J., Baugh, C.M., Cole, S., Frenk, C.S., Lacey, C.G., 2000a. MNRAS 316, 107–119.
Benson, A.J., Bower, R., 2010. Monthly Notices of the Royal Astronomical Society , no–no.
Benson, A.J., Bower, R.G., Frenk, C.S., Lacey, C.G., Baugh, C.M., Cole, S., 2003. Astrophysical Journal 599, 38–49.
Benson, A.J., Bower, R.G., Frenk, C.S., White, S.D.M., 2000b. Monthly Notices of the Royal Astronomical Society 314, 557–565.
Benson, A.J., Cole, S., Frenk, C.S., Baugh, C.M., Lacey, C.G., 2000c. MNRAS 311, 793–808.
Benson, A.J., Dzanovic, D., Frenk, C.S., Sharples, R., 2007. Monthly Notices of the Royal Astronomical Society 379, 841–866.
Benson, A.J., Kamionkowski, M., Hassani, S.H., 2005. Monthly Notices of the Royal Astronomical Society 357, 847–858.
Benson, A.J., Lacey, C.G., Baugh, C.M., Cole, S., Frenk, C.S., 2002a. MNRAS 333, 156–176.
Benson, A.J., Lacey, C.G., Baugh, C.M., Cole, S., Frenk, C.S., 2002b. Monthly Notices of the Royal Astronomical Society 333, 156–176.
Benson, A.J., Lacey, C.G., Frenk, C.S., Baugh, C.M., Cole, S., 2004. MNRAS 351, 1215–1236.
Benson, A.J., Madau, P., 2003. Monthly Notices of the Royal Astronomical Society 344, 835–846.
Benson, A.J., Nusser, A., Sugiyama, N., Lacey, C.G., 2001a. MNRAS 320, 153–176.
Benson, A.J., Pearce, F.R., Frenk, C.S., Baugh, C.M., Jenkins, A., 2001b. Monthly Notices of the Royal Astronomical Society 320, 261–280.
Benson, A.J., Sugiyama, N., Nusser, A., Lacey, C.G., 2006. MNRAS 369, 1055–1080.
Berezinsky, V., Dokuchaev, V., Eroshenko, Y., 2006. Physical Review D 73, 63504.
Berti, E., Volonteri, M., 2008. Astrophysical Journal 684, 822–828.
Bertin, G., Romeo, A.B., 1988. Astronomy and Astrophysics 195, 105–113.
Bertone, G., Hooper, D., Silk, J., 2005. Physics Reports 405, 279–390.
Bertschinger, E., 1985. Astrophysical Journal Supplement Series 58, 39–65.
Bertschinger, E., 1998. Annual Review of Astronomy and Astrophysics 36, 599–654.
Bett, P., Eke, V., Frenk, C.S., Jenkins, A., Helly, J., Navarro, J., 2007. MNRAS 376, 215–232.
Bett, P., Eke, V., Frenk, C.S., Jenkins, A., Okamoto, T., 2009.
Binney, J., 1977a. Astrophysical Journal 215, 483–491.
Binney, J., 1977b. Monthly Notices of the Royal Astronomical Society 181, 735–746.
Binney, J., Tremaine, S., 2008.
Birnboim, Y., Dekel, A., 2003. Monthly Notices of the Royal Astronomical Society 345, 349–364.
Birzan, L., Rafferty, D.A., McNamara, B.R., Wise, M.W., Nulsen, P.E.J., 2004. Astrophysical Journal 607, 800–809.
Blaizot, J., Guiderdoni, B., Devriendt, J.E.G., Bouchet, F.R., Hatton, S., 2003. Astrophysics and Space Science 284, 373–376.
Blaizot, J., Guiderdoni, B., Devriendt, J.E.G., Bouchet, F.R., Hatton, S.J., Stoehr, F., 2004. MNRAS 352, 571–588.
Blaizot, J., Szapudi, I., Colombi, S., Budavàri, T., Bouchet, F.R., Devriendt, J.E.G., Guiderdoni, B., Pan, J., Szalay, A., 2006. MNRAS 369, 1009–1020.
Blanchet, L., Qusailah, M.S.S., Will, C.M., 2005. Astrophysical Journal 635, 508–515.
Bland-Hawthorn, J., 2009. in: The Galaxy Disk in Cosmological Context, International Astronomical Union. pp. 241–254.
Blandford, R.D., Payne, D.G., 1982. Monthly Notices of the Royal Astronomical Society 199, 883–903.
Blandford, R.D., Znajek, R.L., 1977. Monthly Notices of the Royal Astronomical Society 179, 433–456.
Blumenthal, G.R., Faber, S.M., Flores, R., Primack, J.R., 1986. Astrophysical Journal 301, 27–34.
Blumenthal, G.R., Faber, S.M., Primack, J.R., Rees, M.J., 1984. Nature 311, 517–525.
Bode, P., Ostriker, J.P., Turok, N., 2001. Astrophysical Journal 556, 93–107.
Boehm, C., Schaeffer, R., 2005. Astronomy and Astrophysics 438, 419–442.
Bond, J.R., Cole, S., Efstathiou, G., Kaiser, N., 1991. Astrophysical Journal 379, 440–460.
Bondi, H., Hoyle, F., 1944. Monthly Notices of the Royal Astronomical Society 104, 273.
Book, L.G., Benson, A.J., 2010. http://adsabs.harvard.edu/abs/2010arXiv1001.2305B.
Booth, C.M., Schaye, J., 2009. Monthly Notices of the Royal Astronomical Society 398, 53–74.
Borgani, S., Governato, F., Wadsley, J., Menci, N., Tozzi, P., Lake, G., Quinn, T., Stadel, J., 2001. Astrophysical Journal 559, L71–L74.
van den Bosch, F.C., 2002. Monthly Notices of the Royal Astronomical Society 331, 98–110.
van den Bosch, F.C., Abel, T., Croft, R.A.C., Hernquist, L., White, S.D.M., 2002. Astrophysical Journal 576, 21–35.
van den Bosch, F.C., Abel, T., Hernquist, L., 2003. Monthly Notices of the Royal Astronomical Society 346, 177–185.
Bournaud, F., Combes, F., 2002. Astronomy and Astrophysics 392, 83–102.
Bournaud, F., Jog, C.J., Combes, F., 2005. Astronomy and Astrophysics 437, 69–85.
Bower, R.G., 1991. Monthly Notices of the Royal Astronomical Society 248, 332–352.
Bower, R.G., Benson, A.J., Lacey, C.G., Baugh, C.M., Cole, S., Frenk, C.S., 2001. MNRAS 325, 497–508.
Bower, R.G., Benson, A.J., Malbon, R., Helly, J.C., Frenk, C.S., Baugh, C.M., Cole, S., Lacey, C.G., 2006. MNRAS 370, 645–655.
Bower, R.G., McCarthy, I.G., Benson, A.J., 2008. MNRAS 390, 1399–1410.
Boyarsky, A., Lesgourgues, J., Ruchayskiy, O., Viel, M., 2008.
Boylan-Kolchin, M., Ma, C., Quataert, E., 2008. MNRAS 383, 93–101.
Boyle, L., Kesden, M., Nissanke, S., 2008. Physical Review Letters 100, 151101.
Bromm, V., Coppi, P.S., Larson, R.B., 2002. Astrophysical Journal 564, 23–51.
Bromm, V., Yoshida, N., Hernquist, L., McKee, C.F., 2009. Nature 459, 49–54.
Brook, C.B., Kawata, D., Gibson, B.K., Freeman, K.C., 2004. Astrophysical Journal 612, 894–899.

Brook, C.B., Kawata, D., Scannapieco, E., Martel, H., Gibson, B.K., 2007. Astrophysical Journal 661, 10–18.
Brooks, A.M., Governato, F., Quinn, T., Brook, C.B., Wadsley, J., 2009. Astrophysical Journal 694, 396–410.
Brüggen, M., Lucia, G.D., 2008. Monthly Notices of the Royal Astronomical Society 383, 1336–1342.
Brüggen, M., Scannapieco, E., 2009. Monthly Notices of the Royal Astronomical Society 398, 548–560.
Bruzual, G., Charlot, S., 2003. MNRAS 344, 1000–1028.
Bullock, J.S., Dekel, A., Kolatt, T.S., Kravtsov, A.V., Klypin, A.A., Porciani, C., Primack, J.R., 2001a. The Astrophysical Journal 555, 240–257.
Bullock, J.S., Johnston, K.V., 2005. Astrophysical Journal 635, 931–949.
Bullock, J.S., Kolatt, T.S., Sigad, Y., Somerville, R.S., Kravtsov, A.V., Klypin, A.A., Primack, J.R., Dekel, A., 2001b. Monthly Notices of the Royal Astronomical Society 321, 559–575.
Bullock, J.S., Kravtsov, A.V., Weinberg, D.H., 2000. Astrophysical Journal 539, 517–521.
Burkert, A., Tremaine, S., 2010. http://adsabs.harvard.edu/abs/2010arXiv1004.0137B.
Busha, M.T., Alvarez, M.A., Wechsler, R.H., Abel, T., Strigari, L.E., 2009.
Cardone, V.F., Piedipalumbo, E., Tortora, C., 2005. MNRAS 358, 1325–1336.
Cattaneo, A., Dekel, A., Devriendt, J., Guiderdoni, B., Blaizot, J., 2006. Monthly Notices of the Royal Astronomical Society 370, 1651–1665.
Cazaux, S., Spaans, M., 2004. ApJ 611, 40–51.
Chabrier, G., 2003. Publications of the Astronomical Society of the Pacific 115, 763–795.
Chakrabarti, S., Whitney, B.A., 2009. Astrophysical Journal 690, 1432–1451.
Chandrasekhar, S., 1943. Astrophysical Journal 97, 255.
Chary, R., 2008. Astrophysical Journal 680, 32–40.
Chiu, W.A., Ostriker, J.P., 2000. Astrophysical Journal 534, 507–532.
Christodoulou, D.M., Kazanas, D., Shlosman, I., Tohline, J.E., 1995a. Astrophysical Journal 446, 472.
Christodoulou, D.M., Shlosman, I., Tohline, J.E., 1995b. Astrophysical Journal 443, 551–562.
Ciardi, B., Ferrara, A., Marri, S., Raimondo, G., 2001. Monthly Notices of the Royal Astronomical Society 324, 381–388.
Ciardi, B., Ferrara, A., White, S.D.M., 2003. Monthly Notices of the Royal Astronomical Society 344, L7–L11.
Ciotti, L., 2009.
Ciotti, L., Ostriker, J.P., Proga, D., 2009. The Astrophysical Journal 699, 89–104.
Clarke, C.J., 1989. Monthly Notices of the Royal Astronomical Society 238, 283–292.
Clarke, C.J., 1991. Monthly Notices of the Royal Astronomical Society 249, 704–706.
Cole, S., 1991. Astrophysical Journal 367, 45–53.
Cole, S., Aragon-Salamanca, A., Frenk, C.S., Navarro, J.F., Zepf, S.E., 1994. Monthly Notices of the Royal Astronomical Society 271, 781.
Cole, S., Helly, J., Frenk, C.S., Parkinson, H., 2008. Monthly Notices of the Royal Astronomical Society 383, 546–556.
Cole, S., Lacey, C., 1996. MNRAS 281, 716.
Cole, S., Lacey, C.G., Baugh, C.M., Frenk, C.S., 2000. MNRAS 319, 168–204.
Cole, S., Norberg, P., Baugh, C.M., Frenk, C.S., Bland-Hawthorn, J., Bridges, T., Cannon, R., Colless, M., Collins, C., Couch, W., Cross, N., Dalton, G., Propris, R.D., Driver, S.P., Efstathiou, G., Ellis, R.S., Glazebrook, K., Jackson, C., Lahav, O., Lewis, I., Lumsden, S., Maddox, S., Madgwick, D., Peacock, J.A., Peterson, B.A., Sutherland, W., Taylor, K., 2001. Monthly Notices of the Royal Astronomical Society 326, 255–273.
Cole, S., Percival, W.J., Peacock, J.A., Norberg, P., Baugh, C.M., Frenk, C.S., Baldry, I., Bland-Hawthorn, J., Bridges, T., Cannon, R., Colless, M., Collins, C., Couch, W., Cross, N.J.G., Dalton, G., Eke, V.R., Propris, R.D., Driver, S.P., Efstathiou, G., Ellis, R.S., Glazebrook, K., Jackson, C., Jenkins, A., Lahav, O., Lewis, I., Lumsden, S., Maddox, S., Madgwick, D., Peterson, B.A., Sutherland, W., Taylor, K., 2005. Monthly Notices of the Royal Astronomical Society 362, 505–534.
Colín, P., Avila-Reese, V., Valenzuela, O., Firmani, C., 2002. Astrophysical Journal 581, 777–793.
Collins, D.C., Xu, H., Norman, M.L., Li, H., Li, S., 2009.
Conroy, C., Gunn, J.E., 2010. The Astrophysical Journal 712, 833–857.
Conroy, C., Gunn, J.E., White, M., 2008.
Conroy, C., Ostriker, J.P., 2008. The Astrophysical Journal 681, 151–166.
Conroy, C., Wechsler, R.H., 2009. The Astrophysical Journal 696, 620–635.
Cooper, A.P., Cole, S., Frenk, C.S., White, S.D.M., Helly, J.C., Benson, A.J., Lucia, G.D., Helmi, A., Jenkins, A., Navarro, J.F., Springel, V., Wang, J., 2009. MNRAS submitted.
Cooray, A., Sheth, R., 2002. Physics Reports 372, 1–129.
Covington, M., Dekel, A., Cox, T.J., Jonsson, P., Primack, J.R., 2008. Monthly Notices of the Royal Astronomical Society 384, 94–106.
Cox, T.J., Jonsson, P., Primack, J.R., Somerville, R.S., 2006. Monthly Notices of the Royal Astronomical Society 373, 1013–1038.
Cox, T.J., Jonsson, P., Somerville, R.S., Primack, J.R., Dekel, A., 2008. Monthly Notices of the Royal Astronomical Society 384, 386–409.
Crain, R.A., Theuns, T., Vecchia, C.D., Eke, V.R., Frenk, C.S., Jenkins, A., Kay, S.T., Peacock, J.A., Pearce, F.R., Schaye, J., Springel, V., Thomas, P.A., White, S.D.M., Wiersma, R.P.C., 2009. Monthly Notices of the Royal Astronomical Society 399, 1773–1794.
Croton, D.J., 2009. Monthly Notices of the Royal Astronomical Society 394, 1109–1119.
Croton, D.J., Springel, V., White, S.D.M., Lucia, G.D., Frenk, C.S., Gao, L., Jenkins, A., Kauffmann, G., Navarro, J.F., Yoshida, N., 2006. MNRAS 365, 11–28.
Davé, R., Spergel, D.N., Steinhardt, P.J., Wandelt, B.D., 2001. Astrophysical Journal 547, 574–589.
Davis, M., Efstathiou, G., Frenk, C.S., White, S.D.M., 1985. Astrophysical Journal 292, 371–394.
Dekel, A., Silk, J., 1986. Astrophysical Journal 303, 39–55.
Devriendt, J.E.G., Guiderdoni, B., 2000. A&A 363, 851–862.
Devriendt, J.E.G., Sethi, S.K., Guiderdoni, B., Nath, B.B., 1998. MNRAS 298, 708–718.
Diaferio, A., Kauffmann, G., Colberg, J.M., White, S.D.M., 1999. MNRAS 307, 537–552.
van Dokkum, P.G., 2008. Astrophysical Journal 674, 29–50.

Dolag, K., Jubelgas, M., Springel, V., Borgani, S., Rasia, E., 2004. Astrophysical Journal 606, L97–L100.
Dolag, K., Stasyszyn, F.A., 2008. 0807.3553 .
Dotter, A., Chaboyer, B., Ferguson, J.W., chul Lee, H., Worthey, G., Jevremovic, D., Baron, E., 2007. Astrophysical Journal 666, 403–412.
Dove, J.B., Shull, J.M., Ferrara, A., 2000. Astrophysical Journal 531, 846–860.
Draine, B.T., Lee, H.M., 1984. Astrophysical Journal 285, 89–108.
Dunkley, J., Komatsu, E., Nolta, M.R., Spergel, D.N., Larson, D., Hinshaw, G., Page, L., Bennett, C.L., Gold, B., Jarosik, N., Weiland, J.L., Halpern, M., Hill, R.S., Kogut, A., Limon, M., Meyer, S.S., Tucker, G.S., Wollack, E., Wright, E.L., 2009. Astrophysical Journal Supplement Series 180, 306–329.
Dutton, A.A., 2009. Monthly Notices of the Royal Astronomical Society 396, 121–140.
Dutton, A.A., van den Bosch, F.C., Dekel, A., Courteau, S., 2007. Astrophysical Journal 654, 27–52.
Edgar, R., 2004. New Astronomy Reviews 48, 843–859.
Efstathiou, G., 2000. Monthly Notices of the Royal Astronomical Society 317, 697–719.
Efstathiou, G., Frenk, C.S., White, S.D.M., Davis, M., 1988. MNRAS 235, 715–748.
Efstathiou, G., Lake, G., Negroponte, J., 1982. Monthly Notices of the Royal Astronomical Society 199, 1069–1088.
Einasto, J., 1965. Trudy Inst. Astrofiz. Alma-Ata 51, 87.
Eisenstein, D.J., Hu, W., 1999. ApJ 511, 5–15.
Eke, V.R., Cole, S., Frenk, C.S., Navarro, J.F., 1996. Monthly Notices of the Royal Astronomical Society 281, 703.
Eke, V.R., Navarro, J.F., Steinmetz, M., 2001. Astrophysical Journal 554, 114–125.
El-Zant, A., Shlosman, I., 2002. Astrophysical Journal 577, 626–650.
Elahi, P.J., Thacker, R.J., Widrow, L.M., Scannapieco, E., 2009. Monthly Notices of the Royal Astronomical Society 395, 1950–1962.
Fakhouri, O., Ma, C., 2008a. Monthly Notices of the Royal Astronomical Society 386, 577–592.
Fakhouri, O., Ma, C., 2008b.
Fakhouri, O., Ma, C., 2009. Monthly Notices of the Royal Astronomical Society 394, 1825–1840.
Fakhouri, O., Ma, C., Boylan-Kolchin, M., 2010. http://adsabs.harvard.edu/abs/2010arXiv1001.2304F.
Fall, S.M., Efstathiou, G., 1980. Monthly Notices of the Royal Astronomical Society 193, 189–206.
Fan, X., Strauss, M.A., Schneider, D.P., Gunn, J.E., Lupton, R.H., Becker, R.H., Davis, M., Newman, J.A., Richards, G.T., White, R.L., Anderson, J.E., Annis, J., Bahcall, N.A., Brunner, R.J., Csabai, I., Hennessy, G.S., Hindsley, R.B., Fukugita, M., Kunszt, P.Z., Ivezic, Z., Knapp, G.R., McKay, T.A., Munn, J.A., Pier, J.R., Szalay, A.S., York, D.G., 2001. Astronomical Journal 121, 54–65.
Fardal, M.A., Katz, N., Gardner, J.P., Hernquist, L., Weinberg, D.H., Davé, R., 2001. The Astrophysical Journal 562, 605–617.
Favata, M., Hughes, S.A., Holz, D.E., 2004. Astrophysical Journal 607, L5–L8.
Federrath, C., Banerjee, R., Clark, P.C., Klessen, R.S., 2010. The Astrophysical Journal 713, 269–290.
Ferland, G.J., Korista, K.T., Verner, D.A., Ferguson, J.W., Kingdon, J.B., Verner, E.M., 1998. Publications of the Astronomical Society of the Pacific 110, 761–778.
Ferramacho, L.D., Blanchard, A., Zolnierowski, Y., 2008.
Ferrara, A., Bianchi, S., Cimatti, A., Giovanardi, C., 1999. ApJ Supplement Series 123, 437–445.
Ferrarese, L., 2002. Astrophysical Journal 578, 90–97.
Ferrarese, L., Merritt, D., 2000. Astrophysical Journal 539, L9–L12.
Field, G.B., 1965. Astrophysical Journal 142, 531.
Finlator, K., Oppenheimer, B.D., Davé, R., 2010. http://adsabs.harvard.edu/abs/2010arXiv1005.4066F.
Finlator, K., Özel, F., Davé, R., 2009. Monthly Notices of the Royal Astronomical Society 393, 1090–1106.
Firmani, C., Avila-Reese, V., 2003. pp. 107–120.
Firmani, C., Hernandez, X., Gallagher, J., 1996. Astronomy and Astrophysics 308, 403–414.
Fitchett, M.J., 1983. Monthly Notices of the Royal Astronomical Society 203, 1049–1062.
Font, A., Benson, A., Bower, R., Frenk, C., 2010. in prep .
Font, A.S., Bower, R.G., McCarthy, I.G., Benson, A.J., Frenk, C.S., Helly, J.C., Lacey, C.G., Baugh, C.M., Cole, S., 2008. MNRAS 389, 1619–1629.
Font, A.S., Johnston, K.V., Bullock, J.S., Robertson, B.E., 2006a. Astrophysical Journal 638, 585–595.
Font, A.S., Johnston, K.V., Bullock, J.S., Robertson, B.E., 2006b. Astrophysical Journal 646, 886–898.
Font, A.S., Navarro, J.F., Stadel, J., Quinn, T., 2001. Astrophysical Journal 563, L1–L4.
Fontanot, F., Lucia, G.D., Monaco, P., Somerville, R.S., Santini, P., 2009a. 0901.1130 .
Fontanot, F., Monaco, P., Silva, L., Grazian, A., 2007. MNRAS 382, 903–914.
Fontanot, F., Somerville, R.S., Silva, L., Monaco, P., Skibba, R., 2009b. MNRAS 392, 553–569.
Forcada-Miro, M.I., White, S.D.M., 1997. http://adsabs.harvard.edu/abs/1997astro.ph.12204F.
François, P., Matteucci, F., Cayrel, R., Spite, M., Spite, F., Chiappini, C., 2004. Astronomy and Astrophysics 421, 613–621.
Freeman, K., Bland-Hawthorn, J., 2002. Annual Review of Astronomy and Astrophysics 40, 487–537.
Frenk, C.S., 2002. Royal Society of London Philosophical Transactions Series A 360, 1277.
Frenk, C.S., White, S.D.M., Bode, P., Bond, J.R., Bryan, G.L., Cen, R., Couchman, H.M.P., Evrard, A.E., Gnedin, N., Jenkins, A., Khokhlov, A.M., Klypin, A., Navarro, J.F., Norman, M.L., Ostriker, J.P., Owen, J.M., Pearce, F.R., Pen, U., Steinmetz, M., Thomas, P.A., Villumsen, J.V., Wadsley, J.W., Warren, M.S., Xu, G., Yepes, G., 1999. Astrophysical Journal 525, 554–582.
Frenk, C.S., White, S.D.M., Davis, M., Efstathiou, G., 1988. Astrophysical Journal 327, 507–525.
Friedli, D., Benz, W., 1993. Astronomy and Astrophysics 268, 65–85.
Fryxell, B., Olson, K., Ricker, P., Timmes, F.X., Zingale, M., Lamb, D.Q., MacNeice, P., Rosner, R., Truran, J.W., Tufo, H., 2000. Astrophysical Journal Supplement Series 131, 273–334.
Galli, D., Palla, F., 1998. A&A 335, 403–420.
Gao, L., Navarro, J.F., Cole, S., Frenk, C.S., White, S.D.M., Springel, V., Jenkins, A., Neto, A.F., 2008. MNRAS 387, 536–544.

Gao, L., Yoshida, N., Abel, T., Frenk, C.S., Jenkins, A., Springel, V., 2007. Monthly Notices of the Royal Astronomical Society 378, 449–468.
Gebhardt, K., Bender, R., Bower, G., Dressler, A., Faber, S.M., Filippenko, A.V., Green, R., Grillmair, C., Ho, L.C., Kormendy, J., Lauer, T.R., Magorrian, J., Pinkney, J., Richstone, D., Tremaine, S., 2000a. Astrophysical Journal 539, L13–L16.
Gebhardt, K., Kormendy, J., Ho, L.C., Bender, R., Bower, G., Dressler, A., Faber, S.M., Filippenko, A.V., Green, R., Grillmair, C., Lauer, T.R., Magorrian, J., Pinkney, J., Richstone, D., Tremaine, S., 2000b. Astrophysical Journal 543, L5–L8.
Glover, S.C.O., Abel, T., 2008. Monthly Notices of the Royal Astronomical Society 388, 1627–1651.
Gnat, O., Sternberg, A., 2007. Astrophysical Journal Supplement Series 168, 213–230.
Gnedin, N.Y., 2000. ApJ 542, 535–541.
Gnedin, N.Y., Abel, T., 2001. New Astronomy 6, 437–455.
Gnedin, N.Y., Hui, L., 1998. Monthly Notices of the Royal Astronomical Society 296, 44–55.
Gnedin, N.Y., Kravtsov, A.V., Chen, H., 2008. Astrophysical Journal 672, 765–775.
Gnedin, N.Y., Tassis, K., Kravtsov, A.V., 2009. Astrophysical Journal 697, 55–67.
Gnedin, O.Y., 2003. Astrophysical Journal 582, 141–161.
Gnedin, O.Y., Kravtsov, A.V., Klypin, A.A., Nagai, D., 2004. Astrophysical Journal 616, 16–26.
Gnedin, O.Y., Ostriker, J.P., 1999. Astrophysical Journal 513, 626–637.
Goerdt, T., Gnedin, O.Y., Moore, B., Diemand, J., Stadel, J., 2007. Monthly Notices of the Royal Astronomical Society 375, 191–198.
Goldreich, P., Lynden-Bell, D., 1965. Monthly Notices of the Royal Astronomical Society 130, 125.
Gonçalves, D.R., Friaça, A.C.S., 1999. Monthly Notices of the Royal Astronomical Society 309, 651–658.
Gonzalez-Perez, V., Baugh, C.M., Lacey, C.G., Almeida, C., 2008.
Gould, A., Rix, H., 2000. Astrophysical Journal 532, L29–L32.
Governato, F., Baugh, C.M., Frenk, C.S., Cole, S., Lacey, C.G., Quinn, T., Stadel, J., 1998. Nature 392, 359–361.
Governato, F., Gardner, J.P., Stadel, J., Quinn, T., Lake, G., 1999. Astronomical Journal 117, 1651–1656.
Governato, F., Willman, B., Mayer, L., Brooks, A., Stinson, G., Valenzuela, O., Wadsley, J., Quinn, T., 2007. Monthly Notices of the Royal Astronomical Society 374, 1479–1494.
Granato, G.L., Lacey, C.G., Silva, L., Bressan, A., Baugh, C.M., Cole, S., Frenk, C.S., 2000. ApJ 542, 710–730.
Greif, T.H., Johnson, J.L., Klessen, R.S., Bromm, V., 2008. Monthly Notices of the Royal Astronomical Society 387, 1021–1036.
Guiderdoni, B., Hivon, E., Bouchet, F.R., Maffei, B., 1998. MNRAS 295, 877–898.
Gunn, J.E., 1977. The Astrophysical Journal 218, 592–598.
Gunn, J.E., Gott, J.R., 1972. Astrophysical Journal 176, 1.
Guo, F., Oh, S.P., 2008. Monthly Notices of the Royal Astronomical Society 384, 251–266.
Gustafsson, M., Fairbairn, M., Sommer-Larsen, J., 2006. Physical Review D 74, 123522.
Haardt, F., Madau, P., 1996. Astrophysical Journal 461, 20.
Hahn, O., Teyssier, R., Carollo, C.M., 2010. Monthly Notices of the Royal Astronomical Society 405, 274–290.
Hamilton, A.J.S., Kumar, P., Lu, E., Matthews, A., 1991. The Astrophysical Journal 374, L1–L4.
Harris, G.J., Lynas-Gray, A.E., Miller, S., Tennyson, J., 2007. Monthly Notices of the Royal Astronomical Society 374, 337–343.
Hatton, S., Devriendt, J.E.G., Ninin, S., Bouchet, F.R., Guiderdoni, B., Vibert, D., 2003. Monthly Notices of the Royal Astronomical Society 343, 75–106.
Heitmann, K., Higdon, D., White, M., Habib, S., Williams, B.J., Lawrence, E., Wagner, C., 2009. The Astrophysical Journal 705, 156–174.
Heitmann, K., White, M., Wagner, C., Habib, S., Higdon, D., 2008.
Helly, J.C., Cole, S., Frenk, C.S., Baugh, C.M., Benson, A., Lacey, C., 2003a. Monthly Notices of the Royal Astronomical Society 338, 903–912.
Helly, J.C., Cole, S., Frenk, C.S., Baugh, C.M., Benson, A., Lacey, C., Pearce, F.R., 2003b. MNRAS 338, 913–925.
Henriques, B.M.B., Thomas, P.A., Oliver, S., Roseboom, I., 2009. Monthly Notices of the Royal Astronomical Society 396, 535–547.
Hernquist, L., Spergel, D.N., Heyl, J.S., 1993. Astrophysical Journal 416, 415.
Hollenbach, D., McKee, C.F., 1979. ApJ Supplement Series 41, 555–592.
Hopkins, P.F., Croton, D., Bundy, K., Khochfar, S., van den Bosch, F., Somerville, R.S., Wetzel, A., Keres, D., Hernquist, L., Stewart, K., Younger, J.D., Genel, S., Ma, C., 2010. http://adsabs.harvard.edu/abs/2010arXiv1004.2708H.
Hoyle, F., 1949. in: Problems in Cosmical Aerodynamics, Central Air Documents Officem Ohio.
Hoyle, F., Lyttleton, R.A., 1939. p. 405.
Hubble, E.P., 1929. Astrophysical Journal 69, 103–158.
Hubble, E.P., 1936.
Jahnke, K., Maccio, A., 2010. http://adsabs.harvard.edu/abs/2010arXiv1006.0482J.
Jenkins, A., Binney, J., 1990. Monthly Notices of the Royal Astronomical Society 245, 305–317.
Jenkins, A., Frenk, C.S., Pearce, F.R., Thomas, P.A., Colberg, J.M., White, S.D.M., Couchman, H.M.P., Peacock, J.A., Efstathiou, G., Nelson, A.H., 1998. Astrophysical Journal 499, 20.
Jiang, C.Y., Jing, Y.P., Faltenbacher, A., Lin, W.P., Li, C., 2008. ApJ 675, 1095–1105.
Jing, Y.P., Suto, Y., 2002. Astrophysical Journal 574, 538–553.
Jog, C.J., Solomon, P.M., 1984. Astrophysical Journal 276, 114–126.
Johnston, K.V., Bullock, J.S., Sharma, S., Font, A., Robertson, B.E., Leitner, S.N., 2008. Astrophysical Journal 689, 936–957.
Jonsson, P., 2006. Monthly Notices of the Royal Astronomical Society 372, 2–20.
Jubelgas, M., Springel, V., Dolag, K., 2004. Monthly Notices of the Royal Astronomical Society 351, 423–435.
Kampakoglou, M., Benson, A.J., 2007. Monthly Notices of the Royal Astronomical Society 374, 775–786.
Kant, I., 1755. J. F. Peterson, Königsberg and Leipzig.
Katz, N., 1992. Astrophysical Journal 391, 502–517.
Katz, N., White, S.D.M., 1993. Astrophysical Journal 412, 455–478.
Kauffmann, G., 1996. MNRAS 281, 487–492.

Kauffmann, G., Charlot, S., 1998. MNRAS 294, 705.
Kauffmann, G., Colberg, J.M., Diaferio, A., White, S.D.M., 1999a. MNRAS 303, 188–206.
Kauffmann, G., Colberg, J.M., Diaferio, A., White, S.D.M., 1999b. MNRAS 307, 529–536.
Kauffmann, G., Guiderdoni, B., White, S.D.M., 1994. MNRAS 267, 981.
Kauffmann, G., Haehnelt, M., 2000. MNRAS 311, 576–588.
Kauffmann, G., White, S.D.M., 1993. Monthly Notices of the Royal Astronomical Society 261, 921–928.
Kauffmann, G., White, S.D.M., Guiderdoni, B., 1993. MNRAS 264, 201.
Kaufmann, T., Bullock, J.S., Maller, A.H., Fang, T., Wadsley, J., 2009. Monthly Notices of the Royal Astronomical Society 396, 191–202.
Kay, S.T., Pearce, F.R., Frenk, C.S., Jenkins, A., 2002. Monthly Notices of the Royal Astronomical Society 330, 113–128.
Kazantzidis, S., Bullock, J.S., Zentner, A.R., Kravtsov, A.V., Moustakas, L.A., 2008. Astrophysical Journal 688, 254–276.
Kazantzidis, S., Zentner, A.R., Kravtsov, A.V., Bullock, J.S., Debattista, V.P., 2009.
Kennicutt, R.C., 1989. Astrophysical Journal 344, 685–703.
Kennicutt, R.C., 1998. Astrophysical Journal 498, 541.
Kereš, D., Katz, N., Fardal, M., Davé, R., Weinberg, D., 2009. MNRAS 395, 160.
Kereš, D., Katz, N., Weinberg, D.H., Davé, R., 2005. Monthly Notices of the Royal Astronomical Society 363, 2–28.
King, A., 2003. Astrophysical Journal 596, L27–L29.
King, A., 2005. Astrophysical Journal 635, L121–L123.
King, A., 2009. Astrophysical Journal 695, L107–L110.
Klypin, A., GottlÃűber, S., Kravtsov, A.V., Khokhlov, A.M., 1999. The Astrophysical Journal 516, 530–551.
Klypin, A., Holtzman, J., Primack, J., Regos, E., 1993. The Astrophysical Journal 416, 1.
Klypin, A.A., Shandarin, S.F., 1983. Monthly Notices of the Royal Astronomical Society 204, 891–907.
Kobayashi, C., Springel, V., White, S.D.M., 2007. Monthly Notices of the Royal Astronomical Society 376, 1465–1479.
Komatsu, E., Dunkley, J., Nolta, M.R., Bennett, C.L., Gold, B., Hinshaw, G., Jarosik, N., Larson, D., Limon, M., Page, L., Spergel, D.N., Halpern, M., Hill, R.S., Kogut, A., Meyer, S.S., Tucker, G.S., Weiland, J.L., Wollack, E., Wright, E.L., 2009. Astrophysical Journal Supplement Series 180, 330–376.
Komatsu, E., Smith, K.M., Dunkley, J., Bennett, C.L., Gold, B., Hinshaw, G., Jarosik, N., Larson, D., Nolta, M.R., Page, L., Spergel, D.N., Halpern, M., Hill, R.S., Kogut, A., Limon, M., Meyer, S.S., Odegard, N., Tucker, G.S., Weiland, J.L., Wollack, E., Wright, E.L., 2010. http://adsabs.harvard.edu/abs/2010arXiv1001.4538K.
Komissarov, S.S., Barkov, M.V., Vlahakis, N., Königl, A., 2007. Monthly Notices of the Royal Astronomical Society 380, 51–70.
Kormendy, J., Fisher, D.B., Cornell, M.E., Bender, R., 2009. The Astrophysical Journal Supplement Series 182, 216–309.
Kormendy, J., Freeman, K.C., 2004. p. 377.
Kormendy, J., Kennicutt, R.C., 2004. Annual Review of Astronomy and Astrophysics 42, 603–683.
Kowalski, M., Rubin, D., Aldering, G., Agostinho, R.J., Amadon, A., Amanullah, R., Balland, C., Barbary, K., Blanc, G., Challis, P.J., Conley, A., Connolly, N.V., Covarrubias, R., Dawson, K.S., Deustua, S.E., Ellis, R., Fabbro, S., Fadeyev, V., Fan, X., Farris, B., Folatelli, G., Frye, B.L., Garavini, G., Gates, E.L., Germany, L., Goldhaber, G., Goldman, B., Goobar, A., Groom, D.E., Haissinski, J., Hardin, D., Hook, I., Kent, S., Kim, A.G., Knop, R.A., Lidman, C., Linder, E.V., Mendez, J., Meyers, J., Miller, G.J., Moniez, M., ao, A.M.M., Newberg, H., Nobili, S., Nugent, P.E., Pain, R., Perdereau, O., Perlmutter, S., Phillips, M.M., Prasad, V., Quimby, R., Regnault, N., Rich, J., Rubenstein, E.P., Ruiz-Lapuente, P., Santos, F.D., Schaefer, B.E., Schommer, R.A., Smith, R.C., Soderberg, A.M., Spadafora, A.L., Strolger, L., Strovink, M., Suntzeff, N.B., Suzuki, N., Thomas, R.C., Walton, N.A., Wang, L., Wood-Vasey, W.M., Yun, J.L., 2008. Astrophysical Journal 686, 749–778.
Kravtsov, A.V., Berlind, A.A., Wechsler, R.H., Klypin, A.A., GottlÃűber, S., Allgood, B., Primack, J.R., 2004. The Astrophysical Journal 609, 35–49.
Kravtsov, A.V., Klypin, A., Hoffman, Y., 2002. The Astrophysical Journal 571, 563–575.
Kravtsov, A.V., Klypin, A.A., Khokhlov, A.M., 1997. Astrophysical Journal Supplement Series 111, 73.
Kriek, M., van Dokkum, P.G., Franx, M., Illingworth, G.D., Magee, D.K., 2009. The Astrophysical Journal 705, L71–L75.
Kroupa, P., 2001. Monthly Notices of the Royal Astronomical Society 322, 231–246.
Krumholz, M.R., McKee, C.F., Tumlinson, J., 2009.
Krumholz, M.R., Tan, J.C., 2007. Astrophysical Journal 654, 304–315.
Kuhlen, M., Diemand, J., Madau, P., Zemp, M., 2008. Journal of Physics Conference Series 125, 2008.
Kuijken, K., Gilmore, G., 1989. Monthly Notices of the Royal Astronomical Society 239, 571–603.
Lacey, C., Cole, S., 1993. Monthly Notices of the Royal Astronomical Society 262, 627–649.
Lacey, C., Silk, J., 1991. Astrophysical Journal 381, 14–32.
Lacey, C.G., 1984. Monthly Notices of the Royal Astronomical Society 208, 687–707.
Lacey, C.G., Baugh, C.M., Frenk, C.S., Benson, A.J., ., 2010. http://adsabs.harvard.edu/abs/2010arXiv1004.3545L.
Lacey, C.G., Baugh, C.M., Frenk, C.S., Silva, L., Granato, G.L., Bressan, A., 2008. MNRAS 385, 1155–1178.
Lanzoni, B., Guiderdoni, B., Mamon, G.A., Devriendt, J., Hatton, S., 2005. Monthly Notices of the Royal Astronomical Society 361, 369–384.
Larson, R.B., 1974. Monthly Notices of the Royal Astronomical Society 169, 229–246.
Laursen, P., Razoumov, A.O., Sommer-Larsen, J., 2009. Astrophysical Journal 696, 853–869.
Law, D.R., Steidel, C.C., Erb, D.K., Larkin, J.E., Pettini, M., Shapley, A.E., Wright, S.A., 2009. Astrophysical Journal 697, 2057–2082.
Lawlor, T.M., Young, T.R., Johnson, T.A., MacDonald, J., 2008. Monthly Notices of the Royal Astronomical Society 384, 1533–1543.
Lee, H., Worthey, G., Dotter, A., Chaboyer, B., Jevremovic, D., Baron, E., Briley, M.M., Ferguson, J.W., Coelho, P., Trager, S.C., 2009. Astrophysical Journal 694, 902–923.
Lemson, G., Kauffmann, G., 1999. MNRAS 302, 111–117.
Li, S., Li, H., Cen, R., 2008. Astrophysical Journal Supplement Series 174, 1–12.
Li, Y., Lucia, G.D., Helmi, A., 2010. Monthly Notices of the Royal Astronomical Society 401, 2036–2052.
Libeskind, N.I., Cole, S., Frenk, C.S., Helly, J.C., 2006. Monthly Notices of the Royal Astronomical Society 368, 1381–1391.

Lin, C.C., Shu, F.H., 1964. The Astrophysical Journal 140, 646.
Lin, D.N.C., Pringle, J.E., 1987. Astrophysical Journal 320, L87–L91.
Lintott, C.J., Schawinski, K., Slosar, A., Land, K., Bamford, S., Thomas, D., Raddick, M.J., Nichol, R.C., Szalay, A., Andreescu, D., Murray, P., Vandenberg, J., 2008. Monthly Notices of the Royal Astronomical Society 389, 1179–1189.
Lotz, J.M., Jonsson, P., Cox, T.J., Primack, J.R., 2008. Monthly Notices of the Royal Astronomical Society 391, 1137–1162.
Lotz, J.M., Primack, J., Madau, P., 2004. Astronomical Journal 128, 163–182.
Lucia, G.D., Blaizot, J., 2007. Monthly Notices of the Royal Astronomical Society 375, 2–14.
Lucia, G.D., Kauffmann, G., White, S.D.M., 2004. MNRAS 349, 1101–1116.
Lucia, G.D., Springel, V., White, S.D.M., Croton, D., Kauffmann, G., 2006. MNRAS 366, 499–509.
Lynden-Bell, D., 1967. Monthly Notices of the Royal Astronomical Society 136, 101.
Lynden-Bell, D., Kalnajs, A.J., 1972. Monthly Notices of the Royal Astronomical Society 157, 1.
Macció, A.V., Kang, X., Fontanot, F., Somerville, R.S., Koposov, S.E., Monaco, P., 2009.
Machida, M.N., Matsumoto, T., ichiro Inutsuka, S., 2008. Astrophysical Journal 685, 690–704.
Madau, P., 1995. Astrophysical Journal 441, 18–27.
Madau, P., Ferguson, H.C., Dickinson, M.E., Giavalisco, M., Steidel, C.C., Fruchter, A., 1996. Monthly Notices of the Royal Astronomical Society 283, 1388–1404.
Madau, P., Haardt, F., 2009. Astrophysical Journal 693, L100–L103.
Magorrian, J., Tremaine, S., Richstone, D., Bender, R., Bower, G., Dressler, A., Faber, S.M., Gebhardt, K., Green, R., Grillmair, C., Kormendy, J., Lauer, T., 1998. Astronomical Journal 115, 2285–2305.
Malbon, R.K., Baugh, C.M., Frenk, C.S., Lacey, C.G., 2007. MNRAS 382, 1394–1414.
Maller, A.H., Bullock, J.S., 2004. Monthly Notices of the Royal Astronomical Society 355, 694–712.
Maller, A.H., Dekel, A., Somerville, R., 2002. MNRAS 329, 423–430.
Maller, A.H., Prochaska, J.X., Somerville, R.S., Primack, J.R., 2001. MNRAS 326, 1475–1488.
Maller, A.H., Prochaska, J.X., Somerville, R.S., Primack, J.R., 2003. MNRAS 343, 268–278.
Mandelbaum, R., Seljak, U., Cool, R.J., Blanton, M., Hirata, C.M., Brinkmann, J., 2006. Monthly Notices of the Royal Astronomical Society 372, 758–776.
Mantz, A., Allen, S.W., Rapetti, D., Ebeling, H., 2009. http://adsabs.harvard.edu/abs/2009arXiv0909.3098M.
Mao, S., Mo, H.J., White, S.D.M., 1998. Monthly Notices of the Royal Astronomical Society 297, L71–L75.
Maraston, C., 2005. Monthly Notices of the Royal Astronomical Society 362, 799–825.
Marigo, P., 2001. A&A 370, 194–217.
Markevitch, M., Gonzalez, A., Clowe, D., Vikhlinin, A., 2004. p. 263.
Marochnik, L.S., Suchkov, A.A., 1996.
Marri, S., White, S.D.M., 2003. Monthly Notices of the Royal Astronomical Society 345, 561–574.
Martin, C.L., Kennicutt, R.C., 2001. Astrophysical Journal 555, 301–321.
Martínez-Serrano, F.J., Serna, A., Domínguez-Tenreiro, R., Mollá, M., 2008. MNRAS 388, 39–55.
Mastropietro, C., Moore, B., Mayer, L., Debattista, V.P., Piffaretti, R., Stadel, J., 2005a. Monthly Notices of the Royal Astronomical Society 364, 607–619.
Mastropietro, C., Moore, B., Mayer, L., Wadsley, J., Stadel, J., 2005b. Monthly Notices of the Royal Astronomical Society 363, 509–520.
Mateo, M.L., 1998. Annual Review of Astronomy and Astrophysics 36, 435–506.
Matteo, T.D., Colberg, J., Springel, V., Hernquist, L., Sijacki, D., 2008. Astrophysical Journal 676, 33–53.
Matteo, T.D., Croft, R.A.C., Springel, V., Hernquist, L., 2003. Astrophysical Journal 593, 56–68.
Matteo, T.D., Springel, V., Hernquist, L., 2005. Nature 433, 604–607.
Matteucci, F., Gibson, B.K., 1995. Astronomy and Astrophysics 304, 11.
Matteucci, F., Greggio, L., 1986. Astronomy and Astrophysics 154, 279–287.
Mayer, L., Governato, F., Colpi, M., Moore, B., Quinn, T., Wadsley, J., Stadel, J., Lake, G., 2001a. Astrophysical Journal 547, L123–L127.
Mayer, L., Governato, F., Colpi, M., Moore, B., Quinn, T., Wadsley, J., Stadel, J., Lake, G., 2001b. Astrophysical Journal 559, 754–784.
McCarthy, I.G., Bower, R.G., Balogh, M.L., Voit, G.M., Pearce, F.R., Theuns, T., Babul, A., Lacey, C.G., Frenk, C.S., 2007. Monthly Notices of the Royal Astronomical Society 376, 497–522.
McCarthy, I.G., Frenk, C.S., Font, A.S., Lacey, C.G., Bower, R.G., Mitchell, N.L., Balogh, M.L., Theuns, T., 2008. Monthly Notices of the Royal Astronomical Society 383, 593–605.
McDowell, M.R.C., 1961. The Observatory 81, 240–243.
McKee, C.F., Ostriker, E.C., 2007. Annual Review of Astronomy and Astrophysics 45, 565–687.
McKee, C.F., Ostriker, J.P., 1977. Astrophysical Journal 218, 148–169.
McKernan, B., Maller, A., Ford, K.E.S., 2010. http://adsabs.harvard.edu/abs/2010arXiv1006.0169M.
Meier, D.L., 1999. Astrophysical Journal 522, 753–766.
Meier, D.L., 2001. Astrophysical Journal 548, L9–L12.
Meiksin, A., 2006. Monthly Notices of the Royal Astronomical Society 365, 807–812.
Merritt, D., Milosavljevic, M., Favata, M., Hughes, S.A., Holz, D.E., 2004. Astrophysical Journal 607, L9–L12.
Merritt, D., Navarro, J.F., Ludlow, A., Jenkins, A., 2005. ApJ 624, L85–L88.
Milosavljevic, M., Merritt, D., 2001. Astrophysical Journal 563, 34–62.
Milosavljevic, M., Merritt, D., 2003. Astrophysical Journal 596, 860–878.
Minchev, I., Quillen, A.C., 2006. Monthly Notices of the Royal Astronomical Society 368, 623–636.
Miranda, M., Macciò, A.V., 2007. Monthly Notices of the Royal Astronomical Society 382, 1225–1232.
Mo, H.J., Mao, S., White, S.D.M., 1998. Monthly Notices of the Royal Astronomical Society 295, 319–336.
Monaco, P., Fontanot, F., Taffoni, G., 2007. Monthly Notices of the Royal Astronomical Society 375, 1189–1219.

Monaco, P., Salucci, P., Danese, L., 2000. Monthly Notices of the Royal Astronomical Society 311, 279–296.
Monaco, P., Theuns, T., Taffoni, G., 2002. Monthly Notices of the Royal Astronomical Society 331, 587–608.
Moore, B., Davis, M., 1994. Monthly Notices of the Royal Astronomical Society 270, 209.
Moore, B., Ghigna, S., Governato, F., Lake, G., Quinn, T., Stadel, J., Tozzi, P., 1999. Astrophysical Journal 524, L19–L22.
Moore, B., Katz, N., Lake, G., 1996a. Astrophysical Journal 457, 455.
Moore, B., Katz, N., Lake, G., Dressler, A., Oemler, A., 1996b. Nature 379, 613–616.
Moore, B., Lake, G., Katz, N., 1998. Astrophysical Journal 495, 139.
Munroe, R., 2009.
Murali, C., Weinberg, M.D., 1997a. Monthly Notices of the Royal Astronomical Society 288, 749–766.
Murali, C., Weinberg, M.D., 1997b. Monthly Notices of the Royal Astronomical Society 291, 717.
Murali, C., Weinberg, M.D., 1997c. Monthly Notices of the Royal Astronomical Society 288, 767–776.
Murray, N., Quataert, E., Thompson, T.A., 2005. Astrophysical Journal 618, 569–585.
Nagashima, M., Lacey, C.G., Baugh, C.M., Frenk, C.S., Cole, S., 2005a. MNRAS 358, 1247–1266.
Nagashima, M., Lacey, C.G., Okamoto, T., Baugh, C.M., Frenk, C.S., Cole, S., 2005b. MNRAS 363, L31–L35.
Narayan, R., Yi, I., 1994. Astrophysical Journal 428, L13–L16.
Narayanan, D., Hayward, C.C., Cox, T.J., Hernquist, L., Jonsson, P., Younger, J.D., Groves, B., 2010. Monthly Notices of the Royal Astronomical Society 401, 1613–1619.
Narlikar, J.V., Padmanabhan, T., 2001. Annual Review of Astronomy and Astrophysics 39, 211–248.
Navarro, J.F., Benz, W., 1991. Astrophysical Journal 380, 320–329.
Navarro, J.F., Frenk, C.S., White, S.D.M., 1995. Monthly Notices of the Royal Astronomical Society 275, 56–66.
Navarro, J.F., Frenk, C.S., White, S.D.M., 1996. Astrophysical Journal 462, 563.
Navarro, J.F., Frenk, C.S., White, S.D.M., 1997. ApJ 490, 493.
Navarro, J.F., Hayashi, E., Power, C., Jenkins, A.R., Frenk, C.S., White, S.D.M., Springel, V., Stadel, J., Quinn, T.R., 2004. MNRAS 349, 1039–1051.
Navarro, J.F., White, S.D.M., 1994. Monthly Notices of the Royal Astronomical Society 267, 401–412.
Neistein, E., Dekel, A., 2008. Monthly Notices of the Royal Astronomical Society 388, 1792–1802.
Nemmen, R.S., Bower, R.G., Babul, A., Storchi-Bergmann, T., 2007. Monthly Notices of the Royal Astronomical Society 377, 1652–1662.
Neyman, J., Scott, E.L., 1952. The Astrophysical Journal 116, 144.
Norman, M.L., Reynolds, D.R., So, G.C., 2009.
Nulsen, P.E.J., 1982. Monthly Notices of the Royal Astronomical Society 198, 1007–1016.
Ocvirk, P., Pichon, C., Teyssier, R., 2008. Monthly Notices of the Royal Astronomical Society 390, 1326–1338.
Ohkubo, T., Nomoto, K., Umeda, H., Yoshida, N., Tsuruta, S., 2009.
Okamoto, T., Gao, L., Theuns, T., 2008a. MNRAS 390, 920–928.
Okamoto, T., Nemmen, R.S., Bower, R.G., 2008b. Monthly Notices of the Royal Astronomical Society 385, 161–180.
Omma, H., Binney, J., Bryan, G., Slyz, A., 2004. Monthly Notices of the Royal Astronomical Society 348, 1105–1119.
Oppenheimer, B.D., Davé, R., 2008. Monthly Notices of the Royal Astronomical Society 387, 577–600.
O'Shea, B.W., Bryan, G., Bordner, J., Norman, M.L., Abel, T., Harkness, R., Kritsuk, A., 2004.
O'Shea, B.W., Norman, M.L., 2007. Astrophysical Journal 654, 66–92.
O'Shea, B.W., Norman, M.L., 2008. Astrophysical Journal 673, 14–33.
Ostriker, J.P., Peebles, P.J.E., 1973. Astrophysical Journal 186, 467–480.
Owen, F.N., Eilek, J.A., Kassim, N.E., 2000. The Astrophysical Journal 543, 611–619.
Padilla, N.D., Baugh, C.M., 2002. Monthly Notices of the Royal Astronomical Society 329, 431–444.
Parkinson, H., Cole, S., Helly, J., 2008. Monthly Notices of the Royal Astronomical Society 383, 557–564.
Parrish, I.J., Quataert, E., Sharma, P., 2009. The Astrophysical Journal 703, 96–108.
Parry, O.H., Eke, V.R., Frenk, C.S., 2009. Monthly Notices of the Royal Astronomical Society 396, 1972–1984.
Peacock, J.A., Dodds, S.J., 1996. Monthly Notices of the Royal Astronomical Society 280, L19–L26.
Peacock, J.A., Smith, R.E., 2000. Monthly Notices of the Royal Astronomical Society 318, 1144–1156.
Peebles, P.J.E., 1968. ApJ 153, 1.
Percival, W.J., Nichol, R.C., Eisenstein, D.J., Frieman, J.A., Fukugita, M., Loveday, J., Pope, A.C., Schneider, D.P., Szalay, A.S., Tegmark, M., Vogeley, M.S., Weinberg, D.H., Zehavi, I., Bahcall, N.A., Brinkmann, J., Connolly, A.J., Meiksin, A., 2007a. Astrophysical Journal 657, 645–663.
Percival, W.J., Nichol, R.C., Eisenstein, D.J., Weinberg, D.H., Fukugita, M., Pope, A.C., Schneider, D.P., Szalay, A.S., Vogeley, M.S., Zehavi, I., Bahcall, N.A., Brinkmann, J., Connolly, A.J., Loveday, J., Meiksin, A., 2007b. Astrophysical Journal 657, 51–55.
Peters, P.C., 1964. Physical Review 136, 1224–1232.
Peters, T., Klessen, R.S., Low, M.M., Banerjee, R., 2010. http://adsabs.harvard.edu/abs/2010arXiv1005.3271P.
Petkova, M., Springel, V., 2009. Monthly Notices of the Royal Astronomical Society 396, 1383–1403.
Pipino, A., Devriendt, J.E.G., Thomas, D., Silk, J., Kaviraj, S., 2008.
Pipino, A., Matteucci, F., 2004. Monthly Notices of the Royal Astronomical Society 347, 968–984.
Pipino, A., Matteucci, F., 2006. Monthly Notices of the Royal Astronomical Society 365, 1114–1122.
Plewa, T., Müller, E., 2001. Computer Physics Communications 138, 101–127.
Pontzen, A., Governato, F., Pettini, M., Booth, C.M., Stinson, G., Wadsley, J., Brooks, A., Quinn, T., Haehnelt, M., 2008. Monthly Notices of the Royal Astronomical Society 390, 1349–1371.
Pope, E.C.D., Pavlovski, G., Kaiser, C.R., Fangohr, H., 2005. Monthly Notices of the Royal Astronomical Society 364, 13–28.
Portinari, L., Chiosi, C., Bressan, A., 1998. A&A 334, 505–539.
Prada, F., Klypin, A.A., Simonneau, E., Betancort-Rijo, J., Patiri, S., Gottlöber, S., Sanchez-Conde, M.A., 2006. ApJ 645, 1001–1011.

Press, W.H., Schechter, P., 1974. Astrophysical Journal 187, 425–438.
Purcell, C.W., Kazantzidis, S., Bullock, J.S., 2009. Astrophysical Journal 694, L98–L102.
Putman, M.E., Bland-Hawthorn, J., Veilleux, S., Gibson, B.K., Freeman, K.C., Maloney, P.R., 2003. The Astrophysical Journal 597, 948–956.
Quilis, V., 2004. Monthly Notices of the Royal Astronomical Society 352, 1426–1438.
Quinlan, G.D., 1996. New Astronomy 1, 35–56.
Quinlan, G.D., Hernquist, L., 1997. New Astronomy 2, 533–554.
Quinn, P.J., Hernquist, L., Fullagar, D.P., 1993. Astrophysical Journal 403, 74–93.
Randall, S.W., Markevitch, M., Clowe, D., Gonzalez, A.H., Bradac, M., 2008. Astrophysical Journal 679, 1173–1180.
Rasmussen, J., Sommer-Larsen, J., Pedersen, K., Toft, S., Benson, A., Bower, R.G., Grove, L.F., 2009. Astrophysical Journal 697, 79–93.
Ratnatunga, K.U., Griffiths, R.E., Ostrander, E.J., 1999. Astronomical Journal 118, 86–107.
Razoumov, A.O., Sommer-Larsen, J., 2006. Astrophysical Journal 651, L89–L92.
Read, J.I., Lake, G., Agertz, O., Debattista, V.P., 2008. Monthly Notices of the Royal Astronomical Society 389, 1041–1057.
Read, J.I., Wilkinson, M.I., Evans, N.W., Gilmore, G., Kleyna, J.T., 2006. Monthly Notices of the Royal Astronomical Society 366, 429–437.
Reed, D.S., Bower, R., Frenk, C.S., Jenkins, A., Theuns, T., 2007. MNRAS 374, 2–15.
Reed, D.S., Bower, R., Frenk, C.S., Jenkins, A., Theuns, T., 2009. Monthly Notices of the Royal Astronomical Society 394, 624–632.
Rees, M.J., Ostriker, J.P., 1977. Monthly Notices of the Royal Astronomical Society 179, 541–559.
Ricker, P.M., Dodelson, S., Lamb, D.Q., 2000. Astrophysical Journal 536, 122–143.
Ricotti, M., Gnedin, N.Y., Shull, J.M., 2001. Astrophysical Journal 560, 580–591.
Ricotti, M., Gnedin, N.Y., Shull, J.M., 2002. Astrophysical Journal 575, 33–48.
Ricotti, M., Shull, J.M., 2000. Astrophysical Journal 542, 548–558.
Rijkhorst, E., Plewa, T., Dubey, A., Mellema, G., 2006. Astronomy and Astrophysics 452, 907–920.
Robertson, B., Bullock, J.S., Cox, T.J., Matteo, T.D., Hernquist, L., Springel, V., Yoshida, N., 2006a. Astrophysical Journal 645, 986–1000.
Robertson, B., Bullock, J.S., Font, A.S., Johnston, K.V., Hernquist, L., 2005. Astrophysical Journal 632, 872–881.
Robertson, B., Cox, T.J., Hernquist, L., Franx, M., Hopkins, P.F., Martini, P., Springel, V., 2006b. Astrophysical Journal 641, 21–40.
Robertson, B.E., Kravtsov, A.V., 2008. Astrophysical Journal 680, 1083–1111.
Robertson, B.E., Kravtsov, A.V., Tinker, J., Zentner, A.R., 2009. Astrophysical Journal 696, 636–652.
Robinson, K., Dursi, L.J., Ricker, P.M., Rosner, R., Calder, A.C., Zingale, M., Truran, J.W., Linde, T., Caceres, A., Fryxell, B., Olson, K., Riley, K., Siegel, A., Vladimirova, N., 2004. The Astrophysical Journal 601, 621–643.
Romano, D., Chiappini, C., Matteucci, F., Tosi, M., 2005. Astronomy and Astrophysics 430, 491–505.
Romeo, A.B., 1992. Monthly Notices of the Royal Astronomical Society 256, 307–320.
Romeo, A.B., 1994. Astronomy and Astrophysics 286, 799–806.
Roskar, R., Debattista, V.P., Quinn, T.R., Stinson, G.S., Wadsley, J., 2008a. Astrophysical Journal 684, L79–L82.
Roskar, R., Debattista, V.P., Stinson, G.S., Quinn, T.R., Kaufmann, T., Wadsley, J., 2008b. Astrophysical Journal 675, L65–L68.
Rosswog, S., 2009.
Roychowdhury, S., Ruszkowski, M., Nath, B.B., Begelman, M.C., 2004. Astrophysical Journal 615, 681–688.
Rozo, E., Wechsler, R.H., Rykoff, E.S., Annis, J.T., Becker, M.R., Evrard, A.E., Frieman, J.A., Hansen, S.M., Hao, J., Johnston, D.E., Koester, B.P., McKay, T.A., Sheldon, E.S., Weinberg, D.H., 2010. The Astrophysical Journal 708, 645–660.
Ruszkowski, M., Brüggen, M., Begelman, M.C., 2004. Astrophysical Journal 611, 158–163.
Ruszkowski, M., Enßlin, T.A., Brüggen, M., Begelman, M.C., Churazov, E., 2008. Monthly Notices of the Royal Astronomical Society 383, 1359–1365.
Sales, L.V., Navarro, J.F., Abadi, M.G., Steinmetz, M., 2007. Monthly Notices of the Royal Astronomical Society 379, 1475–1483.
Salpeter, E.E., 1955. The Astrophysical Journal 121, 161.
Sanchez, A.G., Crocce, M., Cabre, A., Baugh, C.M., Gaztanaga, E., 2009.
Santoro, F., Shull, J.M., 2006. Astrophysical Journal 643, 26–37.
Scannapieco, C., Tissera, P.B., White, S.D.M., Springel, V., 2005. Monthly Notices of the Royal Astronomical Society 364, 552–564.
Scannapieco, C., Tissera, P.B., White, S.D.M., Springel, V., 2006a. Monthly Notices of the Royal Astronomical Society 371, 1125–1139.
Scannapieco, E., Kawata, D., Brook, C.B., Schneider, R., Ferrara, A., Gibson, B.K., 2006b. Astrophysical Journal 653, 285–299.
Scannapieco, E., Oh, S.P., 2004. Astrophysical Journal 608, 62–79.
Schade, D., Carlberg, R.G., Yee, H.K.C., Lopez-Cruz, O., Ellingson, E., 1996. Astrophysical Journal 464, L63.
Schawinski, K., 2009.
Schawinski, K., Thomas, D., Sarzi, M., Maraston, C., Kaviraj, S., Joo, S., Yi, S.K., Silk, J., 2007. Monthly Notices of the Royal Astronomical Society 382, 1415–1431.
Schaye, J., 2004. Astrophysical Journal 609, 667–682.
Schmidt, M., 1959. Astrophysical Journal 129, 243.
Schreiber, N.M.F., Genzel, R., Bouche, N., Cresci, G., Davies, R., Buschkamp, P., Shapiro, K., Tacconi, L.J., Hicks, E.K.S., Genel, S., Shapley, A.E., Erb, D.K., Steidel, C.C., Lutz, D., Eisenhauer, F., Gillessen, S., Sternberg, A., Renzini, A., Cimatti, A., Daddi, E., Kurk, J., Lilly, S., Kong, X., Lehnert, M.D., Nesvadba, N., Verma, A., McCracken, H., Arimoto, N., Mignoli, M., Onodera, M., 2009.
Seljak, U., Makarov, A., McDonald, P., Anderson, S.F., Bahcall, N.A., Brinkmann, J., Burles, S., Cen, R., Doi, M., Gunn, J.E., Ivezic, Z., Kent, S., Loveday, J., Lupton, R.H., Munn, J.A., Nichol, R.C., Ostriker, J.P., Schlegel, D.J., Schneider, D.P., Tegmark, M., Berk, D.E., Weinberg, D.H., York, D.G., 2005. Physical Review D 71, 103515.
Sellwood, J.A., 2010. http://adsabs.harvard.edu/abs/2010arXiv1006.4855S.
Sellwood, J.A., Binney, J.J., 2002. Monthly Notices of the Royal Astronomical Society 336, 785–796.
Sellwood, J.A., Nelson, R.W., Tremaine, S., 1998. Astrophysical Journal 506, 590–599.
Sersic, J.L., 1968.
Sesana, A., Haardt, F., Madau, P., 2007. Astrophysical Journal 660, 546–555.

Sesana, A., Haardt, F., Madau, P., 2008. Astrophysical Journal 686, 432–447.
Shakura, N.I., Sunyaev, R.A., 1973. Astronomy and Astrophysics 24, 337–355.
Shapiro, S.L., 2005. Astrophysical Journal 620, 59–68.
Sharma, S., Steinmetz, M., 2005. ApJ 628, 21–44.
Shaw, D.J., Mota, D.F., 2008. Astrophysical Journal Supplement Series 174, 277–281.
Shen, J., Sellwood, J.A., 2004. Astrophysical Journal 604, 614–631.
Sheth, R.K., Mo, H.J., Tormen, G., 2001. Monthly Notices of the Royal Astronomical Society 323, 1–12.
Shlosman, I., Noguchi, M., 1993. Astrophysical Journal 414, 474–486.
Sijacki, D., Springel, V., Haehnelt, M.G., 2009.
Sijacki, D., Springel, V., Matteo, T.D., Hernquist, L., 2007. Monthly Notices of the Royal Astronomical Society 380, 877–900.
Silk, J., 2001. Monthly Notices of the Royal Astronomical Society 324, 313–318.
Silk, J., Norman, C., 1981. Astrophysical Journal 247, 59–76.
Silk, J., Rees, M.J., 1998. Astronomy and Astrophysics 331, L1–L4.
Silva, L., Granato, G.L., Bressan, A., Danese, L., 1998. ApJ 509, 103–117.
Simard, L., Willmer, C.N.A., Vogt, N.P., Sarajedini, V.L., Phillips, A.C., Weiner, B.J., Koo, D.C., Im, M., Illingworth, G.D., Faber, S.M., 2002. Astrophysical Journal Supplement Series 142, 1–33.
Slosar, A., McDonald, P., Seljak, U., 2007. New Astronomy Review 51, 327–331.
Smith, B.D., Turk, M.J., Sigurdsson, S., O'Shea, B.W., Norman, M.L., 2009. The Astrophysical Journal 691, 441–451.
Smith, R.E., Peacock, J.A., Jenkins, A., White, S.D.M., Frenk, C.S., Pearce, F.R., Thomas, P.A., Efstathiou, G., Couchman, H.M.P., 2003. Monthly Notices of the Royal Astronomical Society 341, 1311–1332.
Smoluchowksi, M., 1916. Phys. Zeit. 17, 557.
Somerville, R.S., 2002. ApJ 572, L23–L26.
Somerville, R.S., Barden, M., Rix, H., Bell, E.F., Beckwith, S.V.W., Borch, A., Caldwell, J.A.R., Häußler, B., Heymans, C., Jahnke, K., Jogee, S., McIntosh, D.H., Meisenheimer, K., Peng, C.Y., Sánchez, S.F., Wisotzki, L., Wolf, C., 2008a. ApJ 672, 776–786.
Somerville, R.S., Bullock, J.S., Livio, M., 2003. Astrophysical Journal 593, 616–621.
Somerville, R.S., Hopkins, P.F., Cox, T.J., Robertson, B.E., Hernquist, L., 2008b. Monthly Notices of the Royal Astronomical Society 391, 481–506.
Somerville, R.S., Livio, M., 2003. ApJ 593, 611–615.
Somerville, R.S., Primack, J.R., 1999. Monthly Notices of the Royal Astronomical Society 310, 1087–1110.
Spitzer, L., 1942. Astrophysical Journal 95, 329.
Spitzer, L., 1962.
Spitzer, L., Schwarzschild, M., 1953. Astrophysical Journal 118, 106.
Springel, V., 2005. Monthly Notices of the Royal Astronomical Society 364, 1105–1134.
Springel, V., Hernquist, L., 2005. Astrophysical Journal 622, L9–L12.
Springel, V., Matteo, T.D., Hernquist, L., 2005a. Monthly Notices of the Royal Astronomical Society 361, 776–794.
Springel, V., Wang, J., Vogelsberger, M., Ludlow, A., Jenkins, A., Helmi, A., Navarro, J.F., Frenk, C.S., White, S.D.M., 2008. Monthly Notices of the Royal Astronomical Society 391, 1685–1711.
Springel, V., White, S.D.M., Jenkins, A., Frenk, C.S., Yoshida, N., Gao, L., Navarro, J., Thacker, R., Croton, D., Helly, J., Peacock, J.A., Cole, S., Thomas, P., Couchman, H., Evrard, A., Colberg, J., Pearce, F., 2005b. Nature 435, 629–636.
Springel, V., White, S.D.M., Tormen, G., Kauffmann, G., 2001. MNRAS 328, 726–750.
Stacy, A., Bromm, V., 2007. Monthly Notices of the Royal Astronomical Society 382, 229–238.
Steidel, C.C., Erb, D.K., Shapley, A.E., Pettini, M., Reddy, N.A., BogosavljeviÄĞ, M., Rudie, G.C., Rakic, O., 2010. http://adsabs.harvard.edu/abs/2010arXiv1003.0679S.
Steinmetz, M., Navarro, J.F., 2002. New Astronomy 7, 155–160.
Stewart, K.R., Bullock, J.S., Barton, E.J., Wechsler, R.H., 2009. The Astrophysical Journal 702, 1005–1015.
Stinson, G., 2007.
Stinson, G., Seth, A., Katz, N., Wadsley, J., Governato, F., Quinn, T., 2006. Monthly Notices of the Royal Astronomical Society 373, 1074–1090.
Strigari, L.E., Bullock, J.S., Kaplinghat, M., Simon, J.D., Geha, M., Willman, B., Walker, M.G., 2008. Nature 454, 1096–1097.
Stringer, M.J., Brooks, A.M., Benson, A.J., Governato, F., 2010. http://adsabs.harvard.edu/abs/2010arXiv1001.0594S.
Summers, F.J., Davis, M., Evrard, A.E., 1995. Astrophysical Journal 454, 1.
Swinbank, A.M., Lacey, C.G., Smail, I., Baugh, C.M., Frenk, C.S., Blain, A.W., Chapman, S.C., Coppin, K.E.K., Ivison, R.J., Gonzalez, J.E., Hainline, L.J., 2008. Monthly Notices of the Royal Astronomical Society 391, 420–434.
Tasker, E.J., Bryan, G.L., 2006. Astrophysical Journal 641, 878–890.
Tasker, E.J., Bryan, G.L., 2008. The Astrophysical Journal 673, 810–831.
Tassis, K., Kravtsov, A.V., Gnedin, N.Y., 2008. Astrophysical Journal 672, 888–903.
Taylor, J.E., Babul, A., 2004. Monthly Notices of the Royal Astronomical Society 348, 811–830.
Tegmark, M., Blanton, M.R., Strauss, M.A., Hoyle, F., Schlegel, D., Scoccimarro, R., Vogeley, M.S., Weinberg, D.H., Zehavi, I., Berlind, A., Budavari, T., Connolly, A., Eisenstein, D.J., Finkbeiner, D., Frieman, J.A., Gunn, J.E., Hamilton, A.J.S., Hui, L., Jain, B., Johnston, D., Kent, S., Lin, H., Nakajima, R., Nichol, R.C., Ostriker, J.P., Pope, A., Scranton, R., Seljak, U., Sheth, R.K., Stebbins, A., Szalay, A.S., Szapudi, I., Verde, L., Xu, Y., Annis, J., Bahcall, N.A., Brinkmann, J., Burles, S., Castander, F.J., Csabai, I., Loveday, J., Doi, M., Fukugita, M., Gott, J.R., Hennessy, G., Hogg, D.W., Ivezic, Z., Knapp, G.R., Lamb, D.Q., Lee, B.C., Lupton, R.H., McKay, T.A., Kunszt, P., Munn, J.A., O'Connell, L., Peoples, J., Pier, J.R., Richmond, M., Rockosi, C., Schneider, D.P., Stoughton, C., Tucker, D.L., Berk, D.E.V., Yanny, B., York, D.G., 2004. Astrophysical Journal 606, 702–740.
Tegmark, M., Eisenstein, D.J., Strauss, M.A., Weinberg, D.H., Blanton, M.R., Frieman, J.A., Fukugita, M., Gunn, J.E., Hamilton, A.J.S., Knapp, G.R., Nichol, R.C., Ostriker, J.P., Padmanabhan, N., Percival, W.J., Schlegel, D.J., Schneider, D.P., Scoccimarro, R., Seljak, U., Seo, H.,

Swanson, M., Szalay, A.S., Vogeley, M.S., Yoo, J., Zehavi, I., Abazajian, K., Anderson, S.F., Annis, J., Bahcall, N.A., Bassett, B., Berlind, A., Brinkmann, J., Budavari, T., Castander, F., Connolly, A., Csabai, I., Doi, M., Finkbeiner, D.P., Gillespie, B., Glazebrook, K., Hennessy, G.S., Hogg, D.W., Ivezic, Z., Jain, B., Johnston, D., Kent, S., Lamb, D.Q., Lee, B.C., Lin, H., Loveday, J., Lupton, R.H., Munn, J.A., Pan, K., Park, C., Peoples, J., Pier, J.R., Pope, A., Richmond, M., Rockosi, C., Scranton, R., Sheth, R.K., Stebbins, A., Stoughton, C., Szapudi, I., Tucker, D.L., Berk, D.E.V., Yanny, B., York, D.G., 2006. Physical Review D 74, 123507.
Tegmark, M., Silk, J., Rees, M.J., Blanchard, A., Abel, T., Palla, F., 1997. ApJ 474, 1.
Thacker, R.J., Couchman, H.M.P., 2000. Astrophysical Journal 545, 728–752.
Thacker, R.J., Couchman, H.M.P., 2001. Astrophysical Journal 555, L17–L20.
Thorne, K.S., 1974. Astrophysical Journal 191, 507–520.
Tichy, W., Marronetti, P., 2007. Physical Review D (Particles, Fields, Gravitation, and Cosmology) 76, 061502–5.
Timmes, F.X., Woosley, S.E., Weaver, T.A., 1995. Astrophysical Journal Supplement Series 98, 617–658.
Tinker, J., Kravtsov, A.V., Klypin, A., Abazajian, K., Warren, M., Yepes, G., Gottlöber, S., Holz, D.E., 2008. The Astrophysical Journal 688, 709–728.
Tinker, J.L., Wechsler, R.H., Zheng, Z., 2010. The Astrophysical Journal 709, 67–76.
Tollerud, E.J., Bullock, J.S., Strigari, L.E., Willman, B., 2008. Astrophysical Journal 688, 277–289.
Tolstoy, E., Hill, V., Tosi, M., 2009.
Toomre, A., 1964. Astrophysical Journal 139, 1217–1238.
Tormen, G., Diaferio, A., Syer, D., 1998. Monthly Notices of the Royal Astronomical Society 299, 728–742.
Toth, G., Ostriker, J.P., 1992. Astrophysical Journal 389, 5–26.
Tozzi, P., Norman, C., 2001. Astrophysical Journal 546, 63–84.
Tremaine, S., Gebhardt, K., Bender, R., Bower, G., Dressler, A., Faber, S.M., Filippenko, A.V., Green, R., Grillmair, C., Ho, L.C., Kormendy, J., Lauer, T.R., Magorrian, J., Pinkney, J., Richstone, D., 2002. Astrophysical Journal 574, 740–753.
Tremaine, S., Henon, M., Lynden-Bell, D., 1986. Monthly Notices of the Royal Astronomical Society 219, 285–297.
Trenti, M., Stiavelli, M., 2009. Astrophysical Journal 694, 879–892.
Tumlinson, J., 2006. Astrophysical Journal 641, 1–20.
Turk, M.J., 2009. http://adsabs.harvard.edu/abs/2009PhDT.....5T.
de Vaucouleurs, G., 1959. Handbuch der Physik 53, 275.
de Vaucouleurs, G., de Vaucouleurs, A., Corwin, H.G., Buta, R.J., Paturel, G., Fouque, P., 1991.
Vecchia, C.D., Bower, R.G., Theuns, T., Balogh, M.L., Mazzotta, P., Frenk, C.S., 2004. Monthly Notices of the Royal Astronomical Society 355, 995–1004.
Vecchia, C.D., Schaye, J., 2008. Monthly Notices of the Royal Astronomical Society 387, 1431–1444.
Veilleux, S., Cecil, G., Bland-Hawthorn, J., 2005. Annual Review of Astronomy and Astrophysics 43, 769–826.
Velazquez, H., White, S.D.M., 1999. Monthly Notices of the Royal Astronomical Society 304, 254–270.
Vernaleo, J.C., Reynolds, C.S., 2006. Astrophysical Journal 645, 83–94.
Viel, M., Becker, G.D., Bolton, J.S., Haehnelt, M.G., Rauch, M., Sargent, W.L.W., 2008. Physical Review Letters 100, 41304.
Vikhlinin, A., Kravtsov, A.V., Burenin, R.A., Ebeling, H., Forman, W.R., Hornstrup, A., Jones, C., Murray, S.S., Nagai, D., Quintana, H., Voevodkin, A., 2009. The Astrophysical Journal 692, 1060–1074.
Villalobos, Álvaro., Helmi, A., 2008. Monthly Notices of the Royal Astronomical Society 391, 1806–1827.
Villiers, J.D., Hawley, J.F., Krolik, J.H., Hirose, S., 2005. Astrophysical Journal 620, 878–888.
Vitvitska, M., Klypin, A.A., Kravtsov, A.V., Wechsler, R.H., Primack, J.R., Bullock, J.S., 2002. Astrophysical Journal 581, 799–809.
Voit, G.M., Balogh, M.L., Bower, R.G., Lacey, C.G., Bryan, G.L., 2003. Astrophysical Journal 593, 272–290.
Volonteri, M., Haardt, F., Madau, P., 2003. Astrophysical Journal 582, 559–573.
Volonteri, M., Lodato, G., Natarajan, P., 2008. Monthly Notices of the Royal Astronomical Society 383, 1079–1088.
Volonteri, M., Madau, P., Quataert, E., Rees, M.J., 2005. Astrophysical Journal 620, 69–77.
Volonteri, M., Natarajan, P., 2009.
Wadepuhl, M., Springel, V., 2010. http://adsabs.harvard.edu/abs/2010arXiv1004.3217W.
Wadsley, J.W., Stadel, J., Quinn, T., 2004. New Astronomy 9, 137–158.
Wang, B., Silk, J., 1994. Astrophysical Journal 427, 759–769.
Wang, P., Abel, T., 2009. The Astrophysical Journal 696, 96–109.
Wang, Q.D., Yao, Y., Tripp, T.M., Fang, T., Cui, W., Nicastro, F., Mathur, S., Williams, R.J., Song, L., Croft, R., 2005. Astrophysical Journal 635, 386–395.
Warren, M.S., Quinn, P.J., Salmon, J.K., Zurek, W.H., 1992. ApJ 399, 405–425.
Watanabe, M., Kodaira, K., Okamura, S., 1985. Astrophysical Journal 292, 72–78.
Wechsler, R.H., Bullock, J.S., Primack, J.R., Kravtsov, A.V., Dekel, A., 2002. The Astrophysical Journal 568, 52–70.
Wechsler, R.H., Somerville, R.S., Bullock, J.S., Kolatt, T.S., Primack, J.R., Blumenthal, G.R., Dekel, A., 2001. ApJ 554, 85–103.
Wen, W., Zhao, J., 2004. Progress in Astronomy 22, 235–244.
Wetzel, A.R., Cohn, J.D., White, M., 2008. 0810.3650 .
White, S., 2004. p. 30.
White, S.D.M., Davis, M., Efstathiou, G., Frenk, C.S., 1987a. Nature 330, 451–453.
White, S.D.M., Davis, M., Frenk, C.S., 1984. Monthly Notices of the Royal Astronomical Society 209, 27P–31P.
White, S.D.M., Frenk, C.S., 1991. Astrophysical Journal 379, 52–79.
White, S.D.M., Frenk, C.S., Davis, M., Efstathiou, G., 1987b. Astrophysical Journal 313, 505–516.
White, S.D.M., Rees, M.J., 1978. MNRAS 183, 341–358.
Williams, R.J., Mathur, S., Nicastro, F., 2006. Astrophysical Journal 645, 179–185.
Willman, B., Dalcanton, J.J., Martinez-Delgado, D., West, A.A., Blanton, M.R., Hogg, D.W., Barentine, J.C., Brewington, H.J., Harvanek, M.,

Kleinman, S.J., Krzesinski, J., Long, D., Neilsen, E.H., Nitta, A., Snedden, S.A., 2005. Astrophysical Journal 626, L85–L88.
Wise, J.H., Abel, T., 2007a. Astrophysical Journal 671, 1559–1567.
Wise, J.H., Abel, T., 2007b. Astrophysical Journal 665, 899–910.
Wise, J.H., Abel, T., 2008a. Astrophysical Journal 684, 1–17.
Wise, J.H., Abel, T., 2008b. Astrophysical Journal 685, 40–56.
Wise, J.H., Cen, R., 2009. Astrophysical Journal 693, 984–999.
Wise, J.H., Turk, M.J., Abel, T., 2008. Astrophysical Journal 682, 745–757.
Wright, T., 1750. London.
Wuyts, S., Franx, M., Cox, T.J., Förster Schreiber, N.M., Hayward, C.C., Hernquist, L., Hopkins, P.F., Labbé, I., Marchesini, D., Robertson, B.E., Toft, S., van Dokkum, P.G., 2009. The Astrophysical Journal 700, 799–819.
Wyithe, J.S.B., Loeb, A., 2003. Astrophysical Journal 595, 614–623.
Yajima, H., Umemura, M., Mori, M., Nakamoto, T., 2009. Monthly Notices of the Royal Astronomical Society 398, 715–721.
Yang, X., Mo, H.J., van den Bosch, F.C., 2003. Monthly Notices of the Royal Astronomical Society 339, 1057–1080.
Yoshida, N., Abel, T., Hernquist, L., Sugiyama, N., 2003. Astrophysical Journal 592, 645–663.
Yoshida, N., Omukai, K., Hernquist, L., Abel, T., 2006. Astrophysical Journal 652, 6–25.
Yoshida, N., Stoehr, F., Springel, V., White, S.D.M., 2002. Monthly Notices of the Royal Astronomical Society 335, 762–772.
Younger, J.D., Bryan, G.L., 2007. Astrophysical Journal 666, 647–657.
Younger, J.D., Hayward, C.C., Narayanan, D., Cox, T.J., Hernquist, L., Jonsson, P., 2009. Monthly Notices of the Royal Astronomical Society 396, L66–L70.
Yu, Q., 2002. Monthly Notices of the Royal Astronomical Society 331, 935–958.
Yüksel, H., Beacom, J.F., Watson, C.R., 2008. Physical Review Letters 101, 121301.
Zavala, J., Okamoto, T., Frenk, C.S., 2008. Monthly Notices of the Royal Astronomical Society 387, 364–370.
Zhang, J., Fakhouri, O., Ma, C., 2008. Monthly Notices of the Royal Astronomical Society 389, 1521–1538.
Zhao, D.H., Jing, Y.P., Mo, H.J., Börner, G., 2009. Astrophysical Journal 707, 354–369.
Zhao, H., Hooper, D., Angus, G.W., Taylor, J.E., Silk, J., 2007. Astrophysical Journal 654, 697–701.
Zheng, Z., Coil, A.L., Zehavi, I., 2007. The Astrophysical Journal 667, 760–779.